

Brackish Groundwater in the Eastern Portion of the Sparta Aquifer

Kristie Laughlin, P.G., Sydney Weitkumat, P.G., Olga Bauer

Report 390
August 2023

Texas Water Development Board
www.twdb.texas.gov



Texas Water Development Board

Report 390

Brackish Groundwater in the Eastern Portion of the Sparta Aquifer

By

Kristie Laughlin, P.G.

Sydney Weitkumat, P.G.

Olga Bauer

August 2023

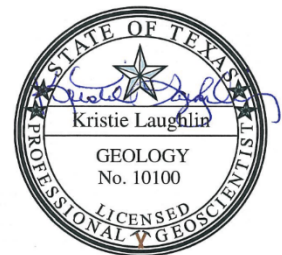


Geoscientist Seal

The contents of this report (including figures, tables, and plates) document the work of the following licensed Texas geoscientists:

Kristie Laughlin, P.G., No. 10100

Ms. Laughlin was responsible for oversight of all aspects of the study and preparing the final report. Primary tasks included stratigraphy, lithology, general geology, geochemistry, and salinity distribution. The seal appearing on this document was authorized on 8/25/2023.



Sydney Weitkunat, P.G., No. 15031

Ms. Weitkunat interpreted stratigraphy, lithology, and total dissolved solids concentration from geophysical well logs, interpolated elevation rasters, and calculating porosity and volumes. She also contributed to preparing the report. The seal appearing on this document was authorized on 8/25/2023.



Olga Bauer

Mrs. Bauer, under the supervision of Ms. Laughlin and Ms. Weitkunat, interpreted stratigraphy, lithology, and total dissolved solids concentration from geophysical well logs, interpolated net sand and elevation rasters, created report figures, contributed to preparing the report, and prepared final geographic information system deliverables and metadata.

Cover photo courtesy of Andy Donnelly
“Prothonotary Warbler”

Texas Water Development Board

Brooke Paup
Chairwoman

George B. Peyton V
Member

L'Oreal Stepney, P.E.
Member

Leading the state's efforts in ensuring a secure water future for Texas and its citizens.

The Texas Water Development Board freely grants permission to copy and distribute its materials. The agency would appreciate acknowledgment.

Published and distributed by the
Texas Water Development Board
P.O. Box 13231, Capitol Station
Austin, Texas 78711-3231

(Printed on recycled paper)

This page is intentionally blank.

Table of contents

Geoscientist Seal	ii
Table of contents	vi
List of figures.....	vii
List of tables.....	viii
List of appendices.....	ix
1 Executive summary	1
Program description	1
Study area	1
Salinity distribution.....	2
Brackish groundwater volumes	3
2 Introduction.....	5
3 Project deliverables.....	7
4 Study area	8
4.1 East Sparta aquifer study area	9
4.2 Previous investigations	15
5 Data collection and analysis.....	19
5.1 Data sources	19
5.2 Data mining	19
5.3 Geophysical logs	22
5.4 State well reports.....	22
6 Geology.....	23
6.1 Depositional history and setting.....	25
6.2 Structure	28
6.3 Faults	28
6.4 Salt domes	29
7 Stratigraphy and lithology.....	30
7.1 Depositional systems	31
7.2 Type logs.....	31
7.3 Stratigraphic interpretation.....	33
7.4 Lithology	43
7.5 Net sand analysis.....	45
8 Aquifer determination and properties.....	48
8.1 Aquifer hydraulic properties	48
8.2 Pumping test data.....	50
8.3 Porosity data	55
8.4 Porosity data analysis	55
9 Measured water quality data.....	59
9.1 Measured sample data	59
9.2 Measured sample quality assurance	59
9.3 Dissolved minerals	63
9.4 Radiochemistry.....	64
9.5 Specific conductance	65
9.6 Total dissolved solids and specific conductance relationship.....	66
10 Calculated water quality data	68

10.1	Well pairs.....	68
10.2	Calculating salinity from geophysical logs.....	69
10.2.1	R_{wa} minimum method.....	69
10.2.2	Input parameters for R_{wa} minimum method.....	72
10.3	Salinity zone delineation.....	75
10.4	Salinity zone analysis.....	76
11	Groundwater volumes.....	80
11.1	Area.....	82
11.2	Saturated thickness.....	82
11.3	Static water level.....	82
11.4	Specific Yield.....	83
11.5	Results.....	83
12	Desalination.....	87
12.1	Treatment Methods.....	87
12.2	Concentrate disposal options.....	87
13	Future improvements.....	88
14	Conclusions.....	89
15	Acknowledgements.....	90
16	References.....	91
17	Appendices.....	97

List of figures

Figure 1-1.	East Sparta aquifer study area.....	2
Figure 1-2.	East Sparta aquifer salinity zones.....	3
Figure 4-1.	Study area nomenclature.....	9
Figure 4.1-1.	Location map of the East Sparta aquifer study area.....	11
Figure 4.1-2.	Administrative boundaries in the East Sparta aquifer study area.....	12
Figure 4.1-3.	East Sparta aquifer study area.....	13
Figure 4.1-4.	Public water supply system boundaries.....	14
Figure 4.2-1.	Published cross sections in the study area.....	17
Figure 4.2-2.	Estimated cross sections in the study area.....	18
Figure 5.2-1.	East Sparta aquifer study area well data locations.....	21
Figure 6-1.	Geological formations outcropping within the study area.....	24
Figure 6.1-1.	Structural components in the Upper Coastal Plains East area (.....	27
Figure 6.3-1.	Graben formation via basin-ward creep in the Luling-Mexia-Talco fault zone.....	28
Figure 6.4-1.	Regional cross section through the Upper Coastal Plains East.....	29
Figure 7.1-1.	Sediment dispersal pattern in a constructive delta:.....	31
Figure 7.2-1.	Strike-oriented cross section through study area type logs.....	32
Figure 7.3-1.	Gamma ray log plots.....	34
Figure 7.3-2.	Spontaneous potential and resistivity logs.....	35

Figure 7.3-3.	Correlation section showing stratigraphic interpretation of the	37
Figure 7.3-4.	Sparta Formation top elevation in feet above mean sea level.	38
Figure 7.3-5.	Sparta Formation bottom elevation in feet above mean sea level.	39
Figure 7.3-6.	Sparta Formation top depth in feet below ground surface.	40
Figure 7.3-7.	Sparta Formation bottom depth in feet below ground surface.	41
Figure 7.3-8.	Sparta Formation thickness in feet.	42
Figure 7.4-1.	Correlation section showing lithologic interpretations for the Sparta Formation.....	44
Figure 7.5-1.	Sparta Formation net sand thickness, in feet.	47
Figure 8.2-1.	Summary of aquifer test data available in the western study area.	51
Figure 8.2-2.	Summary of aquifer test data available in the eastern study area.	52
Figure 8.2-3.	East Sparta aquifer hydraulic properties.	53
Figure 8.2-4.	Area with historically-highest well yields and net sand thickness	54
Figure 8.4-1.	Porosity distribution in the study area.	57
Figure 8.4-2.	Scatter plot of estimated total porosity versus depth in the Sparta sand..	58
Figure 9.2-1.	a) Dominant geochemical signature index map, and b) piper diagram.....	62
Figure 9.5-1.	Total dissolved solids concentration versus specific conductance for Texas Department of Health lab (red) and all other labs (blue).	66
Figure 9.6-1.	Total dissolved solids-specific conductance relationship.....	67
Figure 10.2-1.	Geophysical log for BRACS Well ID 88437 in Trinity county.	71
Figure 10.4-1.	Measured and calculated water quality results with final total dissolved solids concentration (TDS) contours.	78
Figure 10.4-2.	Salinity zones in the study area.....	79
Figure 11-1.	Schematic image showing the difference between unconfined and confined aquifer storage	81

List of tables

Table 1-1.	Total brackish storage volume in the East Sparta aquifer per salinity class (in millions of acre-feet).....	4
Table 2-1.	Groundwater salinity classification used in the study (modified from Winslow and Kister, 1956).	6
Table 4.1-1.	Public water supply systems utilizing the East Sparta aquifer.....	15
Table 6-1.	Simplified stratigraphic column (modified from Baker, 1994).	23
Table 6-2.	Geological formation map-unit symbol labels for Figure 6-1.....	25
Table 7-1.	Stratigraphic units in the study area	30
Table 8.2-1.	Summary of aquifer test data.....	50
Table 9.3-1.	Water quality summary. All units are milligrams per liter, unless otherwise specified.	64

Table 9.4-1. Radionuclide sample results from the Sparta Aquifer exceeding the maximum contaminant level.....	64
Table 9.6-1. East Sparta aquifer total dissolved solids concentration and specific conductance regression summary.....	67
Table 10.1-1. Summary of Sparta Formation well pairs in the study area.....	68
Table 10.2.2-1. Input parameters for the R_{wa} minimum method.....	72
Table 10.2.2-2. Summary of study-wide variables needed to calculate salinity.....	72
Table 10.3-1. Comparison of total dissolved solids concentration (TDS) estimates in both studies for wells with different salinity classifications.	76
Table 10.3-2. Comparison of study parameters for total dissolved solids concentration calculations.	76
Table 11.5-1. Total brackish storage volume in the East Sparta aquifer per salinity class (in millions of acre-feet).....	85
Table 11.5-2. Total brackish storage volume (in acre-feet) of the East Sparta aquifer in each groundwater management area (GMA) by salinity class.....	85
Table 11.5-3. Total brackish storage volume (in acre-feet) of the East Sparta aquifer in each regional water planning area (RWPA) by salinity class.....	85
Table 11.5-4. Total brackish storage volume (in acre-feet) of the East Sparta aquifer in each groundwater conservation district (GCD) per salinity class.....	86

List of appendices

Appendix A. Public water supplies	A-1
Appendix B. BRACS Database.....	B-1
Appendix C. Geophysical logging tools.....	C-1
Appendix D. Comparison of stratigraphic interpretations.....	D-1
Appendix E. Geographic information system datasets	E-1
Appendix F. Porosity calculations	F-1
Appendix G. Modeled water quality data (PhreeqC).....	G-1
Appendix H. Calculation of groundwater volumes	H-1

1 Executive summary

The Texas Water Development Board (TWDB) Brackish Resources Aquifer Characterization System (BRACS) Program was established in 2009 to map and characterize the brackish portions of Texas aquifers to provide useful information and data to regional water planning groups and other entities interested in using brackish groundwater as a water supply. Both Texas industry and public water supply planners are looking at brackish groundwater to supplement stressed freshwater resources. Groundwater contains dissolved minerals, measured in units of milligrams per liter, and can be classified as fresh (0 to 1,000 milligrams per liter), brackish (1,000 to 10,000 milligrams per liter), or saline (greater than 10,000 milligrams per liter). Brackish groundwater is abundant in the state, currently estimated at more than 3.8 billion acre-feet, and is an important water supply component that can be used to meet future water demands. Groundwater desalination strategies in the 2022 State Water Plan represent additional new groundwater supply for nine of the regional planning groups (TWDB, 2023a). Development of these strategies create an additional supply volume of approximately 19,000 acre-feet per year estimated to be online by 2020, with an additional 157,000 acre-feet per year of groundwater recommended to be in service by 2070.

Program description

The goals of the BRACS Program are to 1) map and characterize the brackish parts of the major and minor aquifers of the state in greater detail using existing water well reports, geophysical well logs, and available aquifer data and 2) build datasets that can be used for groundwater exploration and replicable numerical groundwater flow models to estimate aquifer productivity. Since the program was created in 2009, the TWDB has completed 16 brackish aquifer studies; eight of these completed studies are contract reports. There are three ongoing studies, and six remaining aquifers that will need to be characterized by December 1, 2032. At the time of this report's publication, the three brackish aquifer studies currently in progress are 1) the Edwards-Trinity (Plateau) aquifer, 2) the East Queen City and Carrizo-Wilcox aquifers, and 3) the Woodbine Aquifer.

Study area

This report characterizes only the portion of the Sparta Aquifer located east of the Colorado River. The East Sparta aquifer study area includes all or part of 28 counties within the Upper Coastal Plains (Figure 1-1). The study area encompasses portions of regional water planning areas G, H, I, and K, and groundwater management areas 11, 12, 14, and 15. There are 14 groundwater conservation districts located within the East Sparta aquifer study area. The East Sparta aquifer study area includes the outcrop and extends approximately fifteen miles beyond the downdip extent of the official TWDB-designated Sparta Aquifer boundary. The width of the Sparta Formation outcrop ranges from one mile wide south of Bastrop County and ten miles wide in Houston and Anderson counties.

The predominant groundwater use of Sparta Aquifer groundwater is for domestic and livestock purposes, but the aquifer is also relied upon by municipal, industrial, and

irrigation users (George and others, 2011). Currently, there are 19 public water supply systems that have active wells completed in the East Sparta aquifer.

The 2022 State Water Plan includes a water management strategy to develop additional groundwater supplies from the Sparta Aquifer (TWDB, 2023a). This new water management strategy would provide 638 acre-feet per year of additional groundwater supply as a supplement to existing water supplies beyond 2030.

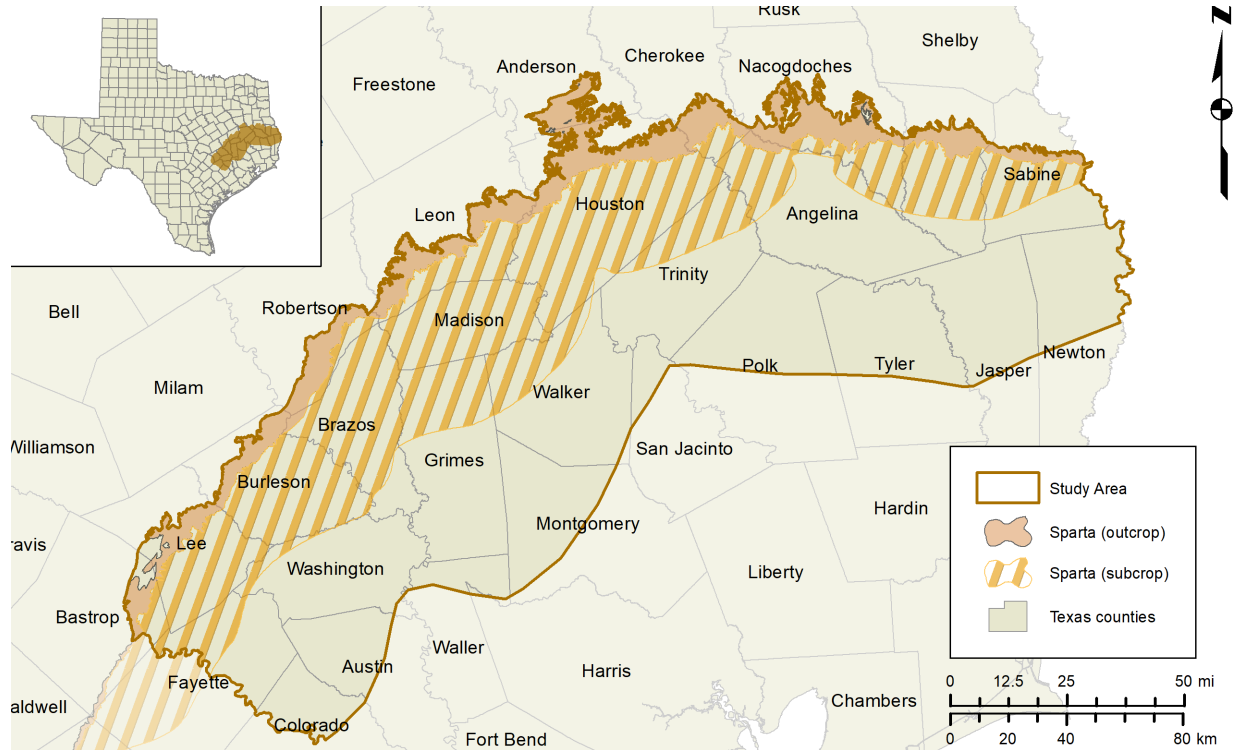


Figure 1-1. East Sparta aquifer study area.

Salinity distribution

A total of 426 wells were used for total dissolved solids concentration calculations. Figure 1-2 shows the salinity zones delineated at 1,000, 3,000, 10,000, and 35,000 milligrams per liter of total dissolved solids concentration.

The salinity distribution in Bastrop, Lee, and Fayette counties reflects reduced recharge within and downdip of a fault zone with large-offset faults where both measured and estimated total dissolved solids concentration values are slightly saline (1,000 to 3,000 milligrams per liter). The slightly saline portion of the aquifer extends approximately 25 miles downdip from the outcrop in this portion of the study area.

The distribution of moderately saline waters in the East Sparta study area encompasses a relatively wide swath of the Sparta Formation under Grimes, Montgomery, Walker, and Washington counties. A narrower band of moderately saline groundwater underlies Austin, Colorado, Trinity, Angelina, San Augustine, and Sabine counties.

The net sand thickness at the southern extent of the 10,000 milligrams per liter contour is less than 50 feet, and the assumption of nearly stagnant groundwater flow can be

attributed to the low sand content in this portion of the study area. The only portion of the study area that is classified as very saline is in Jasper, Newton, Sabine, and Tyler counties.

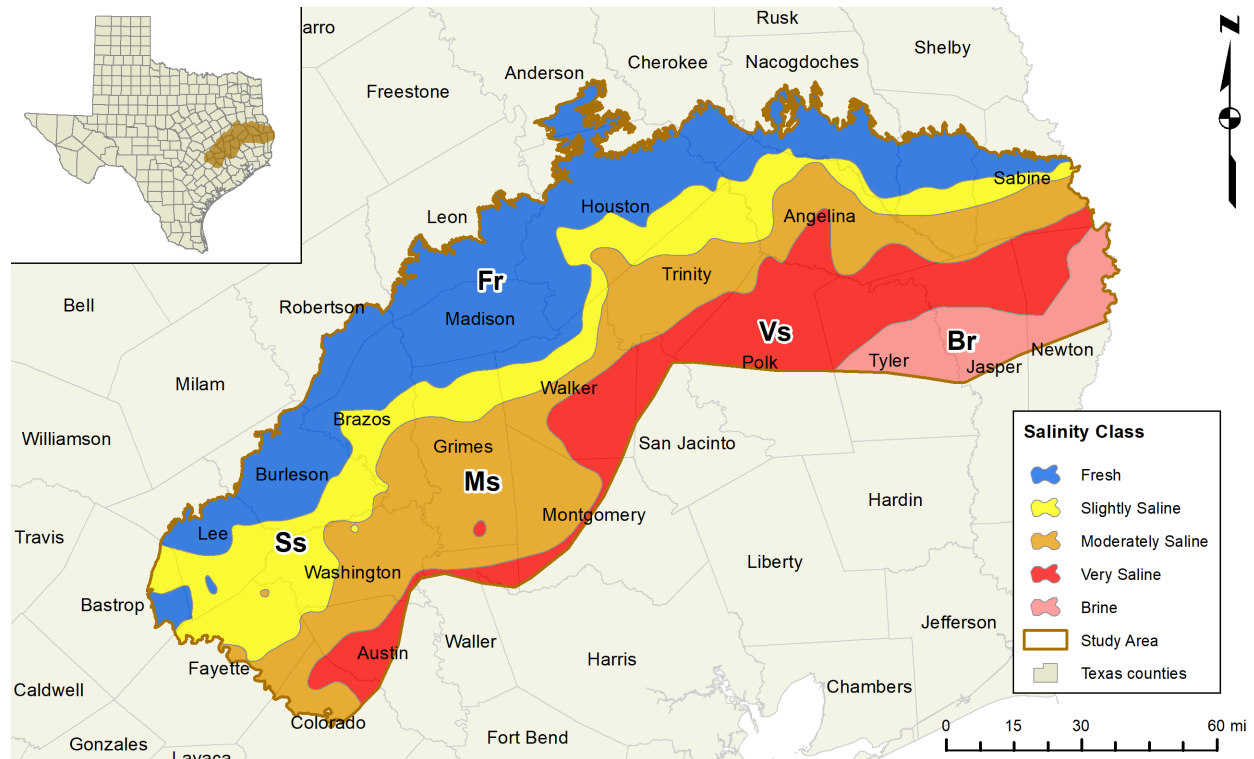


Figure 1-2. East Sparta aquifer salinity zones.

Brackish groundwater volumes

The East Sparta aquifer has a total brackish aquifer storage volume of approximately 50 million acre-feet of brackish groundwater with total dissolved solid concentrations between 1,000 and 9,999 milligrams per liter (Table 1-1). The total brackish aquifer storage volume is the sum of 22.2 and 27.8 million acre-feet of slightly saline and moderately saline groundwater, respectively.

The volumes calculated in this study are estimates to be used to provide insight into the magnitude and distribution of this important resource. We recommend that site-specific studies be conducted to support projects and efforts that will incorporate brackish groundwater resources into water resources planning. It is also important to note that these volume estimates are not the same as the TWDB-calculated total estimated recoverable storage (TERS) volumes, which are confined to the aquifer boundaries used by TWDB groundwater availability models. Furthermore, the area, saturated thickness, and storage parameters used in the calculations for this study are different from those used in TERS reports (Wade and others, 2014a, Wade and Shi, 2014b).

Not all brackish groundwater can be produced or economically developed. These volumes do not consider the effects of land surface subsidence, degradation of water quality, or any changes to surface water-groundwater interaction that may result from extracting groundwater from the aquifer. These volumes should not be used for joint planning or

evaluation of achieving adopted desired future conditions in the same way TERS and modeled available groundwater are used according to the joint planning process described in Texas Water Code § 36.108.

Table 1-1. Total brackish storage volume in the East Sparta aquifer per salinity class (in millions of acre-feet).

Salinity zone	Slightly saline	Moderately saline	Very saline	Brine	Total volume
Total	22.2	27.8	17.7	4.7	72.5

2 Introduction

Brackish groundwater was first mapped in Texas by the U.S. Geological Survey (Winslow and Kister, 1956). This study focused on identifying the occurrence, quantity, and quality of saline aquifers. Nearly two decades later, a Texas Water Development Board (TWDB) study performed a detailed analysis and inventory of the saline aquifers of Texas using a significant quantity of core data (Core Laboratories, 1972). In 2003, a contract study funded by the TWDB estimated that more than 2.5 billion acre-feet of brackish groundwater was available from Texas aquifers, providing a significant future groundwater supply option for regional water planning groups (LBG-Guyton & Associates, 2003).

In 2009, the 81st Texas Legislature initiated the creation of the TWDB Brackish Resources Aquifer Characterization System (BRACS) Program. The goals of the BRACS Program are to 1) map and characterize the brackish parts of the TWDB-designated major and minor aquifers of the state in greater detail using existing water well reports, geophysical well logs, and available aquifer data and 2) build datasets that can be used for both groundwater exploration and replicable numerical groundwater flow models to estimate aquifer productivity.

In 2015, the 84th Texas Legislature passed House Bill 30, which directed the TWDB to identify and designate local or regional brackish groundwater production zones in areas within the state that can be used to reduce the use of fresh groundwater. The TWDB designates official brackish groundwater production zones after evaluating the findings of a brackish aquifer study. House Bill 30 required the TWDB to complete all brackish aquifer studies by December 1, 2022.

In 2019, the 86th Legislature passed Senate Bill 1041, extending the deadline to complete zone designations from December 1, 2022 to December 1, 2032, and House Bill 722 that established a groundwater conservation district permitting framework for developing water supplies from TWDB-designated brackish groundwater production zones.

The TWDB has completed 16 brackish aquifer studies; eight of these completed studies are contract reports. There are three ongoing studies, and six remaining aquifers that will need to be characterized by December 1, 2032. At the time of this report's publication, the three brackish aquifer studies currently in progress are 1) the Edwards-Trinity (Plateau) aquifer, 2) the East Queen City and Carrizo-Wilcox aquifers, and 3) the Woodbine Aquifer.

Table 2-1 (Winslow and Kister, 1956) depicts five salinity classifications used by the TWDB BRACS Program:

- fresh (0–999 milligrams per liter);
- slightly saline (1,000–2,999 milligrams per liter);
- moderately saline (3,000–9,999 milligrams per liter);
- very saline (10,000–34,999 milligrams per liter);
- and brine (>35,000 milligrams per liter).

The term brackish water includes slightly and moderately saline waters (1,000–9,999 milligrams per liter of total dissolved solids concentration). Salinity class codes are used in the report discussion and tables, BRACS Database, and geographic information system file-naming scheme. Colors used in Table 2-1 for each salinity classification are consistent throughout the report and geographic information system datasets.

Table 2-1. Groundwater salinity classification used in the study (modified from Winslow and Kister, 1956).

Groundwater salinity classification	Salinity class code	Total dissolved solids concentration (milligrams per liter)
Fresh	Fr	0 to 999
Slightly saline	Ss	1,000 to 2,999
Moderately saline	Ms	3,000 to 9,999
Very saline	Vs	10,000 to 34,999
Brine	Br	Greater than 35,000

3 Project deliverables

This report discusses previous investigations, data collection and analysis, geology, stratigraphy, lithology, aquifer determination, aquifer properties, measured and calculated water quality, total estimated aquifer storage volumes, and desalination relative to the eastern portion of the Sparta Aquifer (East Sparta aquifer).

Datasets available with this study include:

- subsurface geophysical data,
- water well reports,
- stratigraphy and lithology interpretations based on these subsurface data,
- measured water quality data,
- calculated water salinity data,
- volumetric calculations, and
- all associated geographic information system datasets.

Only non-proprietary data is incorporated into this BRACS aquifer study. Data that is shared with the public by the TWDB will not include any data that is considered by law to be privileged or confidential.

This report, the public BRACS Database, the BRACS Database Data Dictionary (TWDB, 2023), and all geographic information system datasets are available for download from the TWDB BRACS website (TWDB, 2023b). Geophysical well logs are available upon request or can be downloaded from the TWDB Groundwater Data Viewer (TWDB, 2023g).

Information produced from these studies is not intended to serve as a substitute for site-specific evaluations of local aquifer characteristics and groundwater conditions for desalination projects. During design and development of a well field, an entity will need to determine the productivity of the brackish aquifer using monitoring and production wells and groundwater modeling. It is important to note that existing TWDB groundwater availability models are designed for regional assessment and are not applicable to well field analysis. These models are not constructed to analyze the effect of salinity on groundwater flow and in general should not be used for estimating saline water withdrawal. Other significant factors an entity should evaluate before developing brackish groundwater are groundwater quantity and quality changes and potential subsidence.

4 Study area

This report characterizes only the portion of the Sparta Aquifer located east of the Colorado River. The eastern portion of the Sparta Aquifer (East Sparta aquifer) study area investigated for this report is a subset of both the Upper Coastal Plains East study area designated by the TWDB BRACS Program (TWDB, 2023b) and the Texas coastal uplands designated by the U.S. Geological Survey (Hosman and Weiss, 1991).

The BRACS Program calls this physiographic province the Upper Coastal Plains of Texas (Hutchison and others, 2009). The U.S. Geological Survey's Texas coastal uplands aquifer system (Figure 4-1) includes the Yegua-Jackson, Sparta, Queen City, and Carrizo-Wilcox aquifers, in descending chronological order (Hosman and Weiss, 1991).

The eastern Upper Coastal Plains aquifers are relevant groundwater sources for regional water planning purposes in the 2022 Texas State Water Plan. Some water user groups within the Upper Coastal Plains East have indicated that slightly saline groundwater may provide a viable emergency water supply during times of drought (TWDB, 2023a).

The objectives of the study are to:

- collect, analyze, and interpret groundwater wells and geophysical well logs
- map the geological boundaries of the East Sparta aquifer and the bounding aquitards: Weches and Cook Mountain Formations
- map the distribution of total dissolved solids concentration in the East Sparta aquifer
- map the distribution of key chemical parameters of interest to desalination
- map the net sand distribution in the East Sparta aquifer
- estimate the volume of fresh and brackish water in the East Sparta aquifer
- incorporate all information into the publicly available BRACS Database and study geographic information system datasets, and
- present study findings in a peer-reviewed published report.

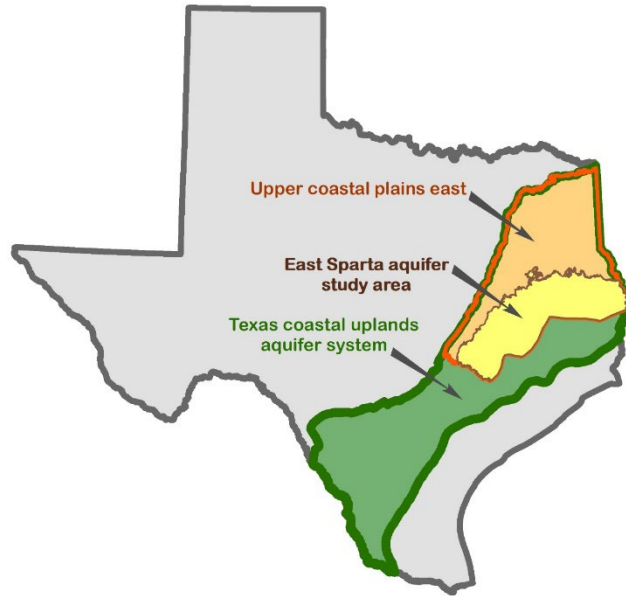


Figure 4-1. Study area nomenclature (modified from Hosman and Weiss, 1991 and TWDB, 2023b).

4.1 East Sparta aquifer study area

The East Sparta aquifer study area includes all or part of 28 counties within the Upper Coastal Plains. Major rivers that transect the East Sparta aquifer include the Sabine, Neches, Trinity, Brazos, and Colorado rivers (Figure 4.1-1).

The study area encompasses portions of regional water planning areas G, H, I, and K, and groundwater management areas 11, 12, 14, and 15 (Figure 4.1-2). There are 14 groundwater conservation districts located within the East Sparta aquifer study area. The East Sparta aquifer study area includes the outcrop and extends approximately fifteen miles beyond the downdip extent of the official TWDB-designated Sparta Aquifer boundary (Figure 4.1-3). The width of the Sparta Formation outcrop ranges from one mile wide south of Bastrop County and ten miles wide in Houston and Anderson counties. The outcrop of the Sparta Formation within the designated Sparta Aquifer boundary generally strikes from west-southwest to east-northeast across the study area.

The predominant groundwater use of Sparta Aquifer groundwater is for domestic and livestock purposes, but the aquifer is also relied upon by municipal, industrial, and irrigation users (George and others, 2011). Currently, there are 19 public water supply systems that have active wells completed in the East Sparta aquifer (Table 4.1-1 and Figure 4.1-4). For further information on all public supply systems in the study area, refer to Appendix A.

The 2022 State Water Plan includes a water management strategy to develop additional groundwater supplies from the Sparta Aquifer (TWDB, 2023a). This new water management strategy would provide 638 acre-feet per year of additional groundwater supply as a supplement existing water supplies beyond 2030.

The City of Bryan proposes using groundwater from twelve existing wells in the Sparta Aquifer and Simsboro Formation of the Carrizo-Wilcox Aquifer as the source water for a proposed aquifer storage and recovery project in the brackish portion of the Simsboro Formation of the Carrizo-Wilcox Aquifer (TWDB, 2023a). The City of College Station also has an ASR project in place to store treated wastewater effluent in both the Sparta and Queen City Aquifers.

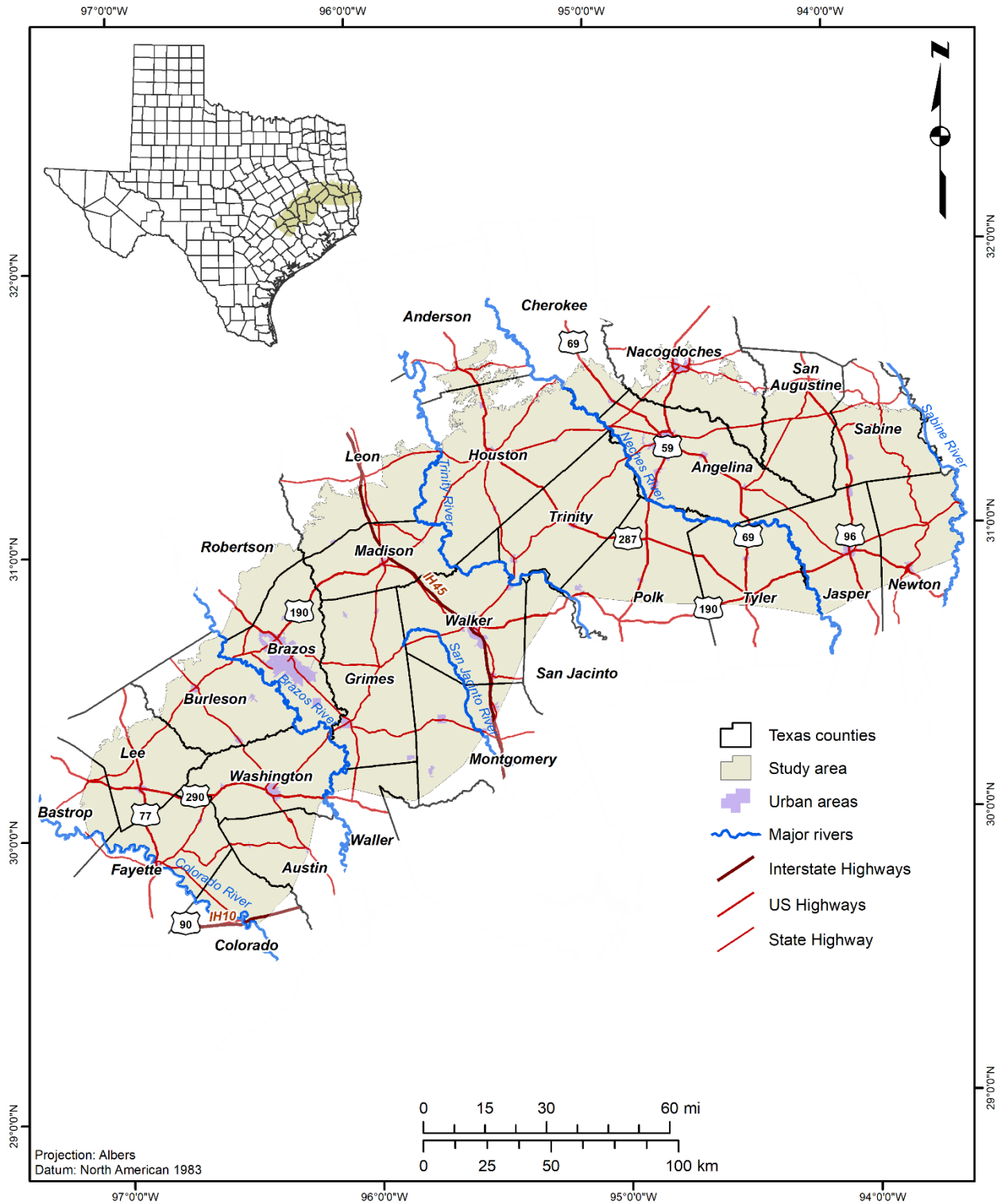


Figure 4.1-1. Location map of the East Sparta aquifer study area.

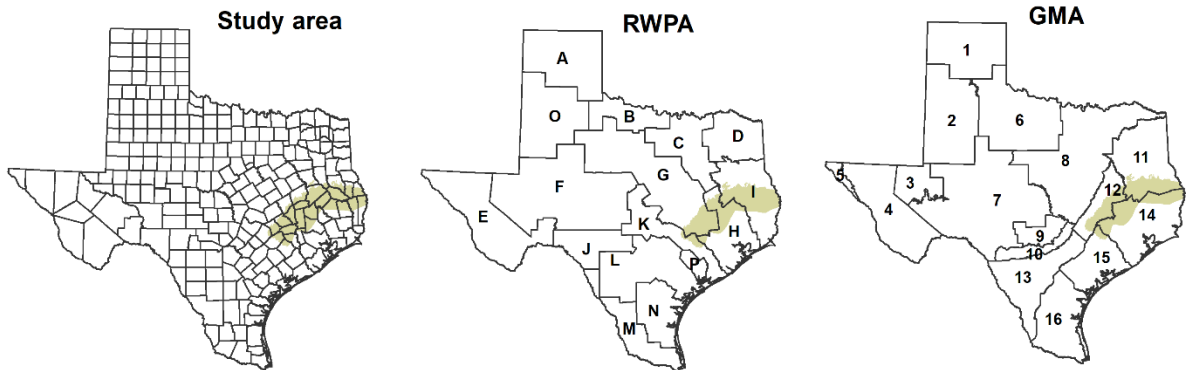
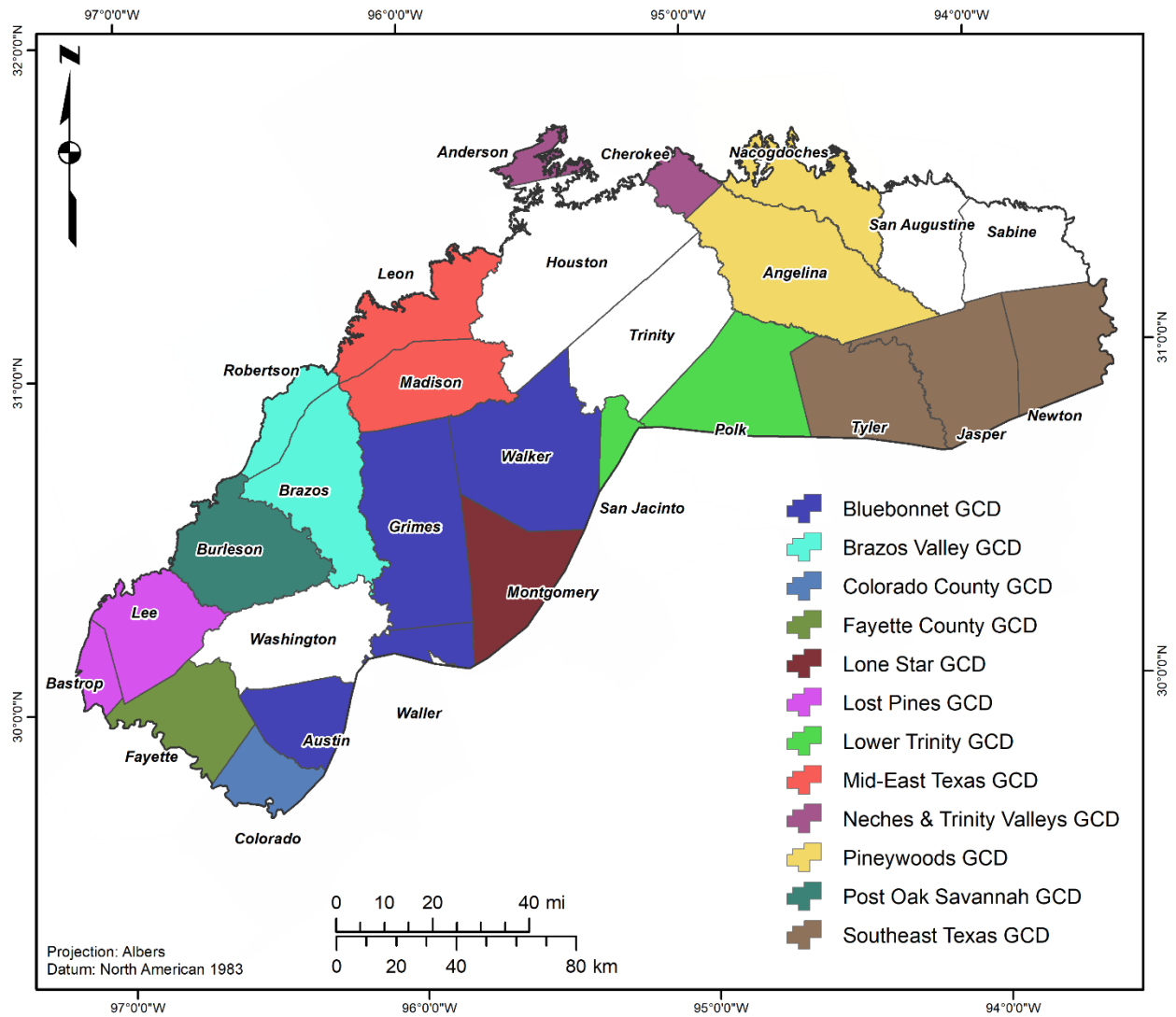


Figure 4.1-2. Administrative boundaries in the East Sparta aquifer study area.

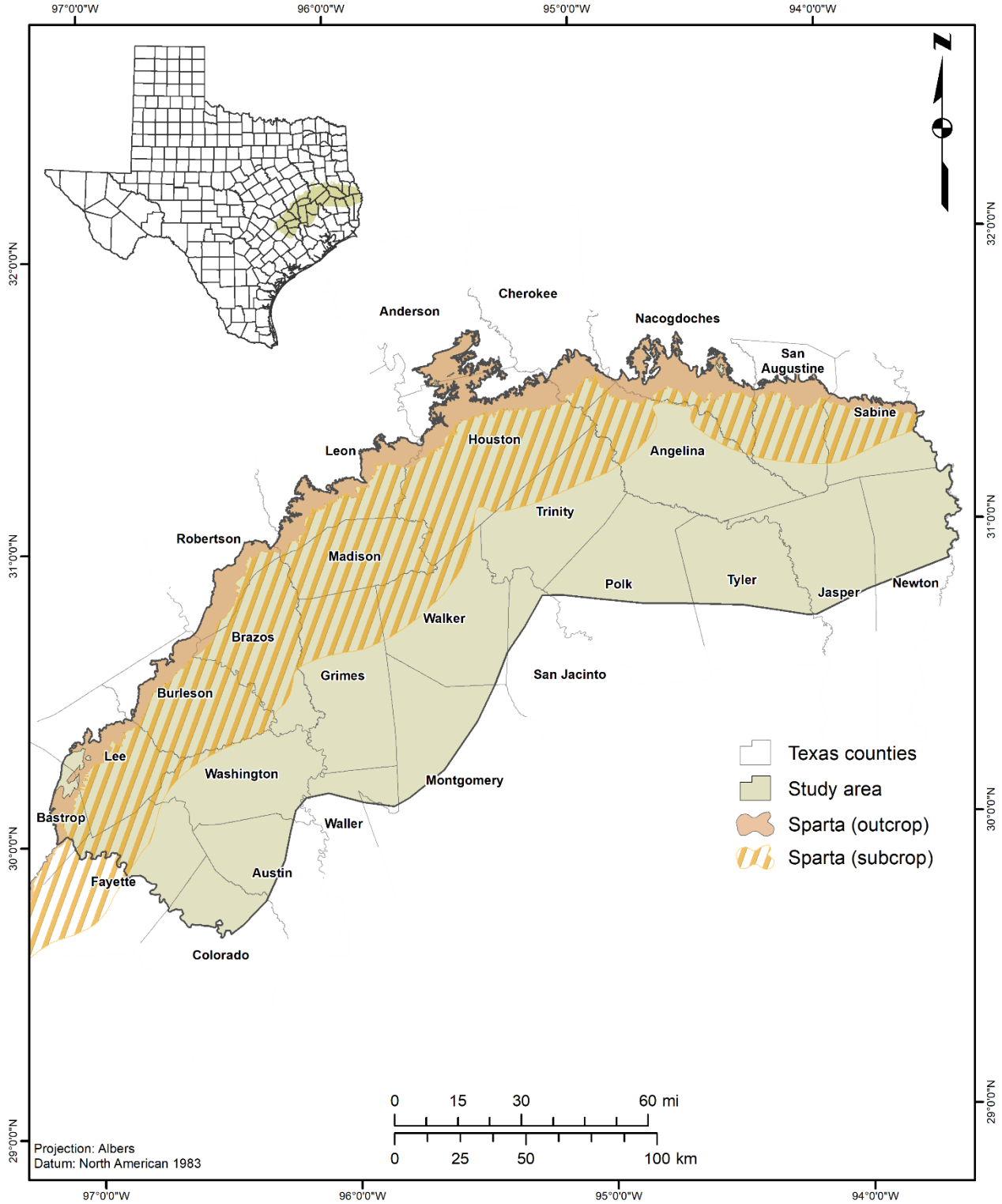


Figure 4.1-3. East Sparta aquifer study area.

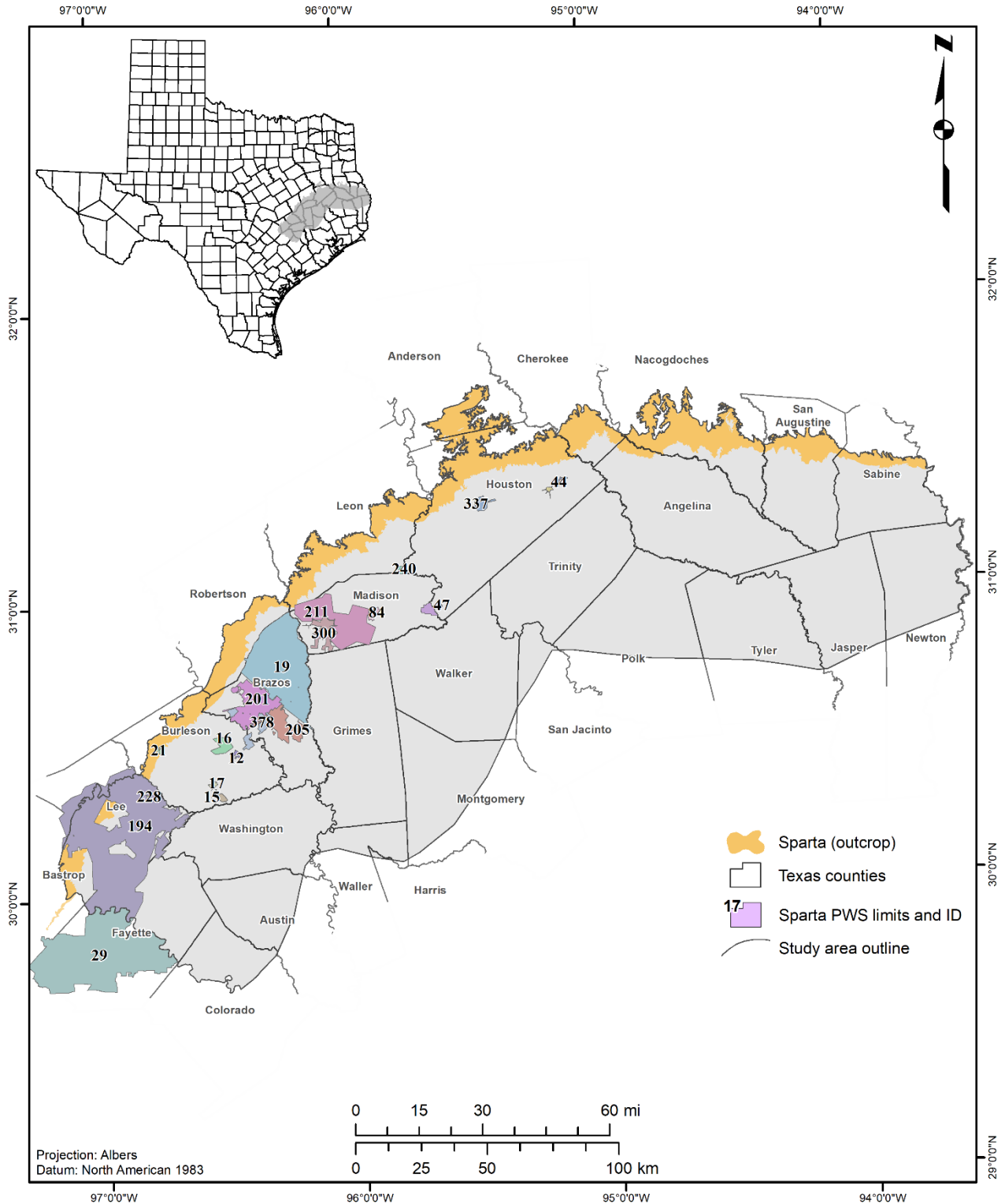


Figure 4.1-4. Public water supply system boundaries with Sparta wells in the East Sparta aquifer study area (data from TWDB Texas Water Service Boundary Viewer, 2023f).

Table 4.1-1. Public water supply systems utilizing the East Sparta aquifer.

Map ID	System ID	System name
12	0260017	City of Snook
15	0260022	Clara Hills Water System
16	0260018	Tunis Water Supply Corporation
17	0260015	Lyons Water Supply Corporation
19	0210005	Wickson Creek Special Utility District
21	0260007	Cade Lakes Water Supply Corporation
29	0750022	Fayette Water Supply Corporation West
44	1130020	Ratcliff Water Supply Corporation
47	1130004	Texas Department of Criminal Justice Eastham Unit
84	1570001	City of Madisonville
194	1570001	Lee County Water Supply Corporation
201	0210001	City of Bryan
205	0210002	City of College Station
211	1570018	High Prairie Water Supply Corporation
228	1440003	Lee County Fresh Water Supply District 1
240	1450017	River Oaks Sunshine Acres
300	1570004	North Zulch Municipal Utility District
302	1130011	City of Kennard
337	1130001	City of Crockett
344	0260002	City of Somerville
370	1570002	Texas Department of Criminal Justice Ferguson Unit
378	0210017	Texas A&M University Main Campus

4.2 Previous investigations

Regional studies with a focus on Sparta Formation depositional systems (Ricoy, 1976; Ricoy and Brown, 1977) and lithofacies (Payne, 1968) were the primary references used for this report. Ricoy’s publications focus on the Sparta Formation depositional environments and the transition of facies that are characteristic of deltaic systems. Ricoy also built geological cross sections based on geophysical logs and determined net sand thickness of Sparta Formation deposits in Texas. Ricoy and Brown (1977) detailed the depositional systems of the Sparta in the Gulf Coast basin of Texas. They defined three primary depositional systems within the area as 1) a high-constructive system in East Texas, 2) a strand plain-barrier bar system in Central Texas, and 3) a high-destructive delta system in South Texas.

Payne (1968; 1970) considered the hydrogeological significance of the Sparta Formation lithofacies and concluded that areas of higher transmissibility have lower concentrations of dissolved solids than areas of low transmissibility.

Other regional contributions include 1) a study of the Sabine Arch (Adams, 2009), 2) the tectonic map of Texas (Ewing, 1991), 3) salt deposition and deformation in the East Texas

Basin (Kreitler and others, 1980), 4) regional cross sections of the Gulf Coast (Baker, 1994), and 5) Lower Cretaceous deposition in East Texas (Bushaw, 1968). The regional cross sections by Baker were especially helpful in confirming formation thickness in and near the outcrop where they transected the study area.

Additionally, Hackley (2012) described the geology and elements of the petroleum system of the middle Eocene Claiborne group. Galloway (2000) wrote an extensive paper incorporating seismic lines to map and interpret Cenozoic fill of stratigraphic sequences of the Gulf of Mexico. The U.S. Geological Survey investigated the Tertiary and Quaternary hydrogeologic units of the Texas coastal uplands aquifer system as part of their Regional Aquifer-System Analysis program (Hosman and Weiss, 1991).

The TWDB published a brackish aquifer study (or BRACS study) for the Upper Coastal Plains in Central Texas (Meyer and others, 2020). This study characterized brackish groundwater zones of all the Upper Coastal Plains aquifers located to the immediate southwest of the East Sparta aquifer study area.

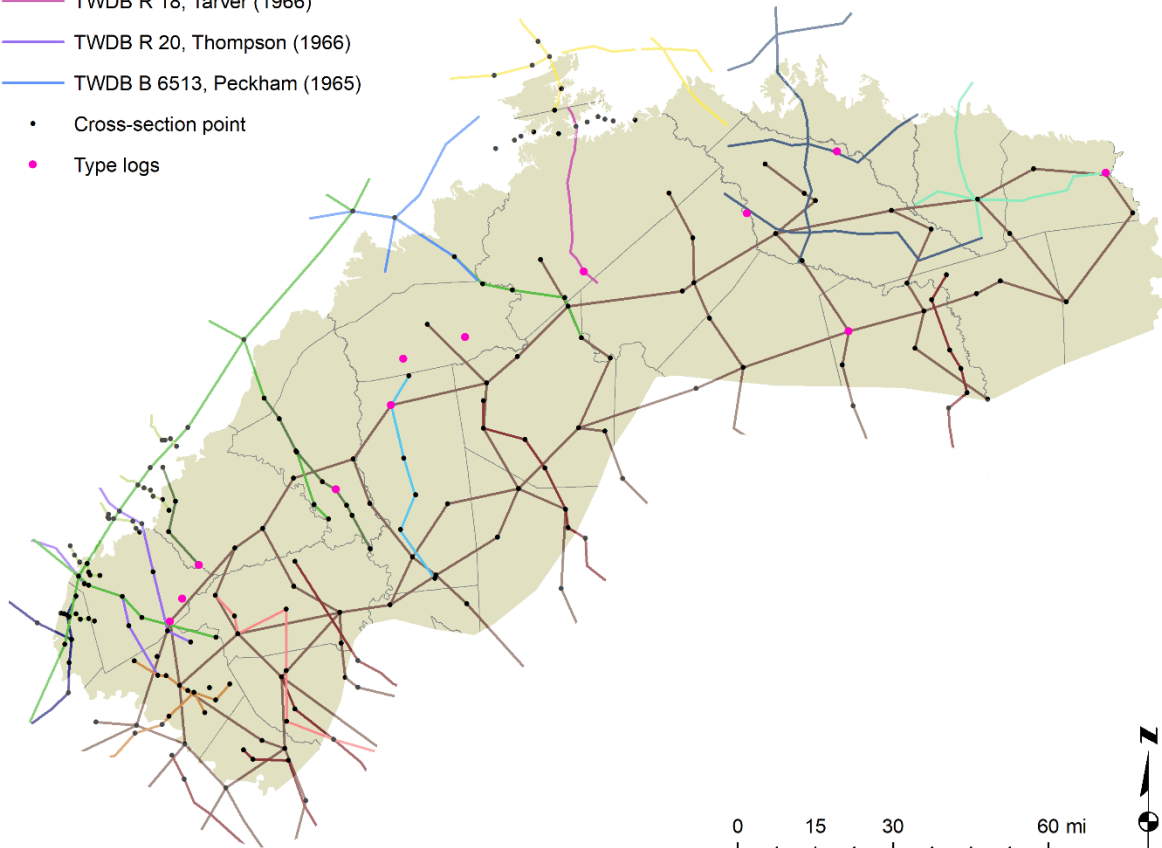
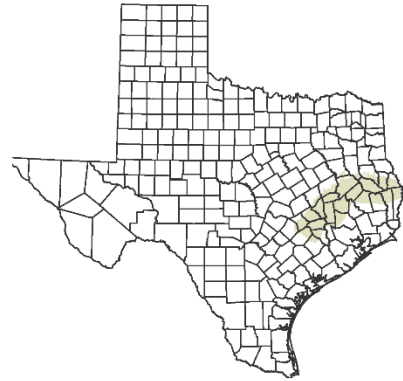
Groundwater availability model reports include 1) the Sparta and Queen City aquifers model report by Kelley and others (2004), 2) the groundwater availability model for the central portion of the Sparta, Queen City, and Carrizo-Wilcox aquifers (Young and others, 2018), and 3) the conceptual model for the northern portion of the Queen City, Sparta, and Carrizo-Wilcox aquifers (Schorr and others, 2020). These reports collectively characterize the geology, hydrogeology, and aquifer properties within the East Sparta aquifer study area. Additionally, numerous county-specific groundwater reports have been published for counties in the study area.

Published cross-section locations and data points have historically been incorporated into the BRACS Database to provide statewide control on geological interpretation from geophysical logs. These data are divided into two subsets and provided the initial stratigraphic framework for this study (Figure 4.2-1 and Figure 4.2-2). The estimated cross sections include at least one well location that was mapped with some degree of uncertainty.

Cross-section line

Report

- INTERA GMA 12 Faulting Study
- Intera Gulf Coast Aquifer Study, Young et al (2010)
- Yegua-Jackson Aquifer Report, Knox et al (2007)
- TWDB R 332, Thorkildson and Price (1991)
- TWDB R 236, Baker (1979)
- TWDB R 186, Baker et al (1974)
- TWDB R 185, Follett (1974)
- TWDB R 150, Guyton (1972)
- TWDB R 109, Follett (1970)
- TWDB R 110, Guyton (1970)
- TWDB R 37, Anders (1967)
- TWDB R 56, Rogers (1967)
- TWDB R 18, Tarver (1966)
- TWDB R 20, Thompson (1966)
- TWDB B 6513, Peckham (1965)
- Cross-section point
- Type logs



Projection: Albers
Datum: North American 1983

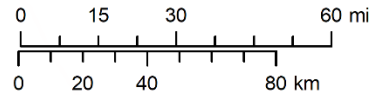


Figure 4.2-1. Published cross sections in the study area.

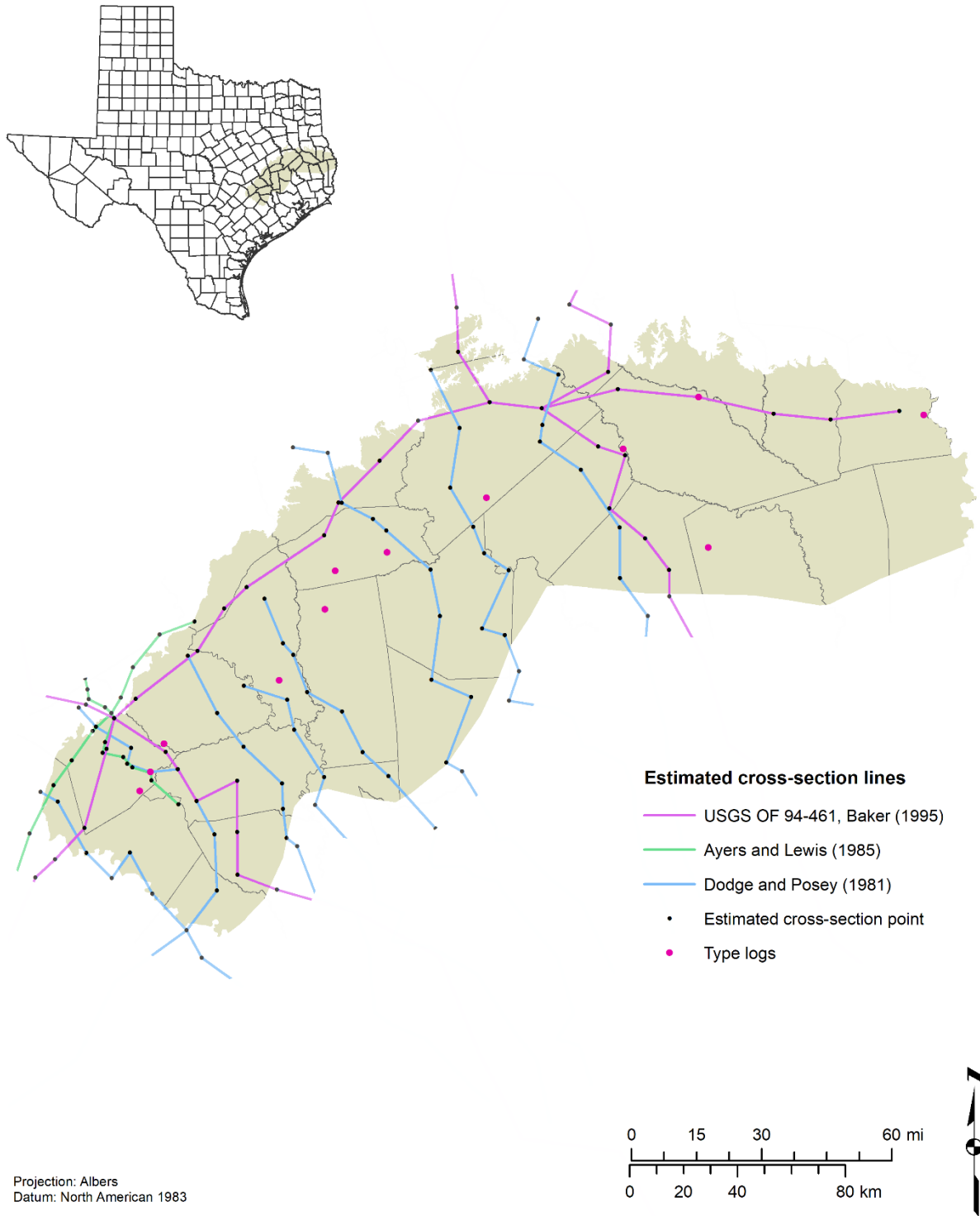


Figure 4.2-2. Estimated cross sections in the study area.

5 Data collection and analysis

Data collection is a significant component of all BRACS studies. Data used to characterize an aquifer during a BRACS study is added to the BRACS Database (TWDB, 2023c). New data were added during each project task, such as stratigraphy, lithology, and aquifer determination. Digital and physical geophysical well logs, water well reports, water geochemical datasets, and groundwater reports were all important sources of information for this study. A description of some of the main tables in the BRACS Database is included in Appendix B.

A typical BRACS study starts with gathering and reviewing previously published studies that are relevant and applicable to the study area. Subsurface data collection and analysis is an ongoing process during the study but is the primary focus after collecting published materials. These data are used to create stratigraphic surfaces and net sand maps of the formation(s) of interest.

5.1 Data sources

The Railroad Commission of Texas Groundwater Advisory Unit Q-log library was an important source of supplemental geophysical logs (RRC, 2021c). We located wells with unknown locations or improved existing well location accuracy using the Railroad Commission of Texas Original Texas Land Survey (RRC, 2023d) and geographic information system. Important supplemental databases and sources of well logs included the Texas Department of Licensing and Regulation Submitted Driller Reports Database (TDLR, 2023), the Underground Injection Control Database (RRC, 2023b), the Texas Commission on Environmental Quality Water Well Report Viewer (TCEQ, 2023b) for wells with assigned state well numbers that were originally filed as paper files, Public Water Supply Database (TCEQ, 2023a), geophysical logs from the U.S. Geological Survey GeoLog Locator (USGS, 2023a), and scanned geophysical logs provided by the Bureau of Economic Geology under a previous TWDB contract.

5.2 Data mining

Figure 5.2-1 shows well data coverage within the study. All well data that are not sourced from the TWDB Groundwater Database (TWDB, 2023e) are appended into the BRACS Database for future reference. Well control used for this study includes wells from both the TWDB Groundwater Database and the Submitted Driller Reports Database. Well control in the study area consists of 4,719 wells: 3,703 oil and gas wells, 944 water wells, and 72 wells classified as “other”. “Other” wells include wastewater disposal, observation wells, and an environmental soil boring.

A goal for BRACS studies is to build a geospatially dense well dataset for public use. To achieve this goal, we attempt to find at least one well drilled through the Sparta Formation within every 2.5-minute grid cell in the study area. Well locations are verified in ArcGIS 10.7®, using the Original Texas Land Survey and county linen maps from the Railroad Commission of Texas. We did not validate the location of every well that we obtained from other agency datasets unless there appeared to be a problem when interpreting geology.

In October 2020, the TWDB contracted work to process 19,163 well files from the TWDB unprocessed geophysical log collection for the entire BRACS Upper Coastal Plains East study area (Standen and others, 2021). Processing logs is a timely yet important procedure that involves checking the location of a well, denoting several foreign key markers that reference the source of information (like state well numbers), and inputting all pertinent information into the BRACS Database. This contract resulted in 11,102 new well records in the database while also improving 1,655 existing well records. The remaining logs were either duplicates that had been previously located in the database and contained no updates, or they were unmappable.

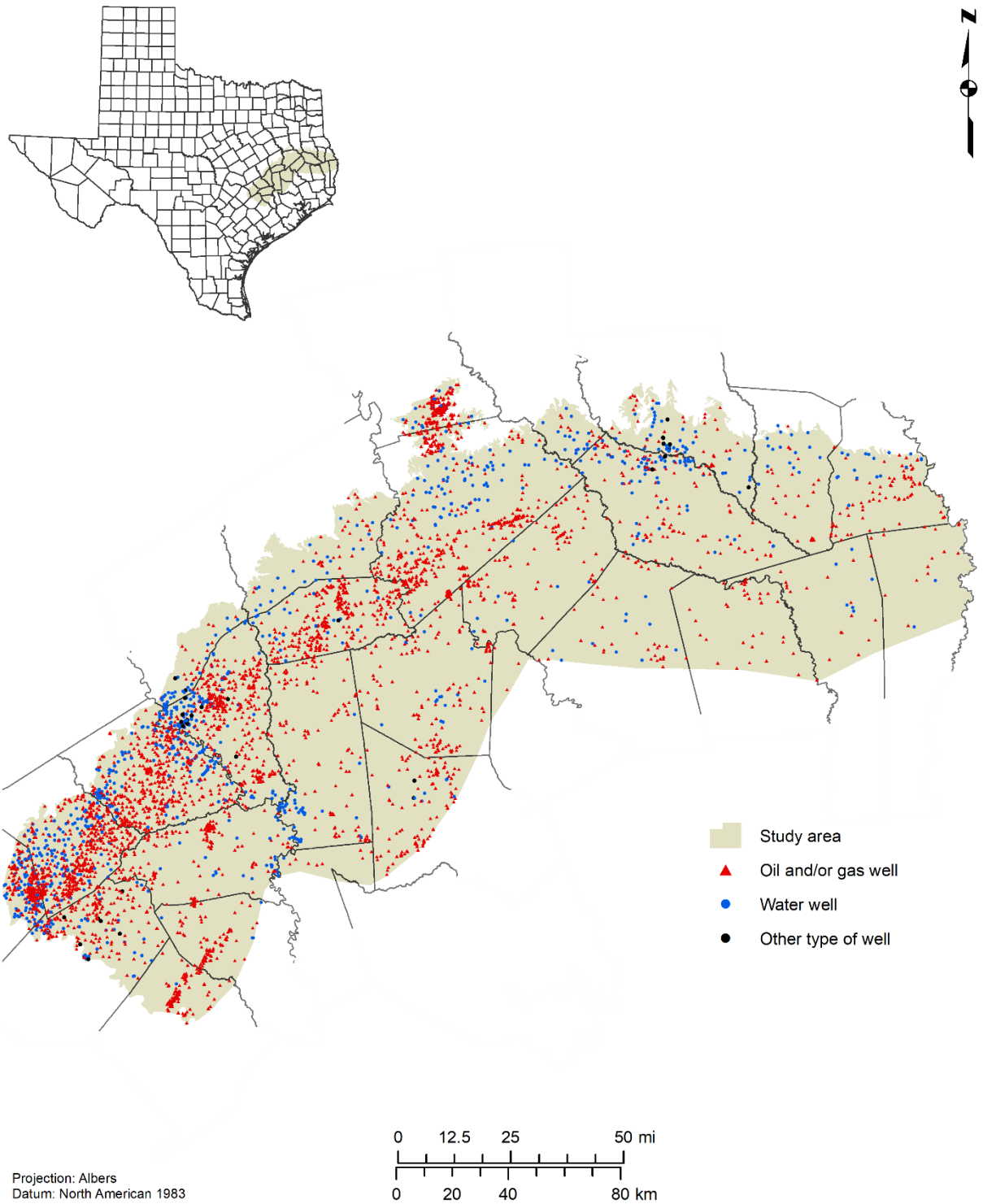


Figure 5.2-1. East Sparta aquifer study area well data locations.

5.3 Geophysical logs

Geophysical logs are used for stratigraphic, lithologic, and interpreted total dissolved solids concentration analyses. Each geophysical well log may have one or more tools used to record subsurface parameters. Appendix C contains a brief description of the log tools used in the study. Many geophysical logs have associated .xml files containing depth calibration data used for geological analysis in software such as IHS-Markit Kingdom®. We used depth-calibrating software developed by BRACS staff to edit geophysical log .tif files and to create .xml files. We depth calibrated 1,090 digital geophysical logs within the East Sparta aquifer study area. Stakeholders can contact the TWDB for instructions on accessing this data.

5.4 State well reports

Well reports from both the TWDB Groundwater Database and the Submitted Driller Reports Database record lithology descriptions, short-term aquifer test data, and water levels. The lithology descriptions are interpreted by BRACS staff and converted into a simplified and consistent nomenclature prior to the determination of sand thickness. For the East Sparta aquifer, the simplified lithology consists of five lithologic classifications: sand (100 percent sand), sand and clay (50 percent sand/50 percent clay), sand with clay (65 percent sand/35 percent clay), clay with sand (35 percent sand/65 percent clay), and clay (100 percent clay).

Aquifer test data are typically for short-term tests. Short-term aquifer tests usually have lower confidence levels than long-term tests that adequately stress the aquifer and provide both drawdown and recovery water level data. Although these are not as reliable as long-term aquifer tests, they are still valuable for reported well yields and specific capacity calculations (well yield volume per foot of drawdown) where no other data exists. Water level data from state well reports can be combined with water levels from the TWDB Groundwater Database to create a static water level elevation surface used for volume calculations.

Water well report data gathered by drillers are considered less accurate than water well data acquired from agencies such as the TWDB or the U.S. Geological Survey. Data submitted via state well reports are not screened for accuracy, whereas data from a government agency is typically reviewed more than once. The user of either data source is responsible for consideration of the data's reliability. Additionally, lithology descriptions are subjective and can be variable. However, water well report data is critical because it provides data where other subsurface data needed to characterize an aquifer is either sparse or non-existent. This data gap normally occurs within and immediately downdip from the outcrop primarily because surface casing in a well may extend through the aquifer of interest, resulting in geophysical logs that do not include data for the shallow subsurface.

6 Geology

The geological formations that outcrop within the East Sparta aquifer study area are primarily Tertiary terrigenous and marine sediments of the Claiborne, Jackson, and Vicksburg groups that were deposited within cyclic transgressive and regressive fluvial-deltaic and associated shallow marine sequences. These materials are overlain by Quaternary surficial alluvial materials (Table 6-1 and Figure 6-1).

Table 6-1. Simplified stratigraphic column (modified from Baker, 1994).

Era	System	Series	Group	Stratigraphic unit	Hydrogeologic unit	
Cenozoic	Quaternary	Holocene		Alluvium and terrace gravels	Gulf Coast Aquifer	
		Pleistocene				
	Tertiary	Pliocene		Goliad Sand		
		Miocene		Fleming Formation		
				Oakville Sandstone		
				Catahoula Sandstone		
		Oligocene	Vicksburg	Undivided	Yegua-Jackson Aquifer	
			Jackson	Undivided		
		Eocene		Yegua Formation		
		Eocene	Claiborne		Cook Mountain Formation	
					Sparta Formation	Sparta Aquifer
					Weches Formation	
				Queen City Sand	Queen City Aquifer	
				Reklaw Formation		
				Carrizo Sand	Carrizo-Wilcox Aquifer	
	Wilcox	Undivided				
Paleocene	Midway	Undivided				
Mesozoic	Cretaceous	Undivided				
	Jurassic					
	Triassic					
Paleozoic				Ouachita facies		

Overlying Formation

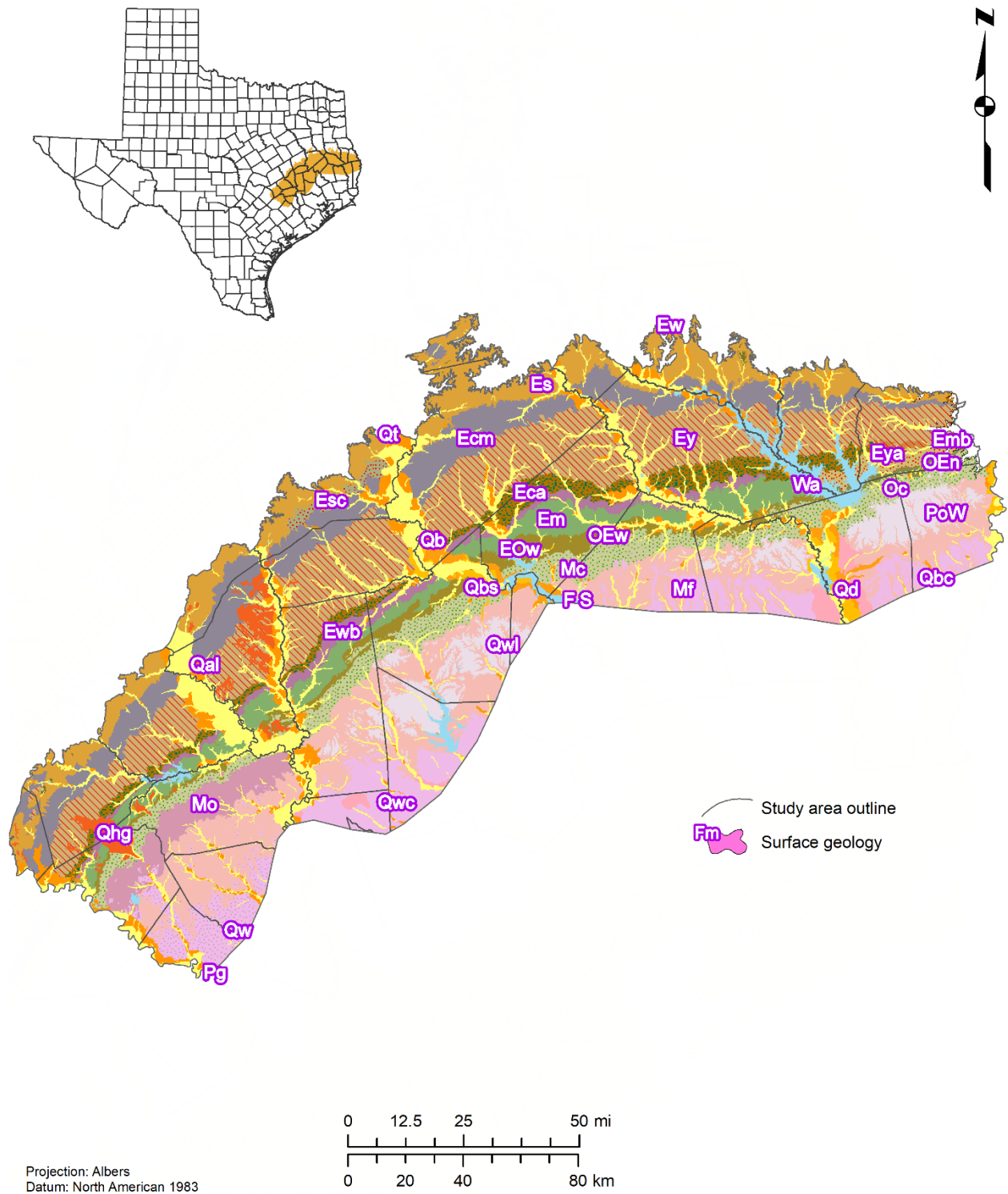





























Figure 6-1. Geological formations outcropping within the study area. Surface geology is based on the Geologic Atlas of Texas (TWDB, 2007). Refer to Table 6-2 for map-unit symbols.

Table 6-2. Geological formation map-unit symbol labels for Figure 6-1.

Symbol	Map-unit symbol	Geological formation name
	Qal	Alluvium
	Qd	Deweyville Formation
	Qt	Fluviatile terrace deposits
	Qhg	Gravel terrace deposits
	Qb or Qbs	Beaumont Formation or Beaumont Formation (sand)
	Qbc	Beaumont Formation (clay)
	Qw, PoW or Qwc	Willis Formation
	Qwl	Willis Formation (landward belt)
	Pg	Goliad Formation
	Mf	Fleming Formation
	Mo	Oakville Sandstone
	Mc or Oc	Catahoula Formation
	Eow or OEw	Whitsett Formation
	OEn	Nash Creek Formation
	Em	Manning Formation
	Ewb	Wellborn Formation
	Eya	Yazoo Formation
	Eca	Caddell Formation
	Emb	Moodys Branch Formation
	Ey	Yegua Formation
	Ecm	Cook Mountain Formation
	Esc	Stone City Formation
	Es	Sparta Sand
	Ew	Weches Formation
	OC	Marathon Limestone and Dagger Flat Sandstone members of the Ozarkian Group
	F S	Fill and Spoil material. Highly variable, mixed mud, silt, sand, and shell
	Wa	Water

6.1 Depositional history and setting

The Paleozoic Ouachita fold belt (Figure 6.1-1) defines the northwestern edge of the East Texas Embayment (Kreitler and others, 1980) and provides the basement for subsequent deposition of the overlying Mesozoic and Cenozoic strata (Figure 6.1-1). The fold belt, which underwent subsidence during the Mesozoic, also functioned as a structural hinge zone dividing fluvial deposition to the west and deltaic sequences to the east (Woodruff

and McBride, 1979). This zone is up to 40 miles wide and underlies the area between the Balcones and Luling-Mexia-Talco fault systems.

During the Late Triassic to Early Jurassic, rifting of the super-continent Pangaea formed the ancestral Gulf of Mexico. The Sabine Uplift (Figure 6.1-1) is a high-standing basement block that formed from rifting and transform faults associated with the formation of the Gulf of Mexico basin (Adams, 2009).

The Louann Salt was deposited during the Middle to Late Jurassic. Geological structure in East Texas is influenced by salt flow. Salt deformation and flow from areas of high to low pressure created salt domes, troughs (turtles), and ridges (pillows) that began forming during the Jurassic when differential pressure developed from the accumulation of overlying deposits. The East Texas and Houston Embayments were primary areas of deposition with sediment influx influenced by the topographic high of the Sabine Uplift to the east (Kreitler and others, 1980). Faulting was initiated by salt mobilization that occurred during the Mesozoic and early Tertiary. The Luling-Mexia-Talco fault zone generally aligns with the updip limit of the Louann Salt (Jackson and Wilson, 1982). The Mount Enterprise fault zone trends southwest to northeast between the Trinity River and the Sabine Uplift in Anderson, Cherokee, and Rusk counties.

During the early Cretaceous, rivers flowed to the southeast, and the Mount Enterprise fault zone was part of a distal alluvial plain (Kreitler and others, 1980). Conditions fluctuated back to a shallow marine setting by the middle of Glen Rose deposition and continued through the Eocene with cyclical deposition of terrigenous, and marine sediments positioned relative to a perpetually migrating fluvial-deltaic interface.

The Middle Eocene marked a relatively inactive tectonic period at the end of the Laramide Orogeny. Rivers drained the newly formed Laramide mountains located in the west, and created wide, sand-rich fluvial systems flowing eastward.

The Sparta Formation received comparatively less sediment and never reached the shelf margin in Texas, marking the termination of Laramide drainage into the Gulf of Mexico (Ewing, 1991). The influx of sediment was relatively low during the time of the Sparta Formation deposition compared to other episodes of Cenozoic deposition (Galloway, 2000), while primary drainage axes shifted from the southern Rockies eastward to the Mississippi Embayment. Runoff from the Sabine Uplift, a topographic high during deposition of the Sparta Formation, drained toward the Mississippi Embayment, resulting in a localized dearth of sediment influx between the southern edge of the uplift and the continental margin.

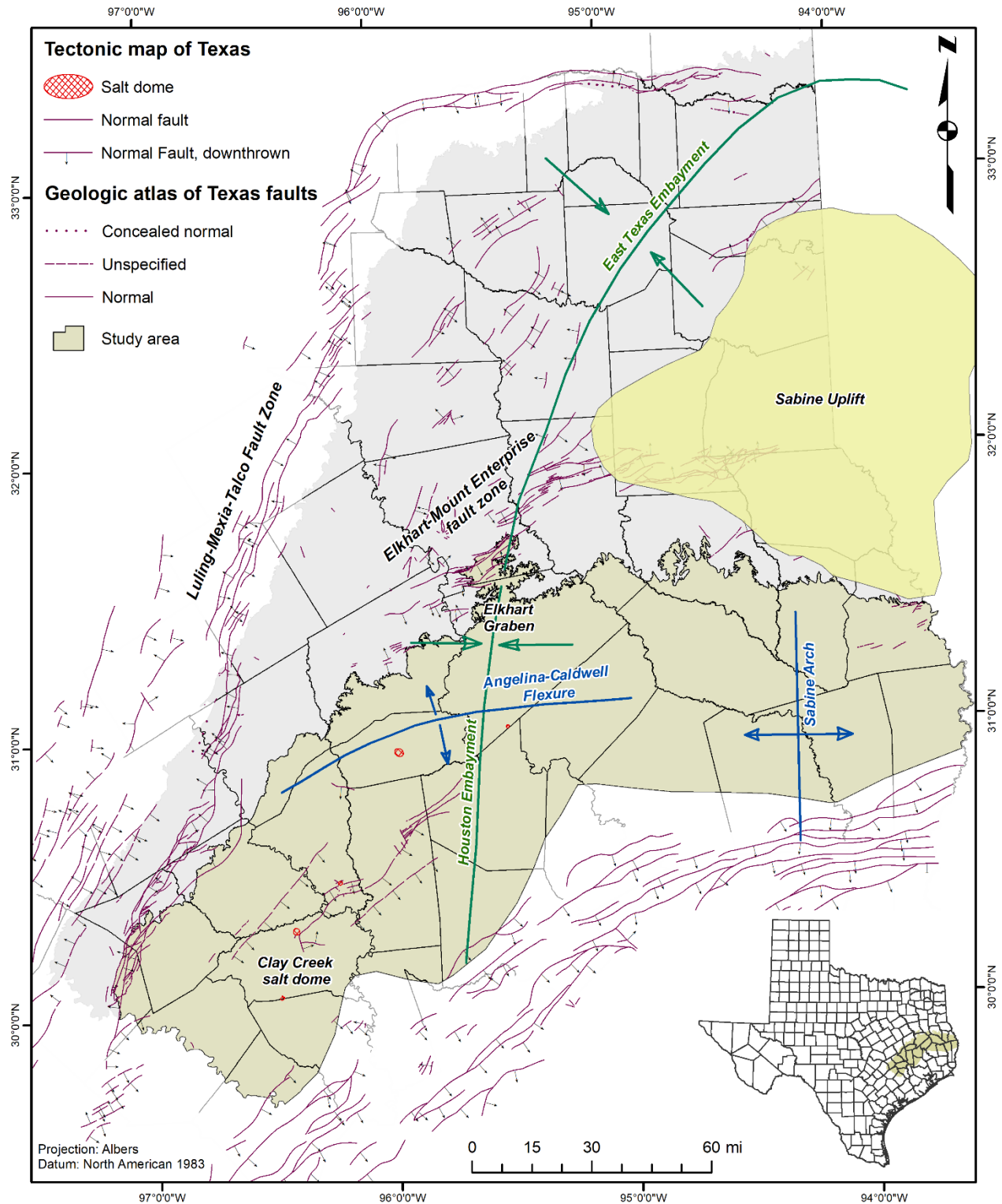


Figure 6.1-1. Structural components in the Upper Coastal Plains East area (modified from Schorr and others, 2018; Ewing, 1991; and TWDB, 2007).

6.2 Structure

The Coastal Plains are the portion of the Gulf of Mexico basin that is not inundated. The interior boundary of the Coastal Plains is generally defined by the Cretaceous formations located north and west of the Luling-Mexia-Talco fault zone (Dillard, 1963). The East Texas Embayment is the part of the Gulf Coastal Plain bounded by the Sabine Uplift to the east, the Luling-Mexia-Talco fault zone to the north and west, and the San Marcos Arch to the south and west (William F. Guyton & Associates, 1972). The Elkhart-Mount Enterprise fault zone divides the inner and shoreward portions of the Coastal Plain. The Angelina-Caldwell Flexure (a hinge line associated with Tertiary sediment loading near the Sabine Uplift) forms a low rim on the southern edge of the East Texas Embayment (Jackson and Wilson, 1982). The Houston Embayment is the southern extent of the East Texas Embayment located south of the Mount Enterprise fault zone (Figure 6.1-1).

6.3 Faults

Grabens of the Luling-Mexia-Talco fault zone formed because underlying salt caused basinward creep of the overlying formations, as illustrated in Figure 6.3-1 (Jackson and Wilson, 1982). The Mount Enterprise fault zone consists of parallel normal growth faults that are downthrown to the north and have no clear origin associated with salt structures, the nearby Angelina-Caldwell Flexure, or the Sabine Uplift (Figure 6.1-1). The Mount Enterprise growth fault is downthrown to the north, and displacement along the fault is approximately 700 feet near the surface and increases with depth. The base of the growth fault terminates at the top of the salt. The downthrow to the north is likely due to 1) the northward movement of formations overlying the Louann Salt, 2) loading due to sediments trapped on north side of fault scarp, and 3) subsequent extension via tensile stress. The Elkhart graben, located on the west end of the Mount Enterprise fault zone, is approximately 4 miles wide by 16 miles long. The central block is downthrown approximately 50 to 300 feet. The graben formed by deformation and collapse of salt (Jackson and Wilson, 1982).

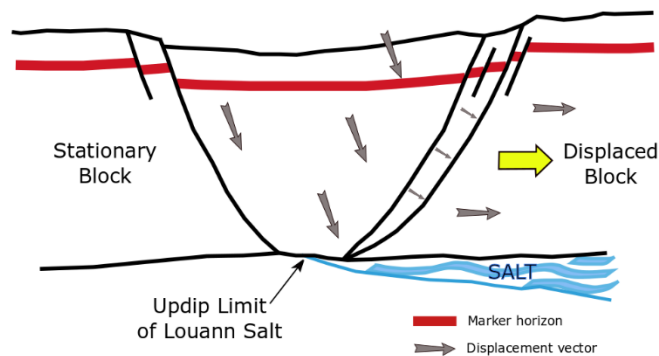


Figure 6.3-1. Graben formation via basin-ward creep in the Luling-Mexia-Talco fault zone (modified from Jackson and Wilson, 1982).

6.4 Salt domes

The East Texas basin, or embayment (Figure 6.1-1), formed during an episode of Triassic continental rifting and rapid fault-controlled subsidence (Jackson and Wilson, 1982). This resulted in the deposition of thick Triassic rift-basin fill, Jurassic evaporites, and Lower Cretaceous fluvial-deltaic deposits. Vertical salt movement caused the evolution of East Texas salt domes from low-amplitude salt pillows to diapirs (Seni and others, 1985). A regional cross-section of the East Texas Basin (Figure 6.4-1) shows five salt domes within the Upper Coastal Plains East area located in Wood, Smith, Anderson, and Houston counties. The Angelina-Caldwell Flexure intersects the cross-section in southern Houston County.

The only salt dome that pierces the Sparta Formation in the study area is the Clay Creek salt dome located in Washington County (Figure 6.1-1). A configuration of radial and cross-cutting faults that overlie the dome affects the Wilcox, Claiborne, and Jackson groups, which have been displaced upwards toward land surface and extensively faulted. The depth to the top of the dome is approximately 2,000 feet (Yin and Groshong, 2006). Based on information obtained from wells above the dome, Burress (1951) constructed a cross-section that shows thinning of the Sparta Formation toward the dome's center indicating that upward movement of the salt occurred simultaneously with the deposition of the sediments.

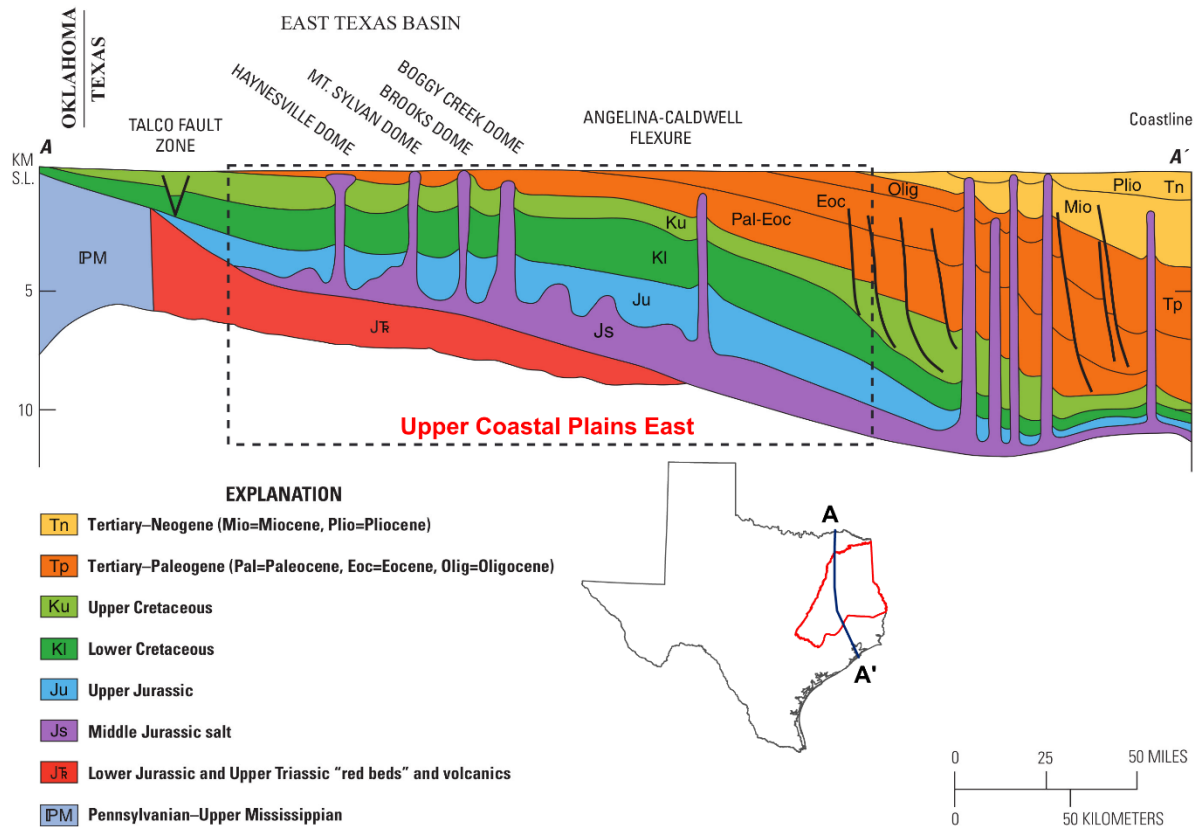


Figure 6.4-1. Regional cross section through the Upper Coastal Plains East (modified from Pearson, 2012).

7 Stratigraphy and lithology

The Sparta Formation is one of several fluvial-deltaic progradations deposited during the Eocene, consisting of terrigenous sand and mudstone interlayered between fossiliferous, glauconitic, marly shelf facies of the underlying Weches Formation and the overlying Cook Mountain Formation (Ricoy, 1976). Table 7-1 shows maximum thickness values for the penetrated formations, as determined from a strike-oriented cross section through the study area type logs.

Table 7-1. Stratigraphic units in the study area (modified from Payne, 1968 and Tarver, 1966).

Group	Stratigraphic unit	Description	Maximum thickness in study area (feet)
Not applicable	Alluvium	River flood plain and terrace deposits composed of gravel, sand, silt, and clay	80
Jackson	Undivided	Tan and red sand, calcareous white sand, and dark brown shale	540
	Yegua Formation	Composed of mostly sand, also sandy clay and clay, lignite common	850
	Cook Mountain Formation	Dark brown shale, some shale is lignitic and fossiliferous, marl, fine- to medium-grained partly gypsiferous sand, occasional limonite within sands, silty shale, iron concretions, some limestone lentils, and bentonite	470
	Sparta Formation	Gray to buff-colored sand, sandy shale and shale, medium-grained massive sand, fining upward to sandy shale, interbedded with clays, minor lignitic dark brown shale, basal contact is a disconformity	380
Claiborne	Weches Formation	Fossiliferous glauconitic marl, sand shale, limestone, with iron concretions and iron-cemented sandstone, gray to dark brown clays, basal contact with Queen City is a disconformity	85
	Queen City Formation	Fine-grained to medium-grained micaceous sand, gray to tan, red immediately below the Weches, interbedded with dark brown sandy shale, occasionally lignitic, some crossbedding	500
	Reklaw Formation	Predominantly thin beds of chocolate-brown glauconitic or lignitic shale with a glauconitic basal sand, iron concretions common	350
	Carrizo Formation	Fine-grained to medium-grained, white to yellow, poorly cemented, massive sand interbedded with thin shale and sandy shale beds, red and cross-bedded near surface basal contact is an unconformity	240
Wilcox	Undivided	Gray green and reddish-brown clays and shales, occasional ignite, thin sands and sandy shales	~3,000
Midway	Undivided		~1,400

7.1 Depositional systems

The Sparta Formation is characterized by three unique depositional environments: a high-destructive wave-dominated delta system in South Texas, an inter-deltaic strand plain and barrier-bar system in Central Texas, and the high-constructive delta system in East Texas (Ricoy, 1976). Most of the study area is within the high-constructive delta system. The transition to the inter-deltaic strand plain system occurs near the northeast Bastrop County line and includes the entire study area within Bastrop County, the southern portion of Lee County, and the southern half of the study area within Fayette County.

The high-constructive delta facies primarily consist of delta plain sandstone and mudstone, delta-front sandstone, and pro-delta mudstone facies. The pro-delta mudstones thicken seaward and underlie the delta-front sands (Figure 7.1-1). East of Texas, the Sparta Formation is significantly thicker in Louisiana, Arkansas, and Mississippi. The Sparta Formation also thickens in northeastern Mexico to the south (Ricoy, 1976).

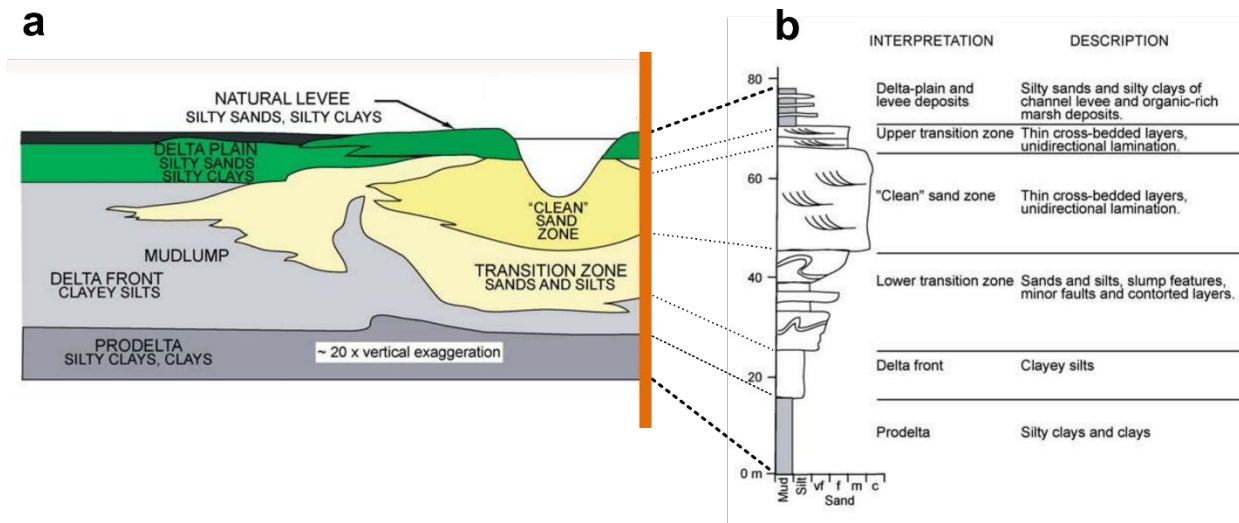


Figure 7.1-1. Sediment dispersal pattern in a constructive delta: a) deposition of delta-plain, delta-front, and prodelta deposits; b) vertical section through coarsening upward sequence of delta front deposits (modified from Olariu and Bhattacharya, 2006).

7.2 Type logs

Maintaining consistent stratigraphy across the study area is one of the challenges inherent to interpreting geological contacts on a regional scale. To facilitate consistency among staff members evaluating geophysical logs, representative type logs were selected by staff within their assigned counties. Ten type logs published in previous reports were identified in the study area (Figure 4.2-1 and Figure 4.2-2). Two additional type logs were added from the Q-log collection to fill in data gaps. Figure 7.2-1 shows a strike-oriented cross section through selected type logs constructed from Lee County to Sabine County to characterize the stratigraphy across the study area. The logs on this cross section were originally published in cross sections presented in TWDB groundwater resources reports for specific counties, including Lee, Brazos, Grimes, Houston, Angelina, and Sabine counties.

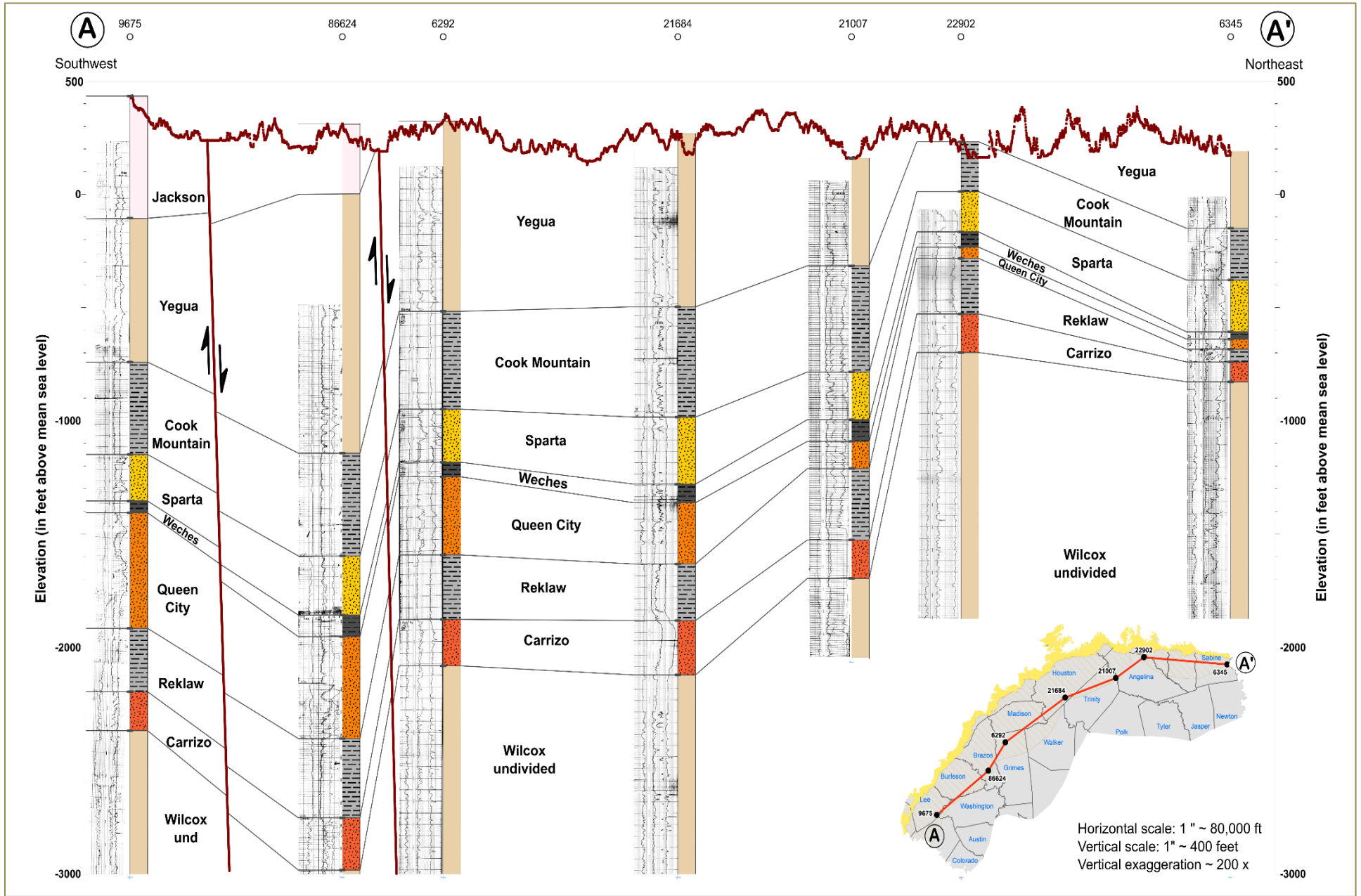


Figure 7.2-1. Strike-oriented cross section through study area type logs.

7.3 Stratigraphic interpretation

Water well reports, geophysical well logs, and published reports were the most important sources used to define the stratigraphic top and bottom of the Sparta Formation in the study area. Regional geologic maps and cross sections were used as a reference (Figure 7.3-3). We used the IHS-Markit Kingdom® geological software to interpret stratigraphic units in 621 geophysical well logs. This software uses depth-calibrated images of geophysical well logs and provides efficient tools for their visualization and interpretation.

Generally, there is less geophysical well log control near the geological formation outcrops due to the presence of well surface casings. There is also less well control at the downdip extent of the study area (southeast and southwest) due to fewer publicly available well logs, shallow well depths, and, in many cases, the deeper sections of well logs were truncated before they were submitted to the state. We used well control outside of the study area boundary to interpolate the geological formation raster surfaces to reduce edge-effect distortion and artifacts. For example, 12 geophysical logs located east of the study area in Sabine Parish, Louisiana were incorporated into the study area stratigraphic raster files to control the edge effect along the Texas-Louisiana state line.

We mapped the stratigraphic units in the subsurface primarily based upon geophysical well log characteristics. Because the Sparta Formation consists of interbedded layers of sand and clay, it can be differentiated from adjacent formations using a combination of geophysical well logs. Typical well logs used for stratigraphic analysis are the spontaneous potential, resistivity, and gamma ray (only available in 25 percent of the wells). Geophysical logging tools used in this study are described in Appendix C.

The example in Figure 7.3-1 demonstrates two gamma ray logs of wells located in Madison County (BRACS Well IDs 101630 and 101629). The interval from approximately 700 feet to 950 feet in Figure 7.3-1 illustrates low gamma ray readings of thicker sand intervals interspersed with moderate to high gamma ray readings representing thinner clay beds, which is a typical gamma ray response of the Sparta Formation in Madison County. The example in Figure 7.3-2 demonstrates spontaneous potential and resistivity logs of a well located in Washington County (BRACS Well ID 4637). On resistivity logs, the Sparta Formation is typically recorded as a distinct series of moderately high resistivity intervals of variable thickness. This well log signature contrasts sharply with low, even resistivity patterns of overlying and underlying formations in the central portion of the study area. Geophysical well logs described in this paragraph were not used for stratigraphic analysis.

We compared stratigraphic picks between this study, Ricoy (1976), and applicable groundwater availability models for the Sparta, Queen City, and Carrizo-Wilcox Aquifers. A summary of the results is included in Appendix D. Overall, this study picked shorter intervals, excluding the more subtle fining-upwards sequences occurring near the top of the Sparta Formation and the coarsening-upwards cycles occurring at the base of the Sparta Formation. Ricoy (1976) picked the longest intervals overall and included most of these sequences. Intervals from the groundwater availability models are a hybrid of these interpretations.

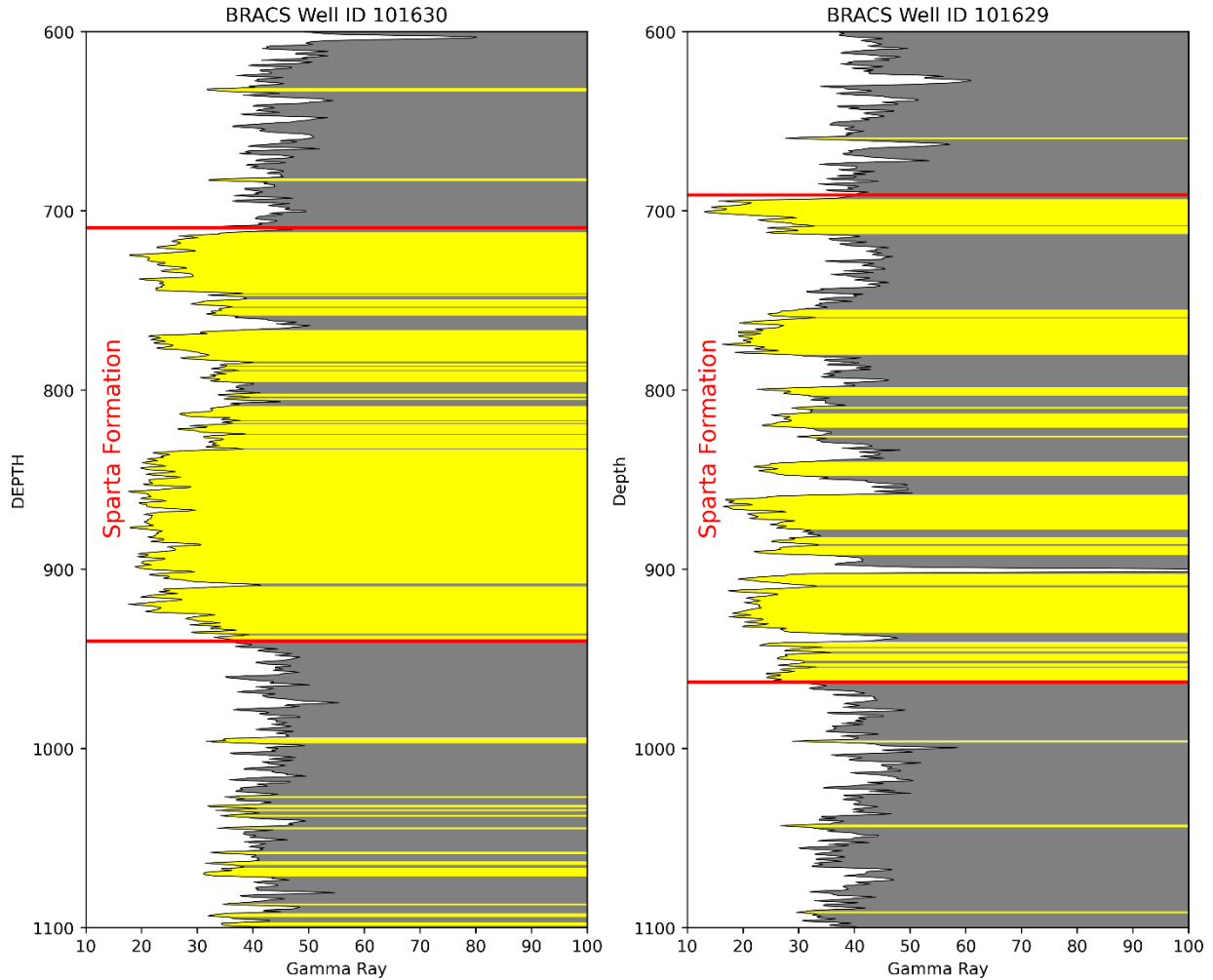


Figure 7.3-1. Gamma ray log plots of BRACS Well IDs 101630 and 101629 for the Sparta Formation in Madison County.

Figure 7.3-3 shows the correlation of five geophysical well logs within the study area using the cross-section feature of the IHS-Markit Kingdom® geological application software. These correlation examples are displayed so that the top of the Weches shale is set at the same level for all five wells. This is known as “flattening” and is frequently used for stratigraphic cross sections.

The stratigraphic top and bottom depths were appended to the geology table in the BRACS Database (tblWell_Geology). The top and bottom depths are based on the measured depth below the measuring datum for the geophysical well log, typically the kelly bushing or rig floor.

The stratigraphic picks were exported to a stratigraphic geographic information system shapefile using a study table (gBRACS_ST_UCPE) populated with a set of custom queries that corrected the depth and elevation values with the kelly bushing height and site elevation based on a statewide seamless 30-meter digital elevation model.

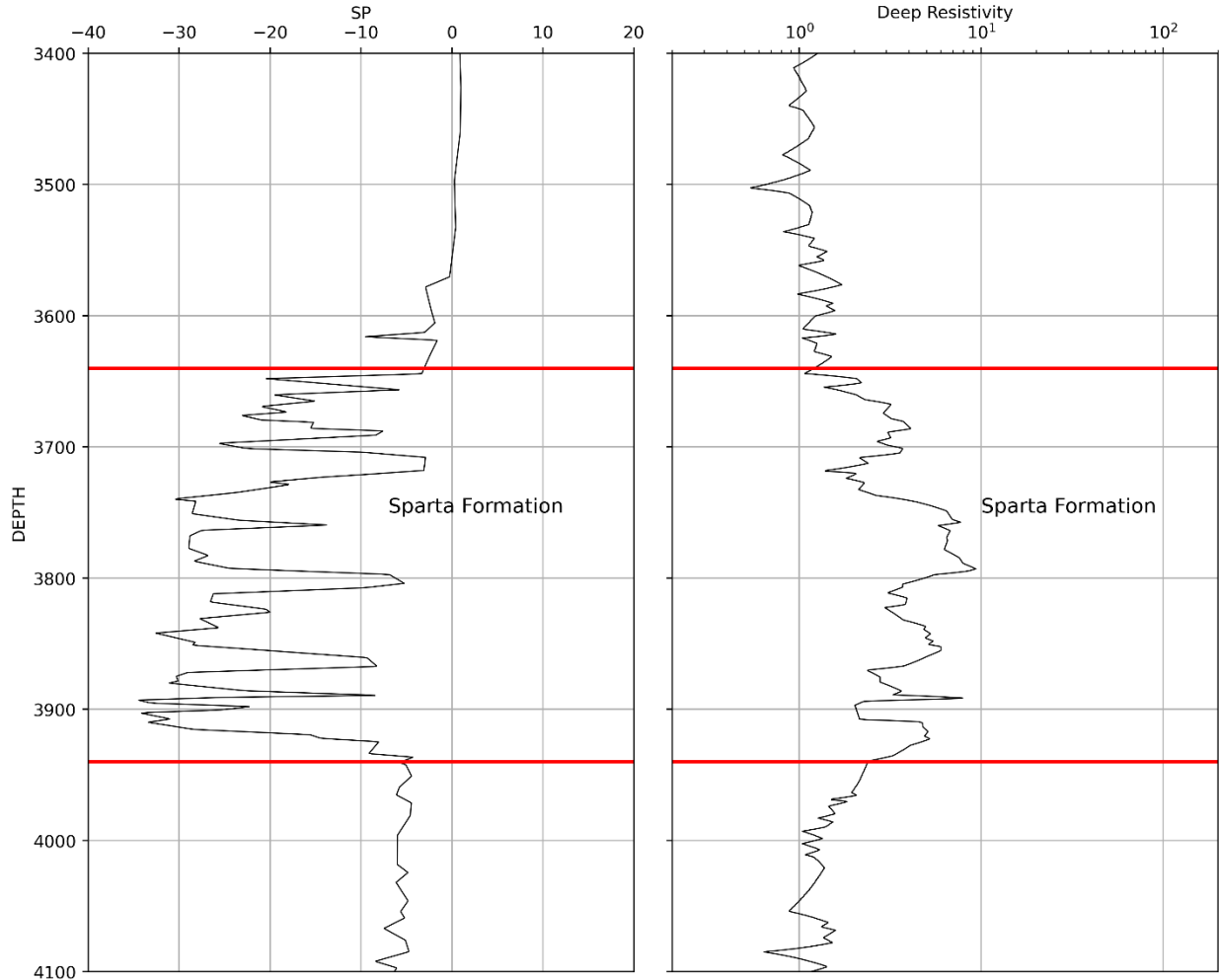


Figure 7.3-2. Spontaneous potential and resistivity logs of BRACS Well ID 4637 for the Sparta Formation in Washington County.

The database table (gBRACS_ST_UCPE) is provided as a study deliverable in the BRACS Database and a table description is provided in the BRACS Database Data Dictionary (TWDB, 2023). The stratigraphic geographic information system shapefile is provided as a study deliverable with metadata (Appendix E).

We prepared top and bottom elevation rasters for the Sparta Formation using stratigraphic picks from a total of 633 and 621 wells, respectively. Wells are located within the study area in addition to some wells located immediately outside of the study area to control raster edge effect. The interpolated elevation rasters were reviewed within the context of regional geological structure and depositional environments for irregularities. Anomalies that resulted from erroneous well locations or stratigraphic picks were updated, exported, and reinterpolated.

Additionally, five guide points were added after the first series of surfaces were created to guide interpolation through the stratigraphically complex area around Clay Creek salt

dome in northern Washington County where spatial density of well control is low. Top elevation values were assigned based on contour lines digitized from Sandeen (1972). Bottom elevation values were assigned using best professional judgement. The location and elevation of guide points used to interpolate rasters are provided in the geographic information system deliverables as point shapefiles.

Using the best available data to map the Sparta Formation surrounding the Clay Creek salt dome, we determined that there is no discernable impact of the salt dome on the Sparta Formation surfaces. We believe this to be an artifact of scale. With much less empirical data to define the formation near the salt dome, and the relative size of the potential dome peaking through the formation in relation to the regional scale of the study, the Sparta Formation appears to be unaffected. We recommend a localized study for those who are planning to drill near this dome.

Figure 7.3-4 and Figure 7.3-5 show the final structure maps for the top and bottom elevations of the Sparta Formation. They show overall smooth surfaces dipping gradually towards the southeast (at about 125 feet per mile). The formation dip increases with depth. The elevation of the top of the Sparta Formation ranges from 430 feet above mean sea level just to the south of the outcrop in Bastrop County to 7,409 feet below mean sea level in Montgomery County. Elevation to the base of the Sparta Formation ranges from 300 feet above mean sea level just to the south of the outcrop in Bastrop County to 7,569 feet below mean sea level in Montgomery County.

Figure 7.3-6 and Figure 7.3-7 show the Sparta Formation top and bottom depth maps, prepared using elevation rasters subtracted from the study area digital elevation model. The depth to the top of the Sparta Formation in the study area is between 0 feet in the outcrop and 7,620 feet in the southernmost part of the study area. The depth to the base ranges between 0 feet on the updip edge of the outcrop and 7,779 feet in the southern most part.

Figure 7.3-8 shows the Sparta Formation thickness, prepared using Raster Calculator in ArcGIS 10.7®, by subtracting the bottom elevation raster from the top elevation raster. The Sparta Formation thickness is approximately 100 feet thick in updip areas near the outcrop and increases to between 250 and 300 feet thick downdip. In the southwest part of the study area, the Sparta Formation appears thinner and varies in thickness from 100 feet updip to between 200 and 250 feet downdip. Depositional axes interpreted by Ricoy and Brown (1977) generally seem to align with areas of greater thickness. Additionally, each type of map has a standardized color ramp for ease of comparison between figures.

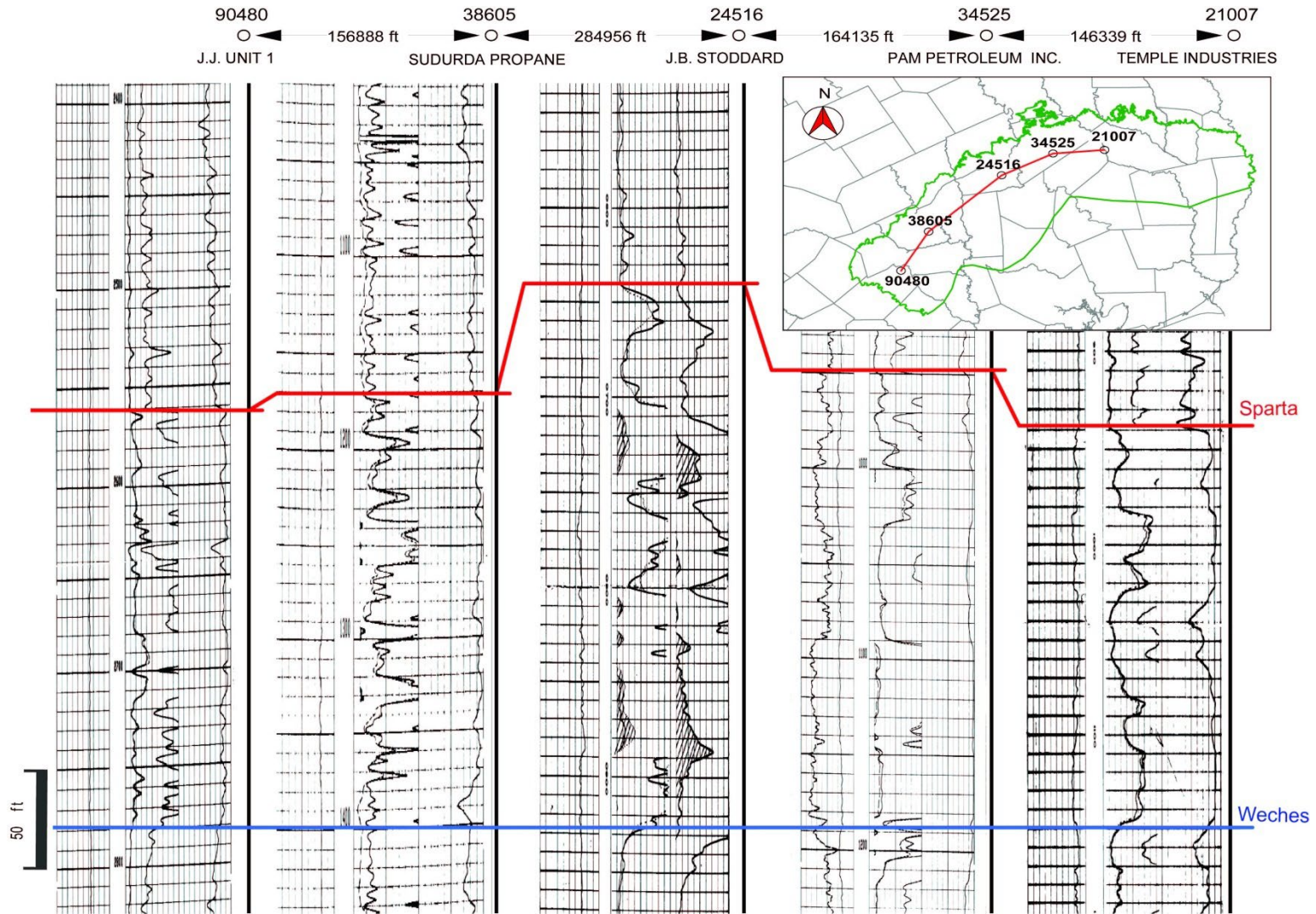


Figure 7.3-3. Correlation section showing stratigraphic interpretation of the Sparta Formation. Geophysical well logs flattened on the top of the Weches. Section orientation is southwest to northeast. Wells are in are in Fayette, Burleson, Madison, Houston, and Angelina counties (from left to right).

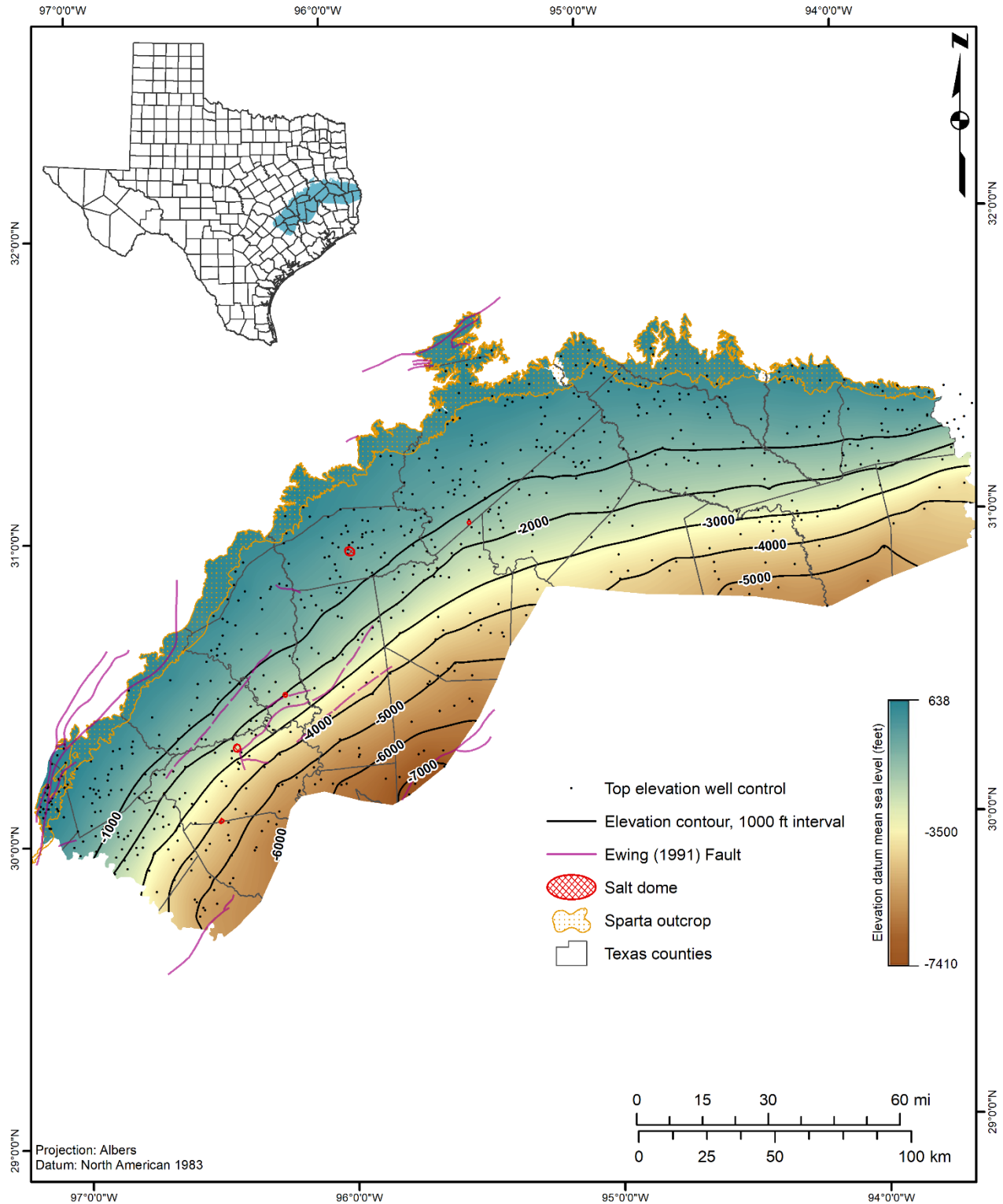


Figure 7.3-4. Sparta Formation top elevation in feet above mean sea level. Faults and salt domes modified from Ewing (1991), Jackson and Wilson (1982), and Seni and others (1985).

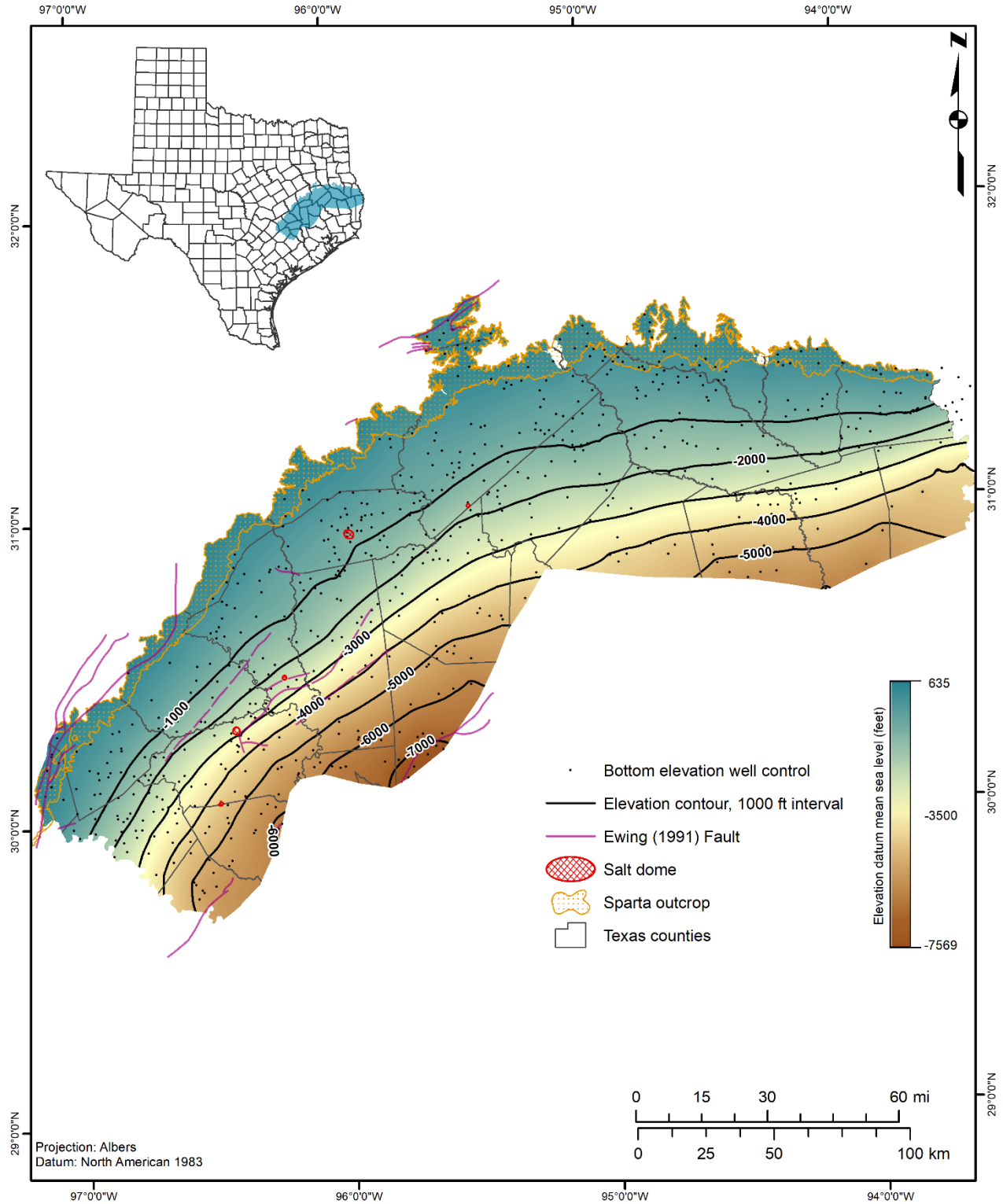


Figure 7.3-5. Sparta Formation bottom elevation in feet above mean sea level. Faults and salt domes modified from Ewing (1991), Jackson and Wilson (1982), and Seni and others (1985).

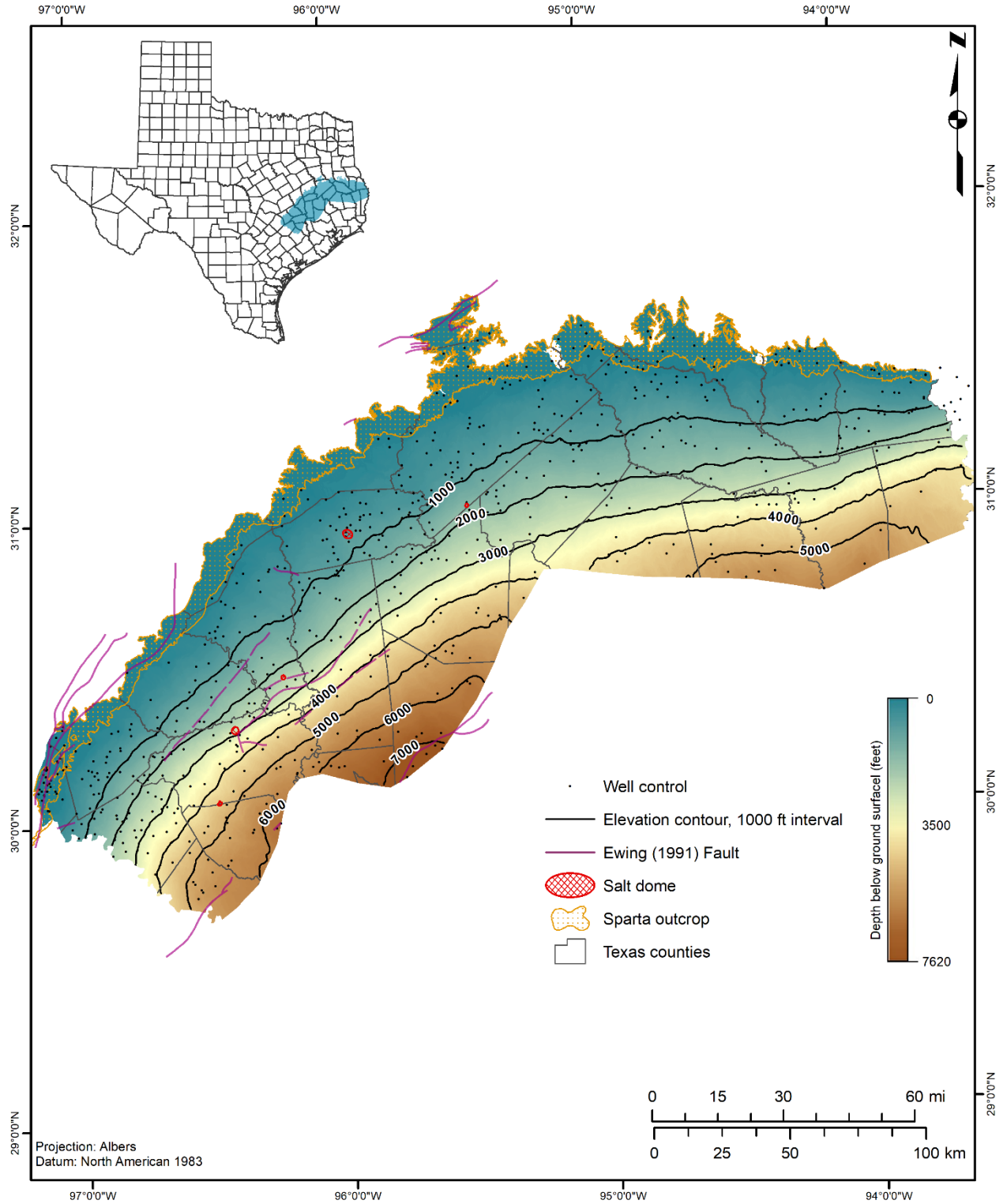


Figure 7.3-6. Sparta Formation top depth in feet below ground surface. Faults and salt domes modified from Ewing (1991), Jackson and Wilson (1982), and Seni and others (1985).

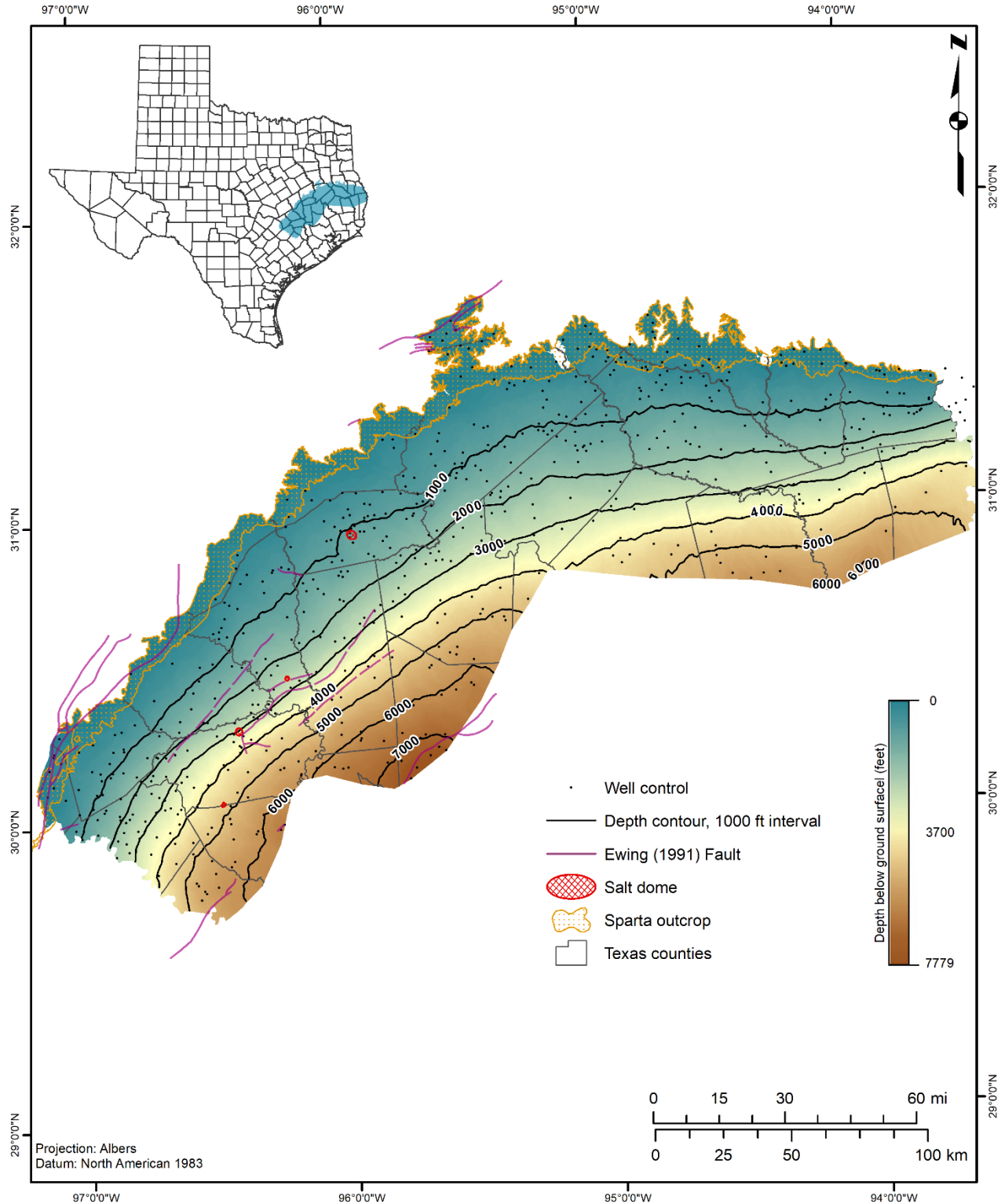


Figure 7.3-7. Sparta Formation bottom depth in feet below ground surface. Faults and salt domes modified from Ewing (1991), Jackson and Wilson (1982), and Seni and others (1985).

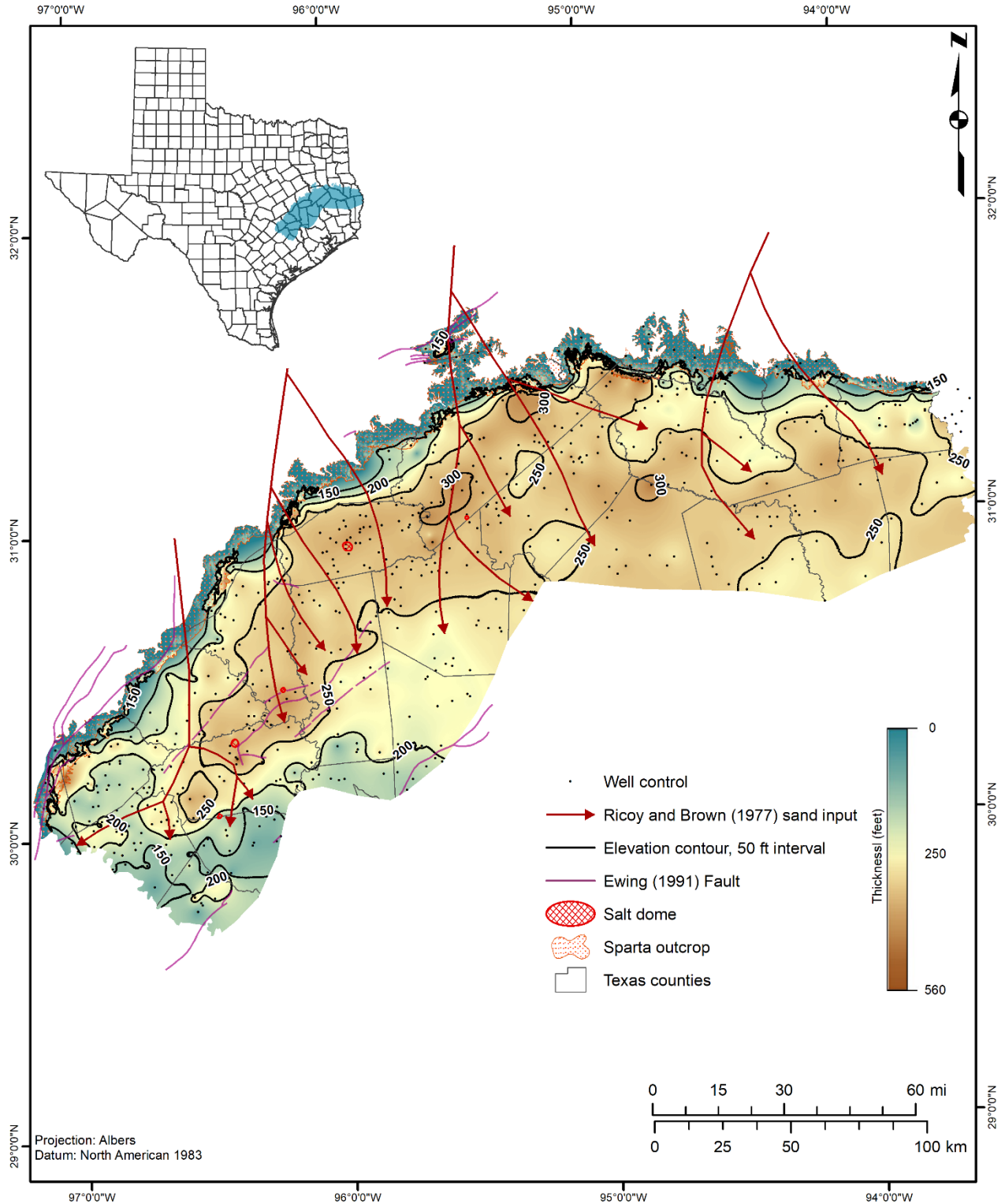


Figure 7.3-8. Sparta Formation thickness in feet. Faults and salt domes modified from Ewing (1991), Jackson and Wilson (1982), and Seni and others (1985).

7.4 Lithology

Formation lithology must be assessed before conducting a net sand analysis and calculating brackish groundwater volume. The Sparta Formation consists mainly of delta-deposited, interbedded layers of sand and clay. While both lithologies can contain groundwater, sand produces groundwater economically whereas clays tend to bind water in place depending on structure.

We used IHS-Markit Kingdom® software to make lithologic picks for geophysical well logs. We used a combination of resistivity tools, a spontaneous potential tool, and a gamma ray tool, where available, to interpret lithology from geophysical well logs (Figure 7.4-1). We evaluated geophysical well log lithology using a five-tier classification system for interpreting the clastic lithology, based either on spontaneous potential or gamma ray logs and induction or resistivity logs. BRACS custom Visual Basic for Applications® code was used to evaluate adjacent units to check for overlaps or gaps (missing sections). The code examines lithologic units to check for overlap and underlap between adjacent lithology records using the sequential record number. The unit contacts were then corrected manually to ensure continuous lithology within the Sparta Formation.

The five simplified classifications included sand (100 percent sand), sand and clay (50 percent sand/50 percent clay), sand with clay (65 percent sand/35 percent clay), clay with sand (35 percent sand/65 percent clay), and clay (100 percent clay). Percentages are approximate and are used to assign a numerical value that can indirectly represent total porosity, or the total void space of the rock.

Where we lacked geophysical log data, lithologic descriptions from drillers logs were simplified, and assigned a percent sand value described above. For example, “brown sandy clay” was assigned a “clay with sand” value (35 percent sand). A mixture of three or more textures or materials may have been reduced to two predominant lithologies. For example, “sand with clay and coal” was translated to a “sand with clay” value (65 percent sand). Percent sand was then multiplied by the thickness of the lithological unit, and then summed for each well, yielding a net sand value for that location. Net sand analysis is discussed further in Section 7.5.

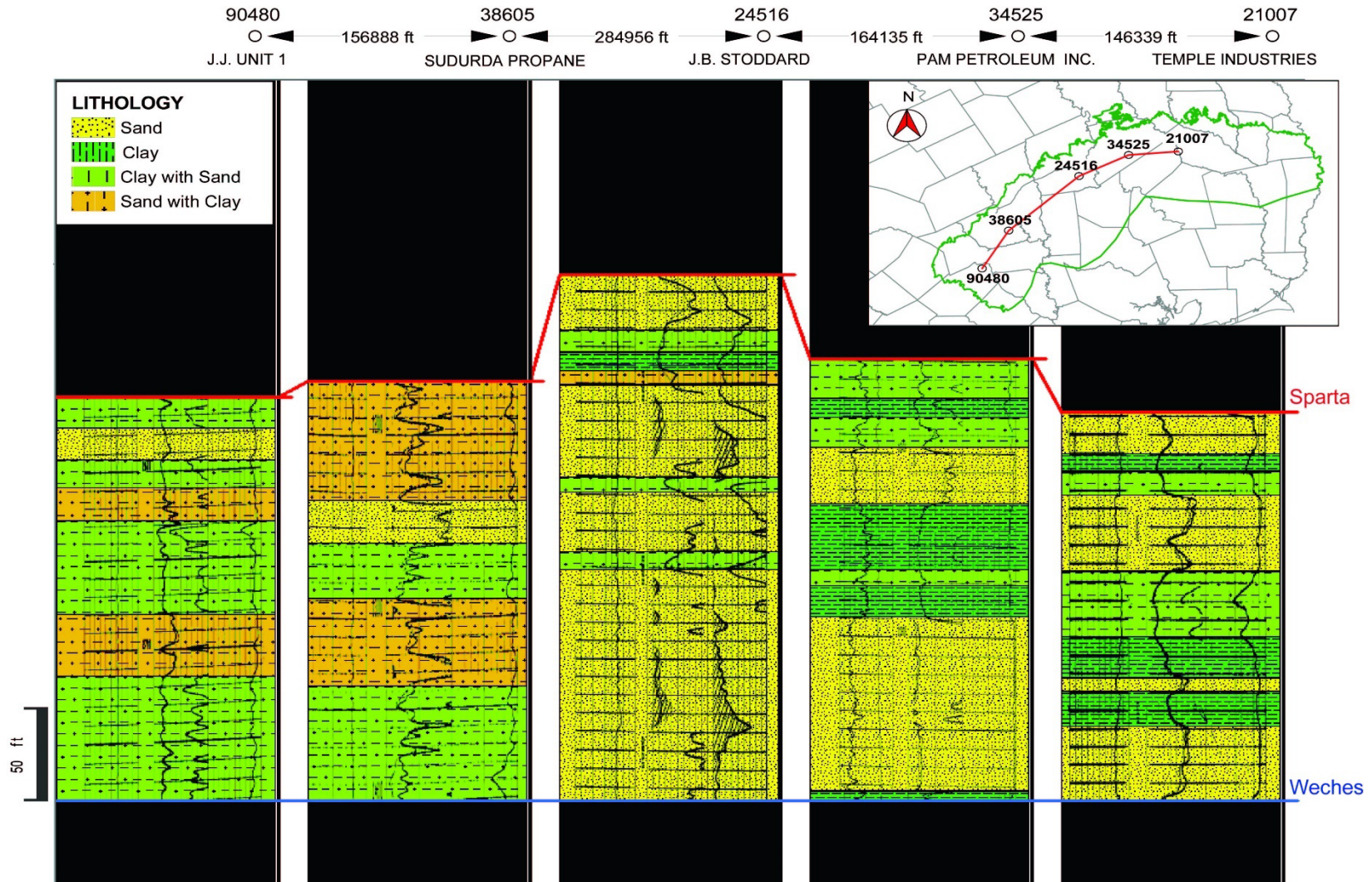


Figure 7.4-1. Correlation section showing lithologic interpretations for the Sparta Formation. Geophysical well logs flattened on the top of the Weches Formation. Section orientation is southwest to northeast. Wells are in Fayette, Burleson, Madison, Houston, and Angelina counties (from left to right).

7.5 Net sand analysis

The geological formations within the study area contain interbedded layers of sand and clay. We prepared maps of net sand within the study area to represent the cumulative sand thickness and sand dispersal pattern during the Sparta Formation deposition. The net sand maps are generated from two sets of information: existing descriptions of formations by water well drillers (also referred to as driller's lithology or description) and our interpretation of geophysical well logs. We evaluated 704 wells (Figure 7.5-1), of which 252 are water wells, 436 are oil and gas wells, and 16 are wells classified as "other" (primarily test holes). We used geophysical well logs for 524 wells and driller descriptions of lithology for the remaining 180 wells.

Because database queries must address lithologic units that are not completely contained within one geological formation (the unit may straddle the formation top, bottom, or both), we wrote specific queries to evaluate each of these scenarios to assign the correct thickness of a lithologic unit to the correct formation. We ran a separate query to assemble the information into a table for export into geographic information system software for spatial analysis. We also developed queries to determine 1) if the geological formation is present at a well site, 2) if the well partially penetrates the geological formation and the percent penetration, 3) if the lithologic description partially describes the entire geological formation, 4) the percent of partial lithologic description due to situations such as a cased hole (recorded as "no record"), and 5) the percent of the partial analysis of the well log (recorded as "partial geologic description"). Well records that do not fully describe a geological formation are used based on best professional judgement. For example, if the percent of lithologic description is high (90 percent or more), all net sand data we calculated was based on depth to top and base of the Sparta Formation raster surfaces.

We created three tables in the BRACS Database containing net sand information for the study area: 1) a table of individual records for each layer containing sand, 2) a table with one record per well with net sand and sand percent for each geological formation encountered, and 3) a table with a decision to use or not use a well for net sand analysis for a specified geological formation. These tables are provided as a study deliverable in the public version of the BRACS Database and table descriptions are provided in the BRACS Database Data Dictionary (TWDB, 2023). The geographic information system point shapefiles are provided as a study deliverable with metadata (Appendix E).

Net sand data points were exported to ArcGIS 10.7®, as point shapefiles and were interpolated using the Spatial Analyst® Topo to Raster tool to create a net sand raster that coincided with the project snap raster grid. Outcrop zero value points representing a zero net sand value were added to force the Topo to Raster tool to thin toward the updip area in the outcrop.

We did not include potentially erroneous data points if the information did not support the regional or local lithology. For example, we looked at net sand points located within "bullseyes" (closed circles) and in several cases these points were eliminated due to vague or imprecise water well driller descriptions of lithology. Water well data was excluded where the lithology descriptions provided by the driller were over-simplified by not splitting into lithological units with enough detail to merit incorporation into the data set for the study

area (such as lumping lithological units into consistent depth intervals describing the primary texture encountered by an entire drill string).

The average net sand value of the Sparta Formation in the study area is 127 feet. However, 15 percent of the wells have net sand values of 200 feet and higher. The distribution of these wells coincides with the thickest part of the Sparta Formation in the study area extending through Madison, northern Walker, and Houston counties. We also noted that increased net sand indicates thicker sand packages, and not just more sand in total.

The net sand thickness pattern is quite variable within the study area. Eastward from Bastrop through Madison and Houston counties, the Sparta Formation is characterized by an increase in net sand, where the maximum sand thickness is 307 feet. Areas of higher sand content within the study area are oriented perpendicular to the depositional axes of the Sparta Formation that intersect the study area (Ricoy and Brown, 1977) and exhibit a lobate geometry. We interpreted these areas as delta front sand deposits, which outline progradation of accumulation lobes (sites of maximum sand deposition) of the Sparta Formation high-constructive delta system developed under conditions of high sediment input.

The southwestern part of the study area is characterized by a decrease in net sand, which appears more uniformly distributed, and the downdip extent of sand in the formation is less than in the rest of study area. The final map of net sand distribution (Figure 7.5-1) shows the depositional setting contrast between fluvial environments during the Sparta Formation deposition in east Texas and strand plain/barrier bar system in central Texas. Most of the study area is within the high-constructive delta system. The southwest transition to the inter-deltaic strand plain system occurs near the northeast Bastrop County line and includes the entire study area within Bastrop County, the southern portion of Lee County, and the southern half of the study area within Fayette County. Ricoy and Brown (1977) document a high-destructive, wave-dominated delta system west of the study area approximately between Fayette and Atascosa counties.

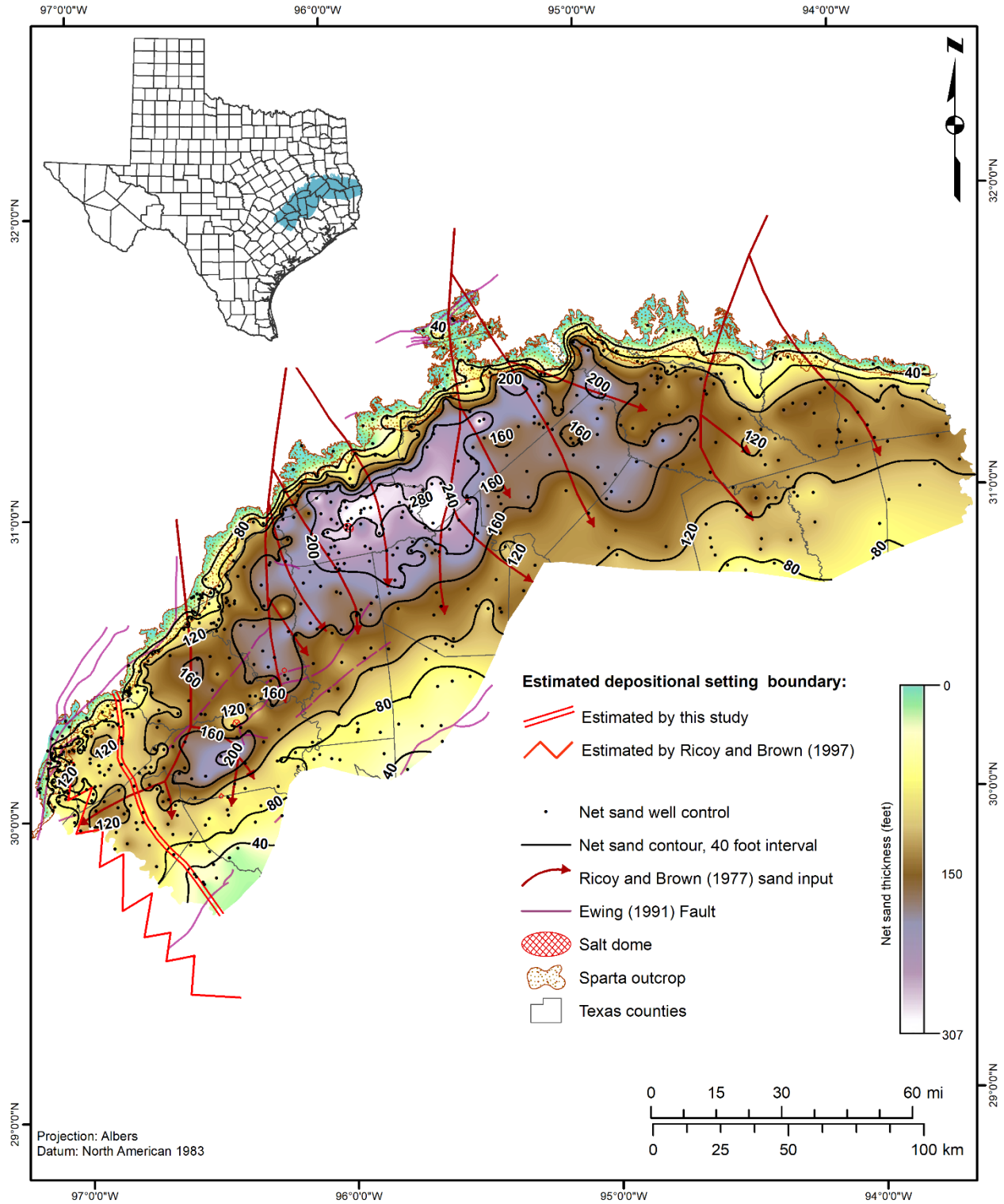


Figure 7.5-1. Sparta Formation net sand thickness, in feet. Axes of significant sand input into the basin are shown in red arrows (modified from Ricoy and Brown, 1977).

8 Aquifer determination and properties

After creating the stratigraphic surfaces and net sand map for the Sparta Formation, we performed an aquifer determination decision process using the stratigraphic surfaces to designate wells completed in the Sparta Aquifer. Aquifer determination consists of a case-by-case review of all water wells within the study area that penetrate the Sparta Formation. This process includes review of wells in the TWDB Groundwater Database that have an existing aquifer code for the Sparta Formation and provides an opportunity to revise any aquifer codes that may have been erroneously assigned an aquifer code for an overlying or underlying aquifer.

An aquifer code for a new or existing well would be assigned by comparing formation tops and bottoms to well screen tops and bottoms. In some cases, formation tops and bottoms are compared to the total depth of a well if no screen data is available. If a screened interval is located between the Sparta Formation top and bottom elevation, then it is designated as a Sparta Aquifer well, unless it is a well that is also screened in sands that are not part of the Sparta Formation.

Of the 6,740 groundwater wells located within the East Sparta aquifer study boundary, 660 wells have the aquifer code 124SPRT (Sparta Formation) designated in the TWDB Groundwater Database. All well data were reviewed and compared against the depth to top and base of the Sparta Formation raster surfaces. Numerous missing well construction records were added to the BRACS Database when available from scanned documents in the TWDB Groundwater Database. A few wells that were previously erroneously designated with the aquifer code 124SPRT within the TWDB Groundwater Database were recoded as either Queen City or Cook Mountain wells, based on the stratigraphy of this study.

Dual-completion wells with aquifer codes indicating well screens set in both the Sparta Formation and any other formation, such as the Queen City Formation or the Spillar Sand Member of the Cook Mountain Formation, were not considered to be representative of the Sparta Aquifer and were excluded from this study. Wells completed in more than one aquifer are mixed waters and were excluded from the water quality and aquifer properties analyses.

8.1 Aquifer hydraulic properties

Aquifer hydraulic properties refer to the intrinsic physical characteristics that control the flow of groundwater through an aquifer. Hydraulic properties include transmissivity, hydraulic conductivity, specific yield, specific capacity, drawdown, pumping rate (well yield), storage coefficients, and porosity. Factors that affect the changes in hydraulic properties include depositional environments, faults or fractures, and aquifer structure, among others. Aquifer properties are generally determined from aquifer test data, which involves analysis of drawdown measurements over time in either one or multiple monitoring wells.

Where aquifer test data from this study were not available, values from other sources were incorporated from the Upper Coastal Plains Central study (Meyer and others, 2020) and specific yield values determined by Young and others (2018).

The primary hydraulic properties we included in this study are defined as follows:

Specific Yield (S_y) – The estimated percent pore volume in the aquifer that can be drained in an unconfined aquifer. Some water will remain trapped in pores when there is insufficient permeability, such as when clays are present. Our study determined this unitless number based on literature review.

Specific capacity (SC) – This term describes the volume of water released per unit decline in water level (unit drawdown). It is calculated by dividing the total pumping rate by the drawdown and is generally reported in gallons per minute per foot.

Hydraulic conductivity (K) – The measure of ease with which groundwater can flow through an aquifer. Greater conductivity indicates greater ease of flow. Dimensions are typically expressed in units of feet per day or gallons per day per square foot.

Transmissivity (T) – This term is related to hydraulic conductivity and describes the ability of groundwater to flow through the thickness of an aquifer, b . The greater the thickness of an aquifer, the greater the transmissivity at a given hydraulic conductivity. The dimensions are expressed in units of square feet per day or gallons per day per foot and the relationship of transmissivity to hydraulic conductivity and aquifer thickness is as follows:

$$T = K \times b \quad \text{(Equation 8-1)}$$

where: T = transmissivity (feet²/day)

K = hydraulic conductivity (feet/day)

b = aquifer thickness (feet)

Storativity (S) – The product of effective aquifer thickness and specific storage (S_s). This term is used to refer to the volume of water a unit thickness of confined aquifer will release when the water level in the aquifer is lowered.

$$S = S_s \times b \quad \text{(Equation 8-2)}$$

where: S = storativity (unitless)

S_s = specific storage (1/feet)

b = aquifer thickness (feet)

We compiled or calculated hydraulic property measurements for the Sparta Formation in 247 wells in the study area. 101 wells are associated with state well numbers. Many of the well yields are from tests conducted decades ago and may not be indicative of what a properly designed, large capacity well may be capable of producing. Further, the accuracy of results depends greatly upon factors such as test duration and spacing of monitoring wells. Users of the hydraulic property data presented in our study should evaluate the data in the proper context. The data is recorded in the BRACS Database table “tblBRACS_AquiferTestInformation”.

8.2 Pumping test data

Sources of aquifer test information for this study include: scanned well records and remarks from the TWDB Groundwater Database (TWDB, 2023e), the Texas Department of Licensing and Regulation Submitted Driller Reports Database (TDLR, 2023), the Texas Commission on Environmental Quality Water Well Report Viewer (TCEQ, 2023b), and the Public Water Supply Database (TCEQ, 2023a), and various county reports (see references).

Specific capacity, well yield, transmissivity, and hydraulic conductivity results are summarized in Table 8.2-1. Figure 8.2-1 and Figure 8.2-2 show western and eastern portions of the study area, respectively, with locations of the available specific capacity, well yield, transmissivity, and hydraulic conductivity data. Figure 8.2-3 is a multi-view map series illustrating the range of values of each aquifer test parameter across the entire study area.

Aquifer test coverage is greater in the western part of the study area with the majority of datapoints reporting at least well yield. The available aquifer tests occurred between October 1936 and March 2017. It should be noted that older aquifer tests may not reflect present conditions, especially in areas that have experienced a sustained increase in pumping volumes over time. BRACS Well ID 87422 reported the largest transmissivity in 1944 at 12,000 gallons per day per foot and is owned by the City of Bryan, located in Brazos County. The greatest well yield was found in BRACS Well ID 92596 within Madison County. The historically highest well yields in the study area generally coincide with the greatest net sand values (Figure 8.2-4). Otherwise, there is no notable pattern within the pumping test data results. The TWDB Groundwater Database contains much more information than is presented here, such as drawdown and sometimes chemistry for these wells, but is available publicly as a resource if needed.

Table 8.2-1. Summary of aquifer test data.

	Specific capacity (gpm/ft) ^a	Well yield (gpm) ^b	Transmissivity (gpd/ft) ^c	Hydraulic conductivity (gpd/ft ²) ^d
Count	114	225	18	13
Minimum	0.07	1	330	22
Maximum	50	1,511	12,000	632
Average	3.26	154	18,654	178

^agpm/ft = gallons per minute per foot of drawdown

^bgpm = gallons per minute of discharge

^cgpd/ft = gallons per day per foot

^dgpd/ft² = gallons per day per foot squared

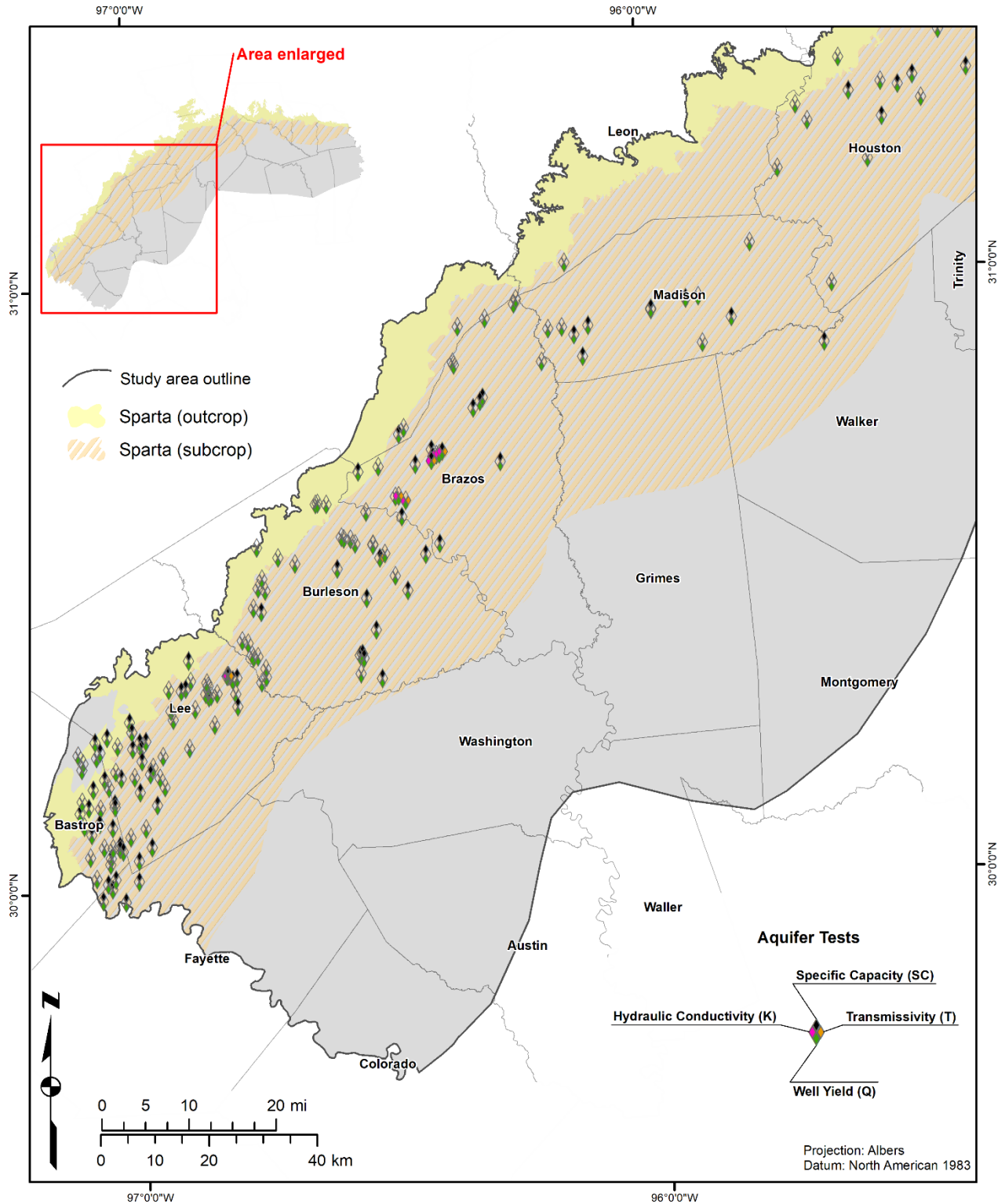


Figure 8.2-1. Summary of aquifer test data available in the western study area.

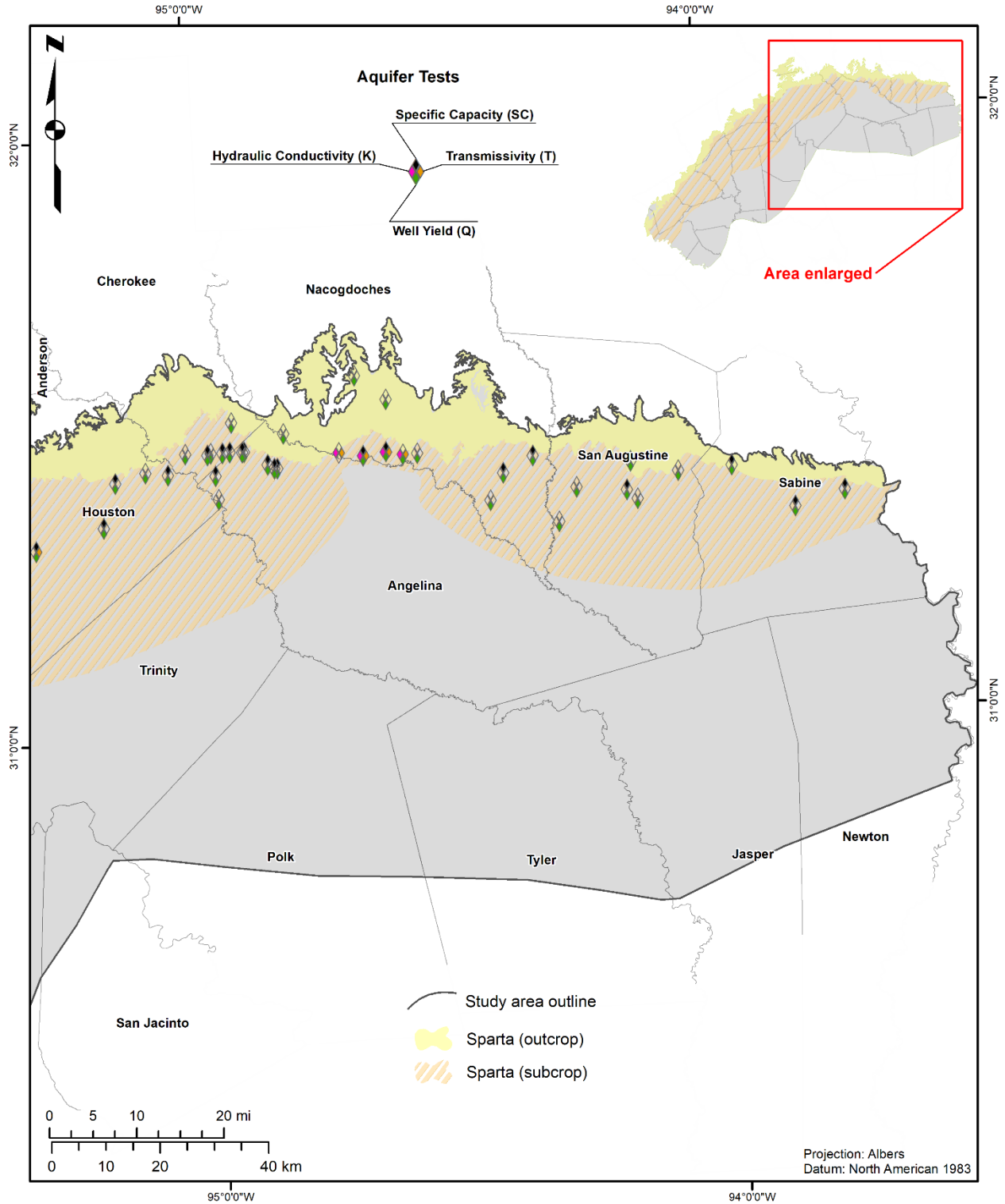


Figure 8.2-2. Summary of aquifer test data available in the eastern study area.

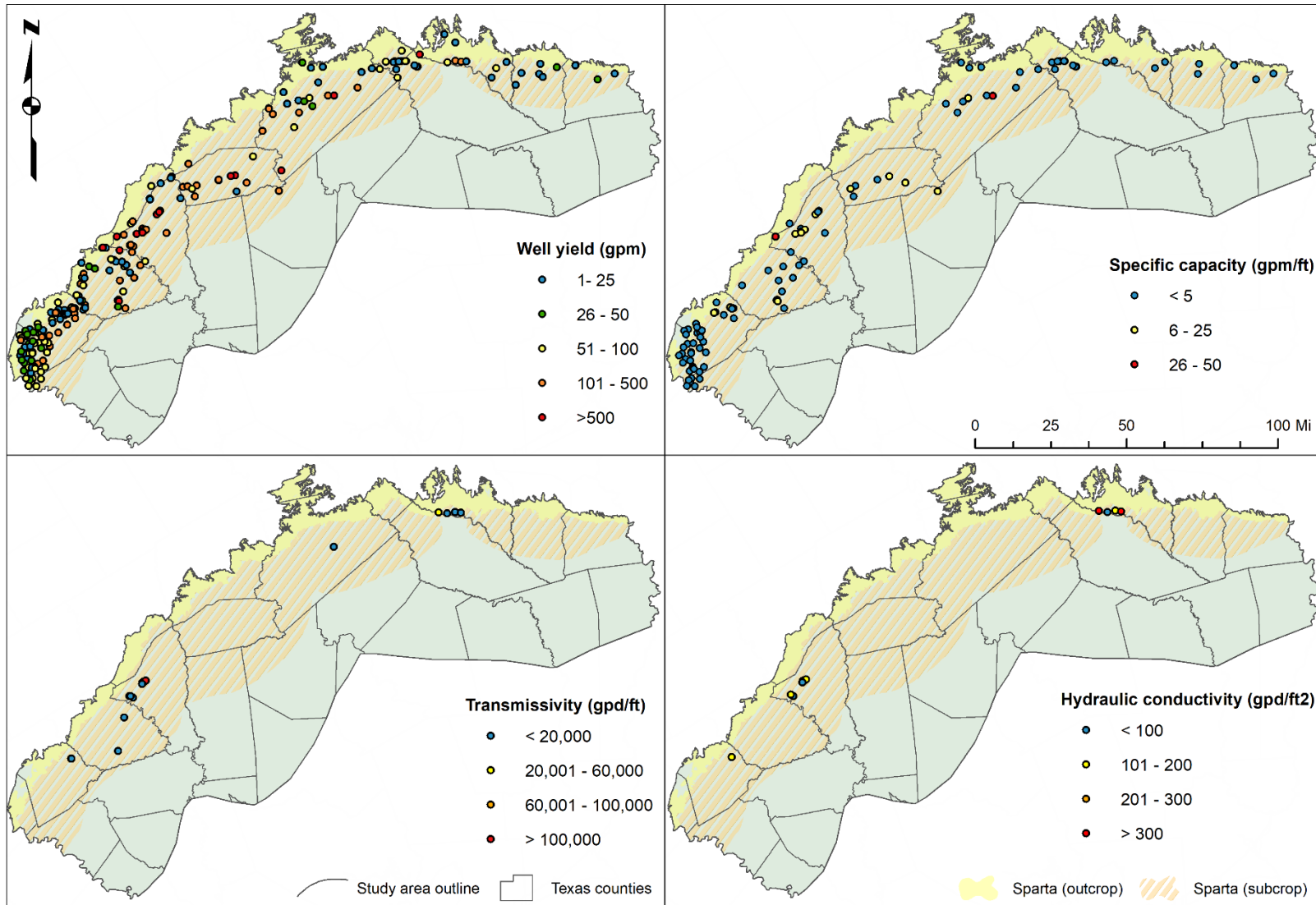


Figure 8.2-3. East Sparta aquifer hydraulic properties. Properties include well yield in gallons per minute (gpm), specific capacity in gallons per minute per foot of drawdown (gpm/ft), transmissivity in gallons per day per foot (gpd/ft), and hydraulic conductivity in gallons per day per foot squared (gpd/ft²). See Table 8.2-1 for a summary of these parameters.

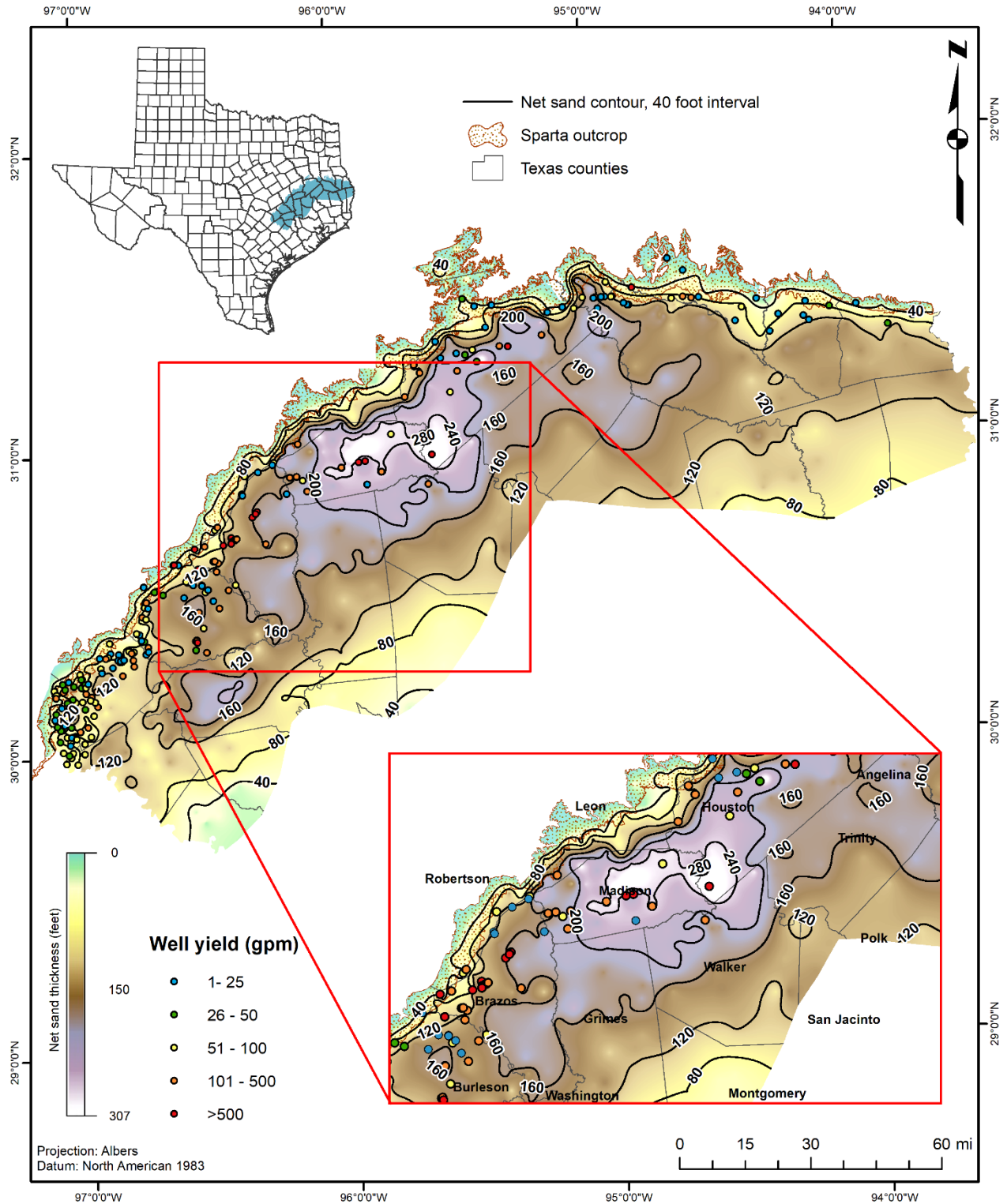


Figure 8.2-4. Area with historically-highest well yields and net sand thickness in the East Sparta aquifer.

8.3 Porosity data

Formation porosity, a measurement of the ratio of pore space (void) volume to total volume, is a required parameter for calculating groundwater volume and total dissolved solids concentration concentrations when using the R_{wa} minimum method. We calculated an estimated total porosity of the water-bearing portion of a clean Sparta sand using density, neutron, and sonic geophysical well log tools. Porosity information was appended to the BRACS Database table (tblGeophysicalLog_Porosity), consisting of all input and output parameters.

Primary porosity decreases with increasing depth due to compaction and cementation (Dutton and Loucks, 2014). Porosity values estimated from geophysical logs are likely a high estimation for sands within the study area since clean, thick (greater than five feet) sands were preferentially selected for interpretation. We selected clay-free and hydrocarbon-free sand units with good caliper curves (no washouts). With respect to density tools, we selected logs exhibiting a density correction factor of between -0.2 and +0.2 grams per cubic centimeter (indicating logging technicians applied a minor correction for mud cake thickness). However, sometimes a thinner sand (about four feet thick) was chosen where such ideal sands were not present.

We used five techniques to estimate total porosity at 34 wells, each technique dependent upon the type of log data available. Neutron-density well logs were calibrated for a sandstone matrix, except for BRACS Well ID 67683, which was converted from a limestone matrix to sandstone using a CNL neutron chart and back calculating the recorded density.

See Appendix F for additional details about the porosity calculations completed for this study.

8.4 Porosity data analysis

Interpreted porosity data are sparse with an average of only one data point per county. Some counties have no available data (Angelina and San Augustine counties) and Fayette County has a maximum of seven data points (Figure 8.4-1). The porosity values estimated using neutron-density logs are more reliable than the individual density tool or sonic tool estimates. The sonic tool is less reliable in unconsolidated sediment and required a compaction correction factor based on an adjacent shale unit. Furthermore, sonic-derived porosity readings most likely do not account for secondary porosity due to fractures and voids (Torres-Verdin, 2017). Nevertheless, the estimated sonic porosity compared favorably with neutron-density porosity values in the same or nearby wells. Most sands contain interbedded clay, so we used concentration of shale calculations to correct when clean, clay-free sands were unavailable. Detailed petrographic analyses were not available for this study but would provide insight as to the identification of and correction for grain-coating (pore-filling) clay that is a product of diagenesis.

Eleven wells used for porosity calculations for the Sparta sand in the Upper Coastal Plains Central study overlapped with this study and were included in the average porosity used for calculating total dissolved solids concentration. Figure 8.4-2 shows a comparison plot of the results for the Upper Coastal Plains Central and East Sparta study area porosity

calculations versus depth. Both studies calculated an average porosity of 34 percent for the Sparta Formation.

As expected, porosity percentage tends to decrease with increasing depth, and ranges from 22 to 45 percent void volume to total. Several of the wells (BRACS Wells IDs 4624, 30964, and 90435) show a higher estimated porosity that coincide with depositional axes of the Sparta through Madison, Grimes, Houston, and Walker counties (Figure 8.4-1).

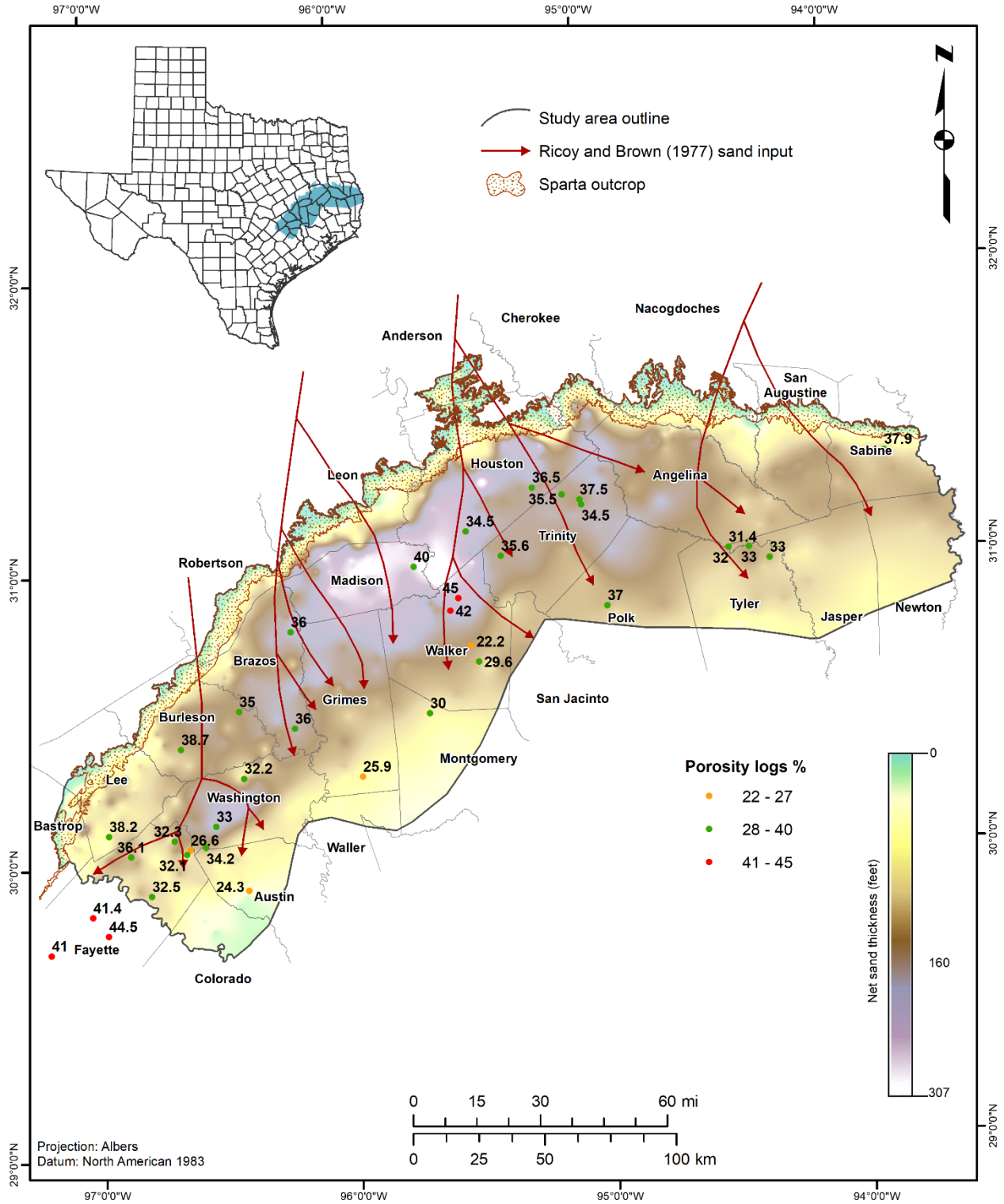


Figure 8.4-1. Porosity distribution in the study area.

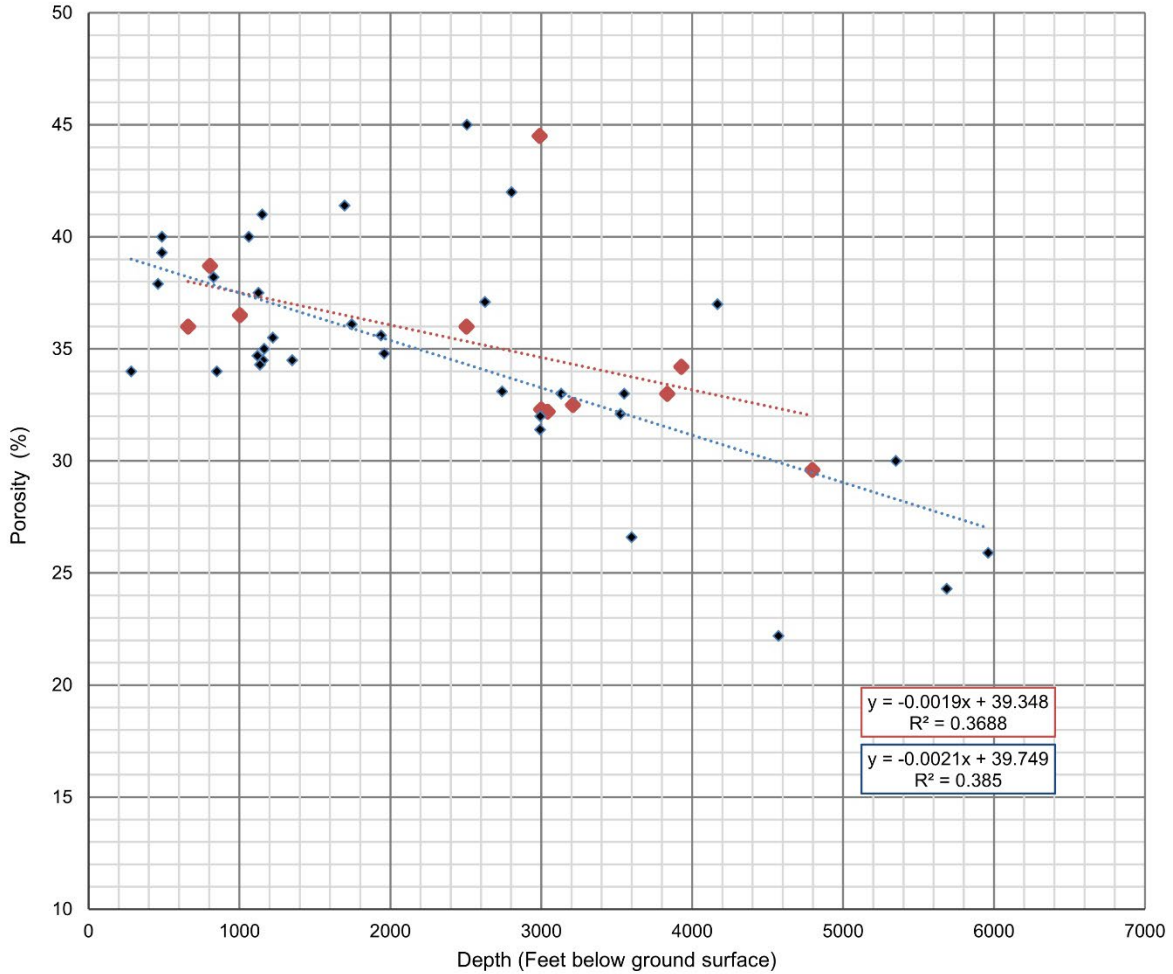


Figure 8.4-2. Scatter plot of estimated total porosity versus depth in the Sparta sand. Upper Coastal Plains Central results that overlap the East Sparta aquifer study area are shown in large red diamonds, and East Sparta aquifer study area results are displayed using small blue diamonds.

9 Measured water quality data

Water quality for a BRACS study includes both measured concentrations of constituents collected via groundwater sampling and total dissolved solids concentration estimates calculated from geophysical logs. The combination of these two data sources is necessary to map groundwater salinity, especially brackish groundwater. Measured concentrations are from the TWDB Groundwater Database (TWDB, 2023e) and the U.S. Geological Survey Produced Waters Database (USGS, 2023b).

9.1 Measured sample data

Sample data for the study was tabulated in the master water quality table. This table is a compilation of all water quality data from the BRACS and TWDB Groundwater Databases. The master water quality table was filtered to only include sample data for wells verified by BRACS staff to be completed in the East Sparta aquifer. The master water quality table is a study deliverable that will also be incorporated in the public version of the BRACS Database, and the next published edition of the BRACS Data Dictionary.

Nine water samples from five oil wells located within the East Sparta aquifer study area (in Washington County) reported as Sparta Formation samples are in the U.S. Geological Survey National Produced Waters Database (USGS, 2023b). These samples of produced water were collected between 1966 and 1969. We confirmed that the produced water samples were collected from the Sparta Formation overlying the Clay Creek salt dome after comparing reported sample intervals and well depths in the database to both the study raster surfaces and the published top elevation contours of the Sparta Formation in the area near the Clay Creek salt dome/oil field (Sandeen, 1972).

The low-resolution coordinate data from the 1960s U.S. Geological Survey National Produced Waters Database (USGS, 2023b) plotted all samples several miles east of the salt dome. Using the Railroad Commission of Texas well viewer (RRC, 2023e) with field names, lease names and well numbers, we believe that three of the wells were completed in the southwestern quadrant of the salt dome. These wells had sample results ranging between 6,802 and 20,617 milligrams per liter total dissolved solids concentration. The remaining two wells with total dissolved solids concentrations of 23,303 and 28,850 milligrams per liter were determined to be unmappable using available data, so the wells were mapped at the centroid of the salt dome. The sample results indicate there is a localized area of very saline groundwater overlying the dome. However, due to geospatial uncertainty, the area has been included as moderately saline rather than very saline in the volume calculations.

9.2 Measured sample quality assurance

A cation-anion balance was performed for quality assurance of the sample data. To perform the cation-anion balance, sample concentrations that were measured in milligrams per liter were converted to milliequivalents per liter (mEq/L) using the following general equations:

Total cations =

$$[(Ca^{2+} \times 0.0499) + (Mg^{2+} \times 0.08229) + (Na^+ \times 0.0435) + (K^+ \times 0.02557) + (Sr^{2+} \times 0.0228)]$$

(Equation 9-1)

where: Ca^{2+} = calcium concentration (mEq/L)

Mg^{2+} = magnesium concentration (mEq/L)

Na^+ = sodium concentration (mEq/L)

K^+ = potassium concentration (mEq/L)

Sr^{2+} = strontium concentration (mEq/L)

Total anions =

$$[(CO_3^{2-} \times 0.03333) + (HCO_3^- \times 0.01639) + (SO_4^{2-} \times 0.02082) + (Cl^- \times 0.02831) + (F^- \times 0.0228) + (NO_3^- \times 0.01613)]$$

(Equation 9-2)

where: CO_3^{2-} = carbonate concentration (mEq/L)

HCO_3^- = bicarbonate concentration (mEq/L)

SO_4^{2-} = sulfate concentration (mEq/L)

Cl^- = chloride concentration (mEq/L)

F^- = fluoride concentration (mEq/L)

NO_3^- = nitrate concentration (mEq/L)

Percent difference between the cation and anion totals in milliequivalents per liter is calculated as follows:

$$\text{Percent difference} = \frac{|C_{ttl} - A_{ttl}|}{\frac{C_{ttl} + A_{ttl}}{2}} \times 100$$

(Equation 9-3)

where: C_{ttl} = total cations

A_{ttl} = total anions

We designated any sample for which the percent difference between the cation and anion total milliequivalents per liter was less than or equal to five percent as balanced. Any sample with a percent difference greater than five was designated as unbalanced and was subsequently excluded from further analysis. Exceptions to the five percent rule include three samples (unbalanced by less than 10 percent) that we manually marked as balanced because their total dissolved solid concentrations are greater than 1,000 milligrams per liter. The slightly saline samples are uncommon and therefore valuable for investigations geared toward characterization of brackish groundwater.

Measured water quality samples from the TWDB Groundwater Database include a flag to indicate whether they are balanced or unbalanced if the difference in the cation and anion milliequivalents per liter is less than or greater than five percent. However, there are some inconsistencies between the ion concentrations and reported balance in the TWDB Groundwater Database. For example, samples that appear to be balanced are flagged as unbalanced. Because of this uncertainty, we recalculated the balance for all TWDB Groundwater Database samples and reflagged them as balanced or unbalanced. Balanced samples are plotted in a piper diagram to identify the geochemical signature of the groundwater samples.

Five out of the nine Sparta Formation produced water samples were balanced with less than five percent error and included in this analysis. Total dissolved solids concentrations for the five produced water samples range between 6,800 and 28,850 milligrams per liter.

Samples excluded from the cation-anion balance were 1) multiple samples at the same location (only the most recent sample was retained), or 2) samples missing critical constituents required for cation-anion balancing, or 3) samples with a total dissolved solids concentration less than 100 milligrams per liter. After parsing data based on these criteria, the remaining 195 samples were included in the cation-anion balance.

Figure 9.2-1 shows a piper diagram for the balanced samples, symbolized by categories of fresh, slightly saline, and moderately saline groundwater classifications. The samples were grouped based upon the total dissolved solids concentration of the sample. The diagram indicates that the groundwater chemistry transitions from predominantly sodium bicarbonate and calcium bicarbonate water in the fresh zone, to a mixed cation sulfate type or mixed cation chloride type in the slightly saline zone, to calcium chloride and sodium chloride type water in the moderately and very saline zones.

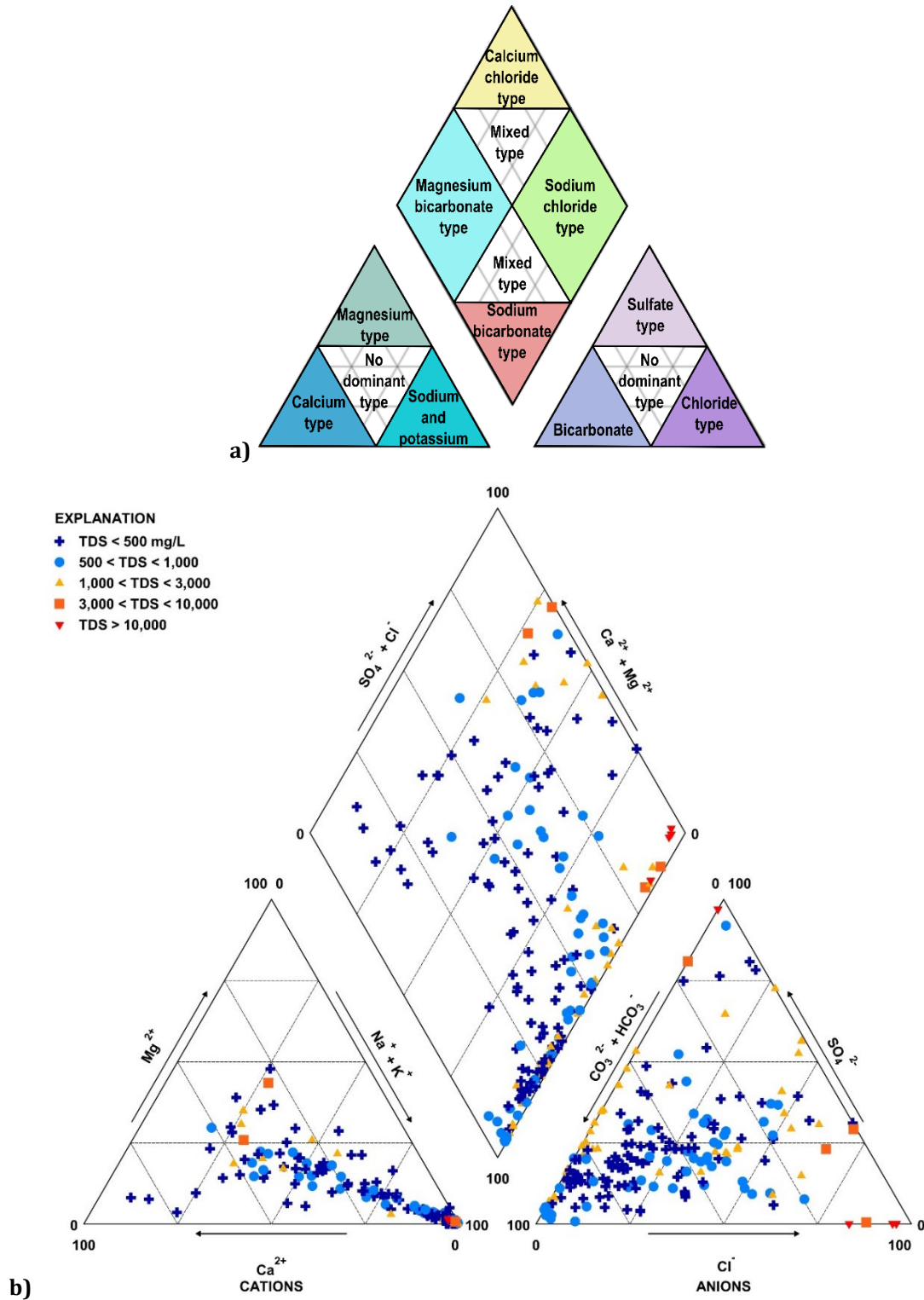


Figure 9.2-1. a) Dominant geochemical signature index map, and b) piper diagram of 195 balanced groundwater samples in the study area. The blue crosses and circles are freshwater, the yellow triangles are slightly saline, the orange squares are moderately saline, and the red triangles symbolize very saline water.

9.3 Dissolved minerals

A total of 677 groundwater samples collected from 357 water wells completed in the East Sparta aquifer were initially compiled.

Three methods for summing constituents to derive measured total dissolved solids values were evaluated for this study:

1. Paired anions and cations with partial bicarbonate
2. Paired anions and cations with 100 percent bicarbonate
3. All anions and cations with 100 percent bicarbonate

The first two summation methods use three, four, or six pairs of anions and cations. For example, the methodology only includes silica and strontium when fluoride and nitrate are also measured, for a total of three, four, or six cation-anion pairs. Additionally, the total dissolved solids concentration in milligrams per liter is summed using either partial bicarbonate for all samples or 100 percent bicarbonate for all samples. The partial bicarbonate concentration is derived by multiplying the bicarbonate concentration by 0.4917, which is the portion of bicarbonate that is not volatilized during heating but is retained and converted to carbonate (Hem, 1985). This is an artifact of the lab method that weighs dry residue upon evaporation to determine dissolved solids concentrations. The adjusted total dissolved solids numbers (using partial bicarbonate) include a bicarbonate correction factor (C_f) of 0.4917, as follows:

$$TDS = \text{measured ion concentrations} + (HCO_3^{2-} \cdot C_f) \quad \text{(Equation 9-4)}$$

where: TDS = total dissolved solids concentration (mg/L)

HCO_3^{2-} = bicarbonate concentration (mg/L)

C_f = bicarbonate correction factor

According to Hem (1985) the total dissolved solids concentration method that uses 100 percent of the bicarbonate concentration is preferable to residue-on-evaporation for total dissolved solids concentrations that are greater than 1,000 milligrams per liter.

The third summation method for total dissolved solids concentration includes 100 percent of measured bicarbonate concentration plus *all* cations (calcium, magnesium, potassium, sodium, strontium, and silica) and any remaining anions (carbonate, chloride, sulfate, fluoride, and nitrate) with measured concentrations, regardless of pairing. Table 9.3-1 shows a comparison of total dissolved solids concentration values using these three methods. The calculated total dissolved solids concentration values increase with 100 percent bicarbonate and again with inclusion of all ions regardless of pairing. Method 2 was selected for this study for salinity mapping to err conservatively. Additionally, the third method does not significantly change the total dissolved solids concentration value. Table 9.3-1 includes the results of Methods 1, 2 and 3. The Method 2 results used for this study are bolded.

Total dissolved solids concentration in the 195 balanced samples range from 101 to 14,576 milligrams per liter. Bicarbonate concentrations range from 1.2 to 1,135 milligrams per liter. Bicarbonate concentrations exceed 50 percent of total dissolved solids concentration

in over 90 percent of the measured samples with salinities less than 1,000 milligrams per liter and comprises 35 percent of total dissolved solids concentration between 1,000 and 1,999 milligrams per liter. Sulfate concentrations range from 0.4 to 2,440 milligrams per liter and exceed 50 percent of total dissolved solids concentration in samples between 3,000 and 3,999 milligrams per liter total dissolved solids concentration. Sample results per analyte that were zero or non-detect (at a concentration lower than the detection limit) were not included in the water quality summary in Table 9.3-1.

Table 9.3-1. Water quality summary. All units are milligrams per liter, unless otherwise specified.

Constituent	Average	Minimum	Maximum	Sample Count
Silica	20	9	88	168
Calcium	29.7	0.1	646	188
Magnesium	11.8	0.1	292	175
Sodium	209	6.9	5,433	189
Potassium	5.1	1.0	19.8	77
Bicarbonate	285	1.2	1,135	188
Carbonate	15.5	1.2	72.0	35
Sulfate	122	0.4	2,440	180
Chloride	152	2	8,500	189
Fluoride	0.5	0.02	4.3	162
Nitrate	13.8	0.02	995	99
Total Dissolved Solids – method 1 (HCO ₃ correction, <=6 ion pairs)	664	79	14,340	189
Total Dissolved Solids – method 2 (no HCO₃ correction, <=6 ion pairs)	808	101	14,576	189
Total Dissolved Solids – method 3 (no HCO ₃ correction, all ions)	831	101	14,592	189
Specific Conductance (micromhos at 25C)	1,149	146	24,500	153
pH (standard units)	7.7	4.2	9.0	171

9.4 Radiochemistry

We found 12 wells sampled for radium-228 in the TWDB Groundwater Database. Ten results were below the maximum contaminant level of five picocuries per liter, and two exceeded the maximum contaminant level, which is the maximum concentration of a regulated contaminant in compliance with Texas public drinking water standards. Twenty-two wells were tested for dissolved uranium and were found to have concentrations below the maximum contamination level of 30 micrograms per liter. Table 9.4-1 presents a summary of these results.

Table 9.4-1. Radionuclide sample results from the Sparta Aquifer exceeding the maximum contaminant level.

State Well Number	Sample Date	Radium-228 (pCi/L) ^a	Dissolved Uranium (µg/L) ^b
		MCL ^c = 5 pCi/L	MCL=30 µg/L
3738704	5/18/2009	6.05 ± 2.6	Not detected
3847204	6/16/2009	6.82 ± 3.5	Not detected

^a Picocuries per liter

^b Micrograms per liter

^c Maximum contamination level

9.5 Specific conductance

Specific conductance (*SC*) is the ability of a material (including groundwater) to conduct electricity through a known volume at a defined temperature. Common units used to measure specific conductance in the United States are micromhos per centimeter ($\mu\text{mhos}/\text{centimeter}$) or microsiemens per centimeter at 25 degrees Celsius. A mho is the reciprocal of the unit of measure for resistance, which is the ohm (Hem, 1985).

Specific conductance values are often related to total dissolved solids concentration by applying a multiplier ranging from 0.4 to as high as 0.96 for high sulfate waters (Hem, 1985).

$$SC = \frac{TDS}{ct} \quad \text{(Equation 9-5)}$$

where:

SC = specific conductance (mS/cm)

TDS = total dissolved solids concentration (mg/L)

ct = multiplier

The multiplier (*ct*) that relates specific conductance to total dissolved solids concentration is typically averaged across an aquifer or portion of an aquifer to determine a representative *ct* for the area of interest. Section 9.6 discusses how *ct* values were derived for three different ranges of total dissolved solids concentrations.

As noted on the TWDB Groundwater Database Data Dictionary webpage (TWDB, 2023e), specific conductance results from the Texas Department of Health in the 1980s and early 1990s were determined to be diluted conductance values. There are 124 samples from the East Sparta aquifer that were analyzed by the Texas Department of Health within this time frame. According to the website, these values were not all successfully corrected by the TWDB. Figure 9.5-1 shows specific conductance and total dissolved solids concentration for these samples compared to results from all other labs. The questionable samples (red dots in Figure 9.5-1) appear to have a different trend line than the samples that were analyzed from all other labs, so the Texas Department of Health samples have been excluded for the purposes of this study.

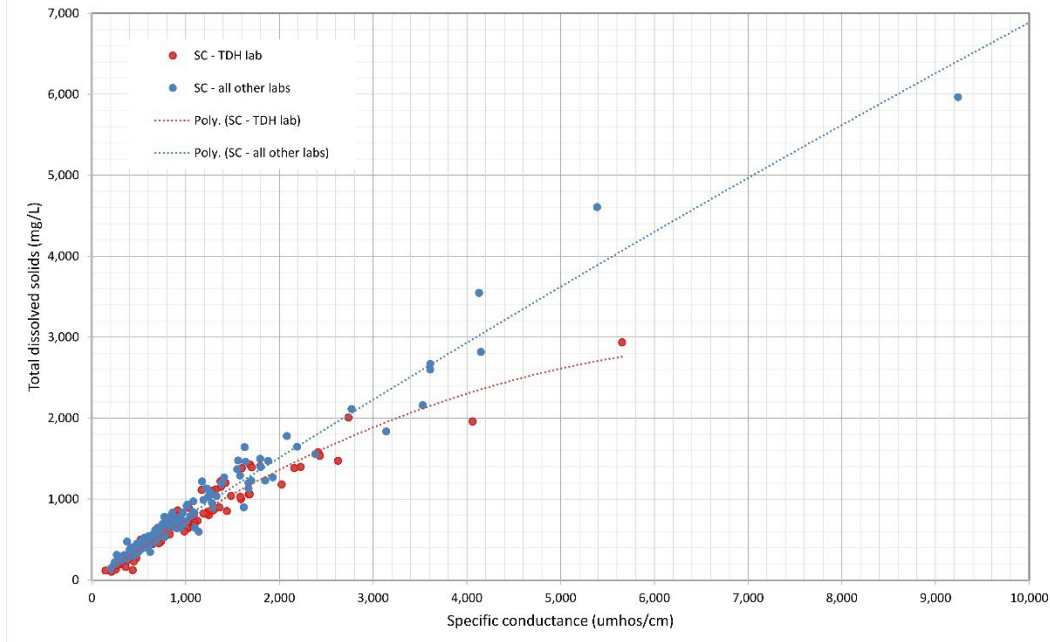


Figure 9.5-1. Total dissolved solids concentration versus specific conductance for Texas Department of Health lab (red) and all other labs (blue).

9.6 Total dissolved solids and specific conductance relationship

This study combined both measured results from lab analyses and calculated values derived from modeled ion concentrations to characterize specific conductance across the complete range of salinity being mapped by this study. The total dissolved solids concentrations included in this characterization range from 100 to 35,000 milligrams per liter. The total dissolved solids-specific conductance relationship is used to capture the influence of divalent ions, because divalent ions appear more resistive than a sodium chloride solution with the same total dissolved solids concentration.

The measured sample data from the TWDB Groundwater Database includes total dissolved solid concentrations up to 14,576 milligrams per liter, which is associated with specific conductance values ranging up to 24,500 µmhos/centimeter. Only five out of 218 samples had a measured total dissolved solids concentration greater than 3,000 milligrams per liter and a specific conductance value greater than 4,000 µmhos/centimeter. Total dissolved solid concentrations with full bicarbonate concentrations were used to develop this relationship with specific conductance to better represent the ion effect, or ion complexing that occurs in natural waters.

Five out of the nine Sparta Aquifer produced water samples were balanced with less than five percent error and included in this analysis. Total dissolved solids concentrations for the five produced water samples range between 6,800 and 28,850 milligrams per liter. The specific conductance values were not reported and were modeled using PHREEQC. The modeled values range from 11,300 to 44,921 µmhos/centimeter.

The modeled sample concentration data was used with PHREEQC (Parkhurst and Appelo, 2013) to calculate the specific conductance for 23 artificial samples with a total dissolved solids concentration ranging between 4,000 and 35,000 milligrams per liter. The five

measured samples with total dissolved solids concentrations greater than 3,000 milligrams per liter were included in the modeled sample data set to help normalize artificial ion concentrations. Calculated specific conductance ranges from 30,000 to 54,150 $\mu\text{mhos}/\text{centimeter}$. Best fit trendlines were generated for each data subset, as shown in Figure 9.6-1. See Appendix G for the modeled sample data set.

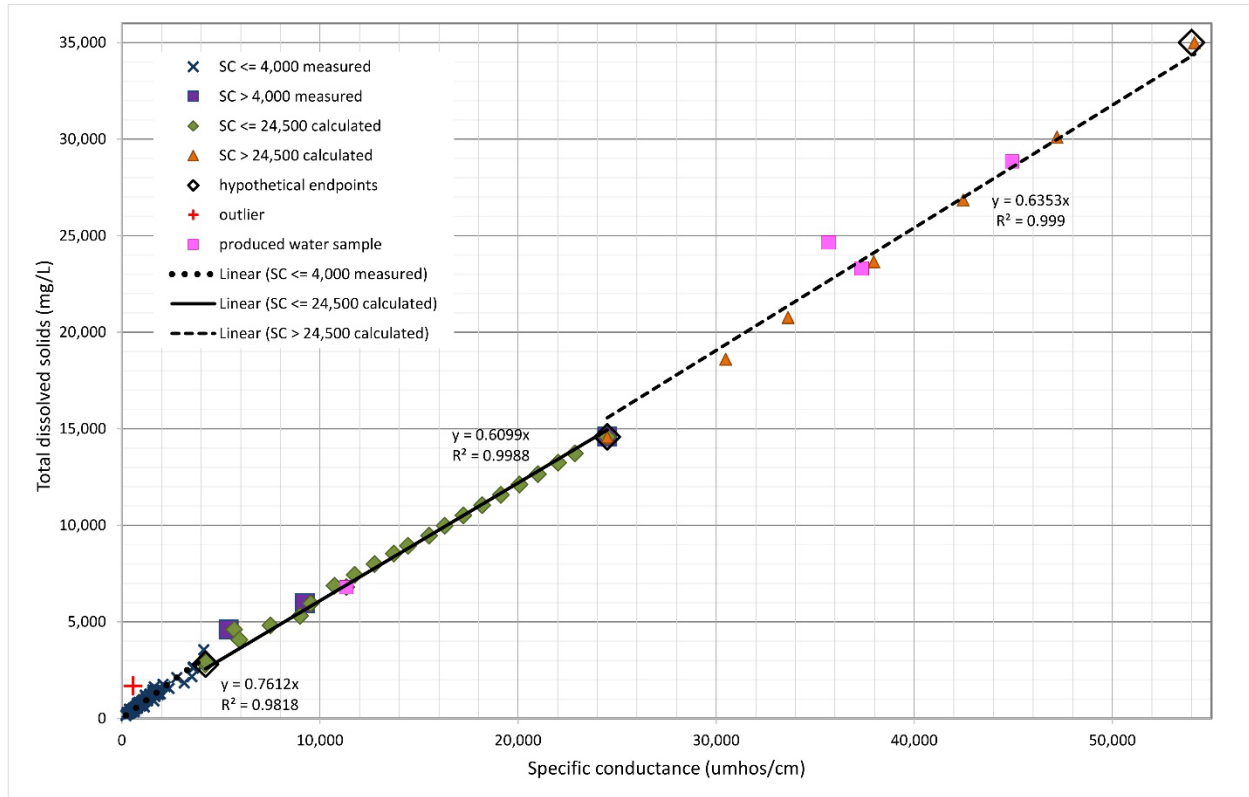


Figure 9.6-1. Total dissolved solids-specific conductance relationship for the East Sparta aquifer.

The trendlines were simplified to include an intercept of zero to derive ct within each data subset. Table 9.6-1 shows the regression summary. The outcome of building the total dissolved solids-specific conductance relationship is the designation of three ct values to characterize the complete salinity range of the Sparta Formation within the study area. These values are bolded in Table 9.6-1.

Table 9.6-1. East Sparta aquifer total dissolved solids concentration and specific conductance regression summary.

Specific conductance range	Linear regression	ct
101-4,150	$y = 0.7612x$	0.76
4,150-24,500	$y = 0.6101x$	0.61
24,500-54,150	$y = 0.6304x$	0.63

10 Calculated water quality data

After the stratigraphic surfaces and net sand maps were created, salinities were calculated as total dissolved solids concentration (in milligrams per liter) from applicable geophysical logs and then mapped collectively with the measured data. Contours were drawn at 1,000, 3,000, and 10,000 milligrams per liter total dissolved solids concentration to delineate salinity zones.

10.1 Well pairs

The workflow for calculating total dissolved solids concentration using geophysical logs and delineating salinity class zones in the study area begins with the establishment of well pairs. Once the well pairs are identified, and the constant values and variables used to calculate salinity are verified, then salinity can be calculated for all geophysical logs in the study area that have both a deep resistivity curve and the required header information. A well pair consists of a well with a measured groundwater sample located proximal to a well with a geophysical log from which a calculated value of total dissolved solids concentration can be derived. The total dissolved solids concentration from the geophysical log is “calibrated” to the sample result by adjusting the parameters that are included in the calculation. The parameter values that are derived from the well pair calibration are then used as study-wide values.

Potential well pairs were identified using a spatial join of the sample locations and geophysical log locations. The maximum distance between a pair of wells was set at two miles. Thirteen well pairs were found with similar measured and calculated salinity values and are summarized in Table 10.1-1.

Table 10.1-1. Summary of Sparta Formation well pairs in the study area.

County	Well log (BRACS ID)	Measured water quality (State Well Number)	Pair separation (miles)	Measured total dissolved solids range (milligrams per liter)	Calculated total dissolved solids (milligrams per liter)
Madison	6337	60-01-201	1.4	167-240	233
Angelina	34160	37-35-703	0	1,018-1,523	1,535
Angelina	34165	37-35-901	0.8	5,396-5,967	6,162
Angelina	34175	37-36-803	0.8	1,431-2,035	1,484
Angelina	34177	37-35-405	0.3	1,000-1,505	1,617
Burleson	38605	59-37-104	1	669-989	995
Madison	38728	38-57-502	1.8	227-297	241
Madison	87454	60-01-401	1.3	183-246	182
Houston	87518	38-44-701	0.7	657-840	657
Madison	87590	60-02-102	1.1	162-249	178
Houston	88257	38-52-701	0.1	988-1,430	1,421
Sabine	88472	36-42-101	0.8	1,223-1,740	1,652
Brazos	97991	59-22-801	0	2,047-2,602	2,550

To compare measured and calculated total dissolved solids concentration for a well pair, the calculated total dissolved solids concentration derived from the geophysical well log is compared to the range of total dissolved solids concentration derived from the three summation methods discussed in Section 9.3. If a calculated value is within the range of measured values or plus-minus ten percent, then it is considered a pair for the purposes of determining characteristic parameter values for the Sparta Formation. For BRACS Well ID 97991 in Brazos County, the range of total dissolved solids concentration is 2,047 to 2,602 milligrams per liter. Using a multiplier (*ct*) of 0.76, a cementation exponent (*m*) of 1.3, a porosity (ϕ) of 0.38, and a NaCl-equivalent correction factor (*Rwe_Rw*) of 1.0, the calculated total dissolved solids concentration is 2,550 milligrams per liter, which falls within the range of the measured groundwater sample.

10.2 Calculating salinity from geophysical logs

There are several methods described by Estep (1998) and (2010) for interpreting total dissolved solids concentration in a formation using geophysical well logs. Calculating total dissolved solids concentration is complicated for many reasons such as the heterogeneity of geology, differing tools used for measurement, and other factors influencing how each calculation method was derived. Most existing geophysical logs for this study were developed for petroleum exploration and production where groundwater composition is predominantly sodium and chloride ions. The geophysical well logs collected for this study were produced between 1920 and 2014. Given the available data and assumptions, we used the *R_{wa}* (resistivity water apparent) minimum method for calculating salinity.

10.2.1 *R_{wa}* minimum method

The *R_{wa}* minimum method (Estep, 1998) is based on Archie's equation (Archie, 1942). Archie's equation is:

$$R_o = R_w \cdot \frac{a}{\phi^m} \cdot \frac{1}{S_w^n} \quad \text{(Equation 10-1a)}$$

where:

R_o = resistivity of the formation (units: ohm-meter)

R_w = resistivity of water (units: ohm-meter)

a = Winsauer tortuosity factor (dimensionless)

ϕ = porosity (units: percent)

m = cementation exponent (dimensionless)

S_w = water saturation (units: percent)

n = saturation exponent (dimensionless)

In a 100-percent water-saturated aquifer (*S_w* = 1), as would be expected in a fresh or brackish aquifer, *S_w* can be eliminated from the equation. Hydrocarbons, in the form of oil or gas, might also contribute to the saturation of the rock, making *S_w* less than 1. Based on recommendations from Estep (1998) and Torres-Verdin (2017), the Winsauer tortuosity factor is assigned as 1. Therefore, the equation could be further simplified to:

$$R_w = R_o \cdot \phi^m \quad \text{(Equation 10-1b)}$$

The deep-investigation geophysical logging resistivity tool measures a combination of the formation rock matrix and groundwater resistivity. The measured resistivity of a formation is due to several parameters: resistivity of formation minerals, sediment grain size, and surface conductance on mineral grains (Alger, 1966). Explanations of the input parameters to calculate total dissolved solids concentration from resistivity logs are described in Section 10.2.2.

A total of 426 wells were used for total dissolved solids concentration salinity class calculations with the R_{wa} minimum method. Equations were coded in Visual Basic for Applications® and completed as a class object within the BRACS Database for automated calculation. Using Microsoft Access allowed us to quickly evaluate parameters for calibration using groundwater chemistry samples as discussed previously. Further, this process ensured consistency and retained all inputs for future use. The software runs the calculations in the following order:

- 1) Determine the temperature at the depth of the formation being investigated (T_f).

$$T_f = (T_{bh} - T_s) \frac{D_f}{D_t} + T_s \quad \text{(Equation 10-2)}$$

Where:

T_{bh} = temperature bottom hole in degrees Fahrenheit

T_f = temperature formation in degrees Fahrenheit

D_f = depth formation in feet

D_t = depth total in feet

T_s = temperature surface in degrees Fahrenheit

- 2) Determine the water-equivalent resistivity (R_w) with the R_{wa} minimum method using a deep resistivity value (R_o). Figure 10.2-1 illustrates how formation resistivity (R_o) is read from a geophysical log.

$$R_w = R_o \cdot \Phi^m \quad \text{(Equation 10-3)}$$

- 3) Correct the water-equivalent resistivity (R_{wc}) based on the NaCl-equivalent correction factor ($R_{we_R_w}$ in BRACS form).

$$R_{wc} = \frac{R_w}{R_{we_R_w}} \quad \text{(Equation 10-4)}$$

- 4) Convert the corrected water-equivalent resistivity (R_{wc}) to the resistivity of the water at 77°Fahrenheit (R_{w77}) using Arp's equation (Torres-Verdin, 2017).

$$R_{w77} = R_{wc} \cdot \frac{T_f + 6.77}{77 + 6.77} \quad \text{(Equation 10-5)}$$

- 5) Convert the resistivity of water at 77°Fahrenheit (R_{w77}) to conductivity of water at 77°Fahrenheit (C_w).

$$C_w = \frac{10,000}{R_{w77}} \quad \text{(Equation 10-6)}$$

- 6) Calculate the interpreted milligrams per liter total dissolved solids concentration using a value for ct for the respective resulting total dissolved solids concentration (TDS) range.

$$TDS = ct \cdot C_w \quad \text{(Equation 10-7)}$$

Figure 10.2-1 illustrates how formation resistivity (R_o) is read from a geophysical log.

There are disadvantages to using the R_{wa} minimum method, including its dependance on empirical input parameters, and the assumption that only water exists in the aquifer (no hydrocarbons). More porosity data would help improve confidence in the calculations.

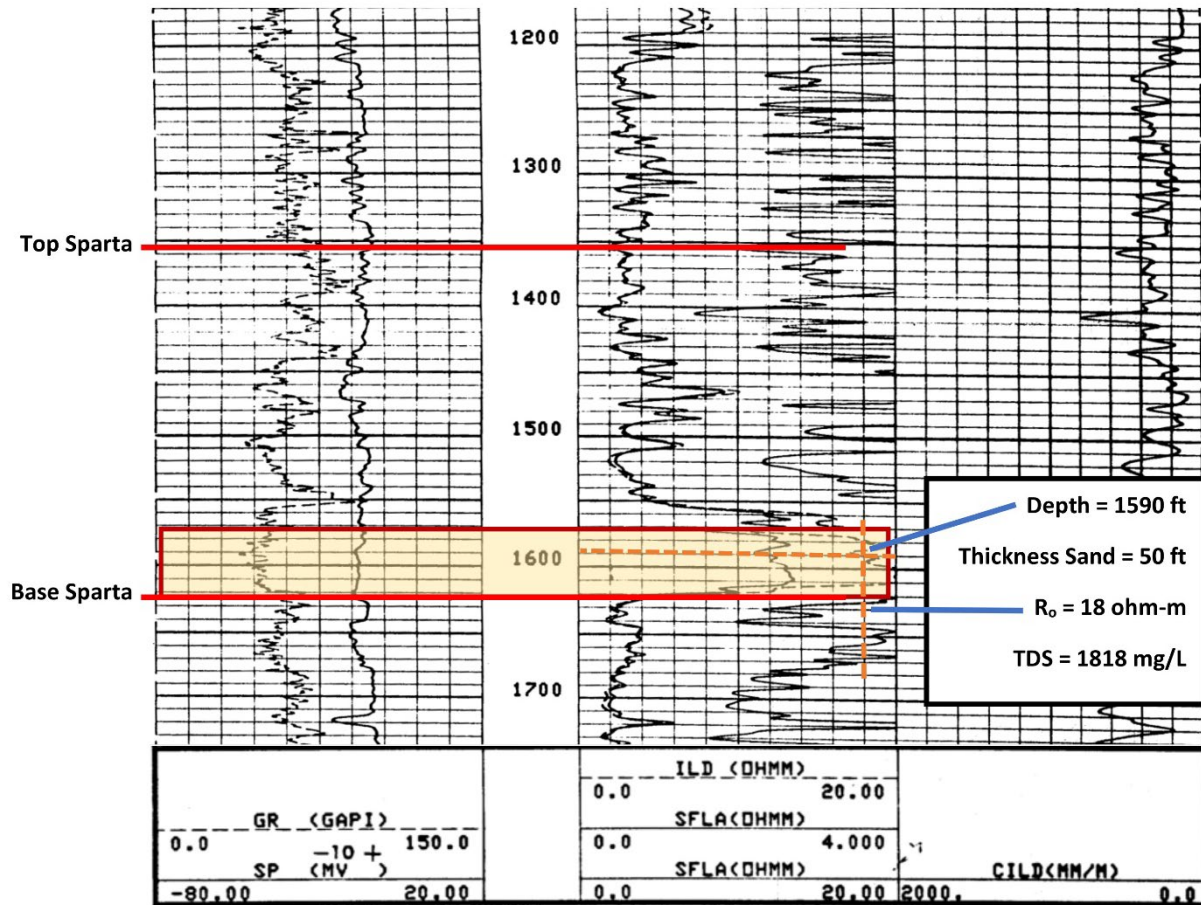


Figure 10.2-1. Geophysical log for BRACS Well ID 88437 in Trinity county. GR is the gamma ray log measured in American Petroleum Institute units (GAPI). SP is the spontaneous potential log measured in millivolts (mV). ILD is the deep induction or resistivity log and the SFLA are spherically focused shallow reading resistivity logs, each measured in ohm-meters (ohm-m). R_o represents the depth reading of the deep resistivity curves, used to calculate total dissolved solids concentration (TDS).

10.2.2 Input parameters for R_{wa} minimum method

There are several input parameters required to calculate total dissolved solids concentration using the R_{wa} minimum method. These parameters are summarized in Table 2-1 and detailed in this section.

Table 2-1. Input parameters for the R_{wa} minimum method.

Parameter	Symbol	Units
Depth total	D_t	Feet
Depth formation	D_f	Feet
Temperature surface	T_s	Degrees Fahrenheit
Temperature bottom hole	T_{bh}	Degrees Fahrenheit
Formation deep resistivity	R_o	Ohm-meter
Porosity	ϕ	Percent
ct conversion factor	ct	dimensionless
Cementation exponent	m	dimensionless
Water quality NaCl correction	R_{we_Rw}	dimensionless

The input parameters that are either predetermined for an entire study area or adjusted per well include: ct (the constant relating total dissolved solids concentration to specific conductance within a specific range of conductance), m (the cementation exponent, which is a study-wide constant), porosity (determined by the closest log with a porosity estimate), and R_{we_Rw} (the NaCl equivalent groundwater correction factor). These input parameters are summarized in Table 2-2.

Table 2-2. Summary of study-wide variables needed to calculate salinity.

Parameter	Description	Type	Value
ct	specific conductance-total dissolved solids constant	Constant dependent on specific conductance (SC)	$ct = 0.76$ for $SC < 4,150$ $ct = 0.61$ for $4,151 < SC < 24,500$ $ct = 0.63$ $SC > 24,500$
m	Cementation exponent	Constant	1.3 (unconsolidated sand)
Porosity	Percent volume of pore space	Variable dependent on location	Ranges from 0.22 to 0.44 in study area; assigned based on proximal geophysical log(s)
R_{we_Rw}	NaCl equivalent correction factor	Variable dependent on total dissolved solids (TDS)	1.33 for 100-999 mg/L TDS 1.28 for 1,000-1,999 mg/L TDS 1.18 for 2,000-2,999 mg/L TDS 1.30 for 3,000-3,999 mg/L TDS 1.0 for $>4,000$ mg/L TDS

Depth total (D_t)

The total depth of the well is required to calculate the formation temperature at the depth of investigation. If a well was logged with multiple depth runs, the total depth of the logging run applicable to the depth of investigation must be used.

Depth formation (D_f)

Depth of the Sparta Formation within the log being investigated is required to calculate the formation temperature. Specifically, this number denotes the depth of the middle of a thick, shale-free, water-saturated sand where the resistivity reading is obtained. This depth, the thickness of the evaluated sand unit, and geologic formation are recorded in the BRACS Database (tblGeophysicalLog_WQ).

Temperature surface (T_s)

The temperature at the well-site surface is required to calculate the formation temperature at the depth of investigation. Contour maps of temperature records from 1951 to 1980 compiled by Larkin and Bomar (1983) were used to determine the average annual temperature at any given well location. A temperature between 65- and 69-degrees Fahrenheit was assigned for each well location.

Temperature bottom hole (T_{bh})

The bottom hole temperature of the logging run applicable to the depth of investigation is needed. If multiple logging runs were completed, care was taken to ensure the correct temperature was read for the correct depth of investigation.

Formation Deep Resistivity (R_o)

The resistivity of the formation is determined with a deep-investigation resistivity logging tool and is a combination of formation rock matrix resistivity and groundwater resistivity. The deep-investigation tool is used because a shallow tool reading is usually affected by mud cake on the wellbore and invaded drilling fluid in the formation. To avoid “shouldering” effects, lowered vertical resolution of well logs due to speed of logging or sampling interval, the formation resistivity was determined by reading resistivity at the peak in a 10 foot or greater layer of shale-free sand that is not affected by hydrocarbons (Torres-Verdin, 2017); Figure 10.2-1).

Formation porosity (ϕ)

The three types of porosity include primary pores, secondary pores, and micropores. For this study, total porosity is measured indirectly from porosity-type logs and used as the estimated total porosity (Torres-Verdin, 2017). Porosity-type logs include neutron-density and acoustic (sonic) logs. Neutron-density was preferred due to their reliability for total porosity estimates, in comparison to acoustic (sonic) logs, which are more accurate in unconsolidated, low porosity mediums, and do not account for secondary porosity due to vugs or fractures (Doveton, 1999). Porosity is described in more detail in the Appendix F.

ct conversion factor (ct)

Information on the designation of the *ct* factor is described in detail in section 9.6. The *ct* values derived to characterize salinity the Sparta Formation within the study area are as follows:

- where specific conductance is less than 4,150 milligrams per liter, *ct* = 0.76,
- where specific conductance is between 4,151 and 24,500 milligrams per liter, *ct* = 0.61, and
- where specific conductance exceeds 24,500 milligrams per liter, *ct* = 0.63.

Cementation exponent (m)

The cementation exponent is a dimensionless parameter determined empirically from detailed core analysis or theoretically based on other known related parameters. It accounts for the effective porosity or connectedness of pore and fracture network. For this study we used a cementation exponent of 1.3, which is within the range of suggestions for unconsolidated sandstones (Torres-Verdin, 2017).

NaCl-equivalent correction factor or water quality correction factor ($R_{we}R_w$)

Most geophysical well logging tools and water quality calculations were developed for petroleum exploration where groundwater is dominated by sodium and chloride ions. However, ions other than NaCl may dominate in fresher water. Different ions such as sulfate (SO_4^{2-}) and bicarbonate (HCO_3^-) are more resistive to electrical current than sodium chloride (NaCl), and the resistivity factors may produce inaccurate results for total dissolved solids concentration calculations without correction.

The NaCl equivalent correction factor was used to correct for erroneously high deep resistivity readings on geophysical logs due to high bicarbonate groundwater. Therefore, the $R_{we}R_w$ correction factor was incorporated into calculated salinities (up to 4,000 milligrams per liter of total dissolved solids concentration) to improve alignment with the measured groundwater sample data.

We used the NaCl equivalent correction technique from Meyer and others (2014) for this study. Cation and anion concentrations were weighted with a multiplier specific to the ion and total dissolved solids concentration of the water sample. We used weighting multipliers from Chart Gen-8, Resistivities of Solutions (Schlumberger, 2009). Adding the NaCl-equivalent milligrams per liter of each constituent yields the NaCl-equivalent milligrams per liter total dissolved solids concentration, or $R_{we}R_w$. Generally, there is an inverse relationship between total dissolved solids concentration and $R_{we}R_w$ since resistivity appears artificially high when influenced by bicarbonate and/or divalent ions such as sulfate (SO_4^{2-}). The correction factors used for this study reflect the decrease of bicarbonate between 100 and 3,999 milligrams per liter and high sulfate measured in samples with 3,000 to 3,999 milligrams per liter total dissolved solids concentration.

The correction factors used for this study are as follows:

- where total dissolved solids concentration are between 100 and 999, $R_{we}R_w = 1.33$,
- where total dissolved solids concentration are between 1,000 and 1,999, $R_{we}R_w = 1.28$,
- where total dissolved solids concentration are between 2,000 and 2,999, $R_{we}R_w = 1.18$
- where total dissolved solids concentration are between 3,000 and 3,999, $R_{we}R_w = 1.30$
- where total dissolved solids concentration equal or exceed 4,000, $R_{we}R_w = 1.0$.

10.3 Salinity zone delineation

Once estimates have been calculated from geophysical logs, preliminary water quality contours can be drawn for the measured (sample data) and calculated (log data) salinity values. Outlier or questionable point values were reviewed and either verified or eliminated from the data set.

The 1,000, 3,000, 10,000, and 35,000 milligrams per liter contour lines were reviewed to verify and/or eliminate data points that were: 1) located within “bullseyes” (closed circles), 2) defining contour pivot points, or turns, where a contour line pivot or wrapped around a data point, or 3) in a different salinity zone from nearby or surrounding data points. For wells near contour pivot points or turns, the well depths of measured groundwater samples were compared to the Sparta Formation top and bottom depth surfaces to verify that the samples were collected from the East Sparta aquifer.

After the total dissolved solids concentration contour lines were finalized (Figure 10.4-1), the salinity zone polygons (Figure 10.4-2) and raster surfaces were created from these data to perform volumetrics calculations.

To compare this study to the Sparta Formation mapped in the Upper Coastal Plains Central study (Meyer and others, 2020), the salinity zone classifications were compared for each well location that included a salinity calculation for the Sparta Formation in both studies. Where the salinity zone classifications differed, then the total dissolved solids concentration calculated for this study was used. The differences can be attributed to the assumptions made regarding input parameters required for the total dissolved solids concentration calculations.

There are five well locations in Fayette County where the salinity zones differ between studies. The Upper Coastal Plains Central classification was moderately saline for the five wells, and for this study, the classification was slightly saline for the same wells (Table 10.3-1). This difference can be attributed to the assumptions made regarding input parameters required for the total dissolved solids concentration calculations. Specifically, the studies used different study-wide values for the cementation factor (m), the total dissolved solids-specific conductance conversion factor (ct), and the sodium chloride equivalent correction factor ($R_{we}R_w$). Additionally, the current study uses porosity from the closest geophysical log, where the Upper Coastal Plains Central study used a study-wide constant for porosity (Table 10.3-2).

Table 10.3-1. Comparison of total dissolved solids concentration (TDS) estimates in both studies for wells with different salinity classifications.

Well ID	East Sparta aquifer study area				Upper Coastal Plains Central			
	Depth	R_o	TDS	Salinity class	Depth	R_o	TDS	Salinity class
38582	1,616	10.6	2,508	Slightly saline	1,615	10.6	3,011	Moderately saline
38584	2,130	9	2,815	Slightly saline	2,132	9	3,397	Moderately saline
42825	2,531	11	2,303	Slightly saline	2,530	10	3,064	Moderately saline
54643	2,223	20	1,295	Slightly saline	2,125	8	3,655	Moderately saline
84977	1,285	11	2,648	Slightly saline	1,280	10	3,557	Moderately saline

Table 10.3-2. Comparison of study parameters for total dissolved solids concentration calculations.

Study	Porosity	m	ct	$R_{we} R_w$
East Sparta aquifer study area	0.22 to 0.45	1.3	0.76	1.18 to 1.32
Upper Coastal Plains Central	0.34	1.75	0.53	1.16

10.4 Salinity zone analysis

The primary drivers affecting salinity distribution in the East Sparta aquifer are net sand thickness and recharge.

The 1,000 milligrams per liter total dissolved solids concentration contour is located from zero to more than 25 miles downdip from the outcrop. The most extensive freshwater area underlies Madison, Houston, and Trinity counties, where the net sand thickness is the greatest (over 200 feet) and the 1,000 milligrams per liter total dissolved solids concentration contour extends the furthest distance downdip.

Areas where the 1,000 milligrams per liter total dissolved solids concentration contour approaches or intersects the outcrop include: the Paige graben area in Bastrop, Lee, and Fayette counties, the Angelina River in Nacogdoches County, and in eastern Sabine County near the Texas-Louisiana state line. These areas generally have a net sand thickness that is less than 100 feet. Additionally, these areas have reduced groundwater recharge due to surface water-groundwater interaction via stream piracy, the structural configuration of large-offset faults in the outcrop, and limited sand influx during deposition, which are elaborated below.

Groundwater and surface water interact with one another where rivers flow over the outcrop of the Sparta Aquifer. When the groundwater table is higher than the surface water level, groundwater discharges to the surface water feature as baseflow, instead of continuing in a downdip direction along the predominant path of regional flow. This dynamic is evident along the Angelina River, or Nacogdoches County line located south of the Sparta Formation outcrop (William F. Guyton & Associates, 1970). The 1,000 and 3,000 milligrams per liter total dissolved solids concentration contours both deviate to within three miles of the outcrop in this area. Some portion of recharge flows into the Angelina River instead of continuing southward into the downdip portion of the aquifer. The

reduced recharge to the downdip portion of the aquifer minimizes flushing of the aquifer with fresher groundwater, increases residence time, and thus creates higher salinity.

The Paige graben has at least one large-offset fault that is located on the northwest side of the graben and has an offset of approximately 700 feet. Several shorter faults were identified on the east side of the graben with 200 to 700 feet of offset.

Young and others (2017) interpreted 20 geophysical logs along two transects of the Paige graben to characterize fault locations and offset and ran a statistical analysis of nearly 100 aquifer pump tests within the Milano fault zone comparing early and late transmissivity values using the Cooper-Jacobs straight line method. A change of slope on a semi-log plot of time and drawdown data suggests a change of aquifer transmissivity. For wells located near faults, the change indicates influence of the fault. In this context, early transmissivity is the portion of time-drawdown data before the slope change, and late transmissivity is the portion of time-drawdown data after the slope change. The analysis concluded that over 60 percent of wells located within four miles of a large-offset fault (offset greater than 500 feet) exhibit low transmissivity because of fault proximity. The investigation further observed that the influence of high-offset faults on groundwater flow is attenuated within eight miles (Young and others, 2017).

The salinity distribution in Bastrop, Lee, and Fayette counties reflects reduced recharge within and downdip of the graben where both measured and estimated total dissolved solids concentration values are slightly saline (1,000 to 3,000 milligrams per liter). The slightly saline portion of the aquifer extends approximately 25 miles downdip from the outcrop in this portion of the study area.

The net sand thickness within the 3,000 milligrams per liter total dissolved solids concentration contour is less than 150 feet in western Sabine County and is less than 80 feet at the Texas-Louisiana state line, which is relatively thin compared to the remainder of the study area. The distribution of moderately saline waters in the East Sparta study area encompasses a relatively wide swath of the Sparta Formation under Grimes, Montgomery, Walker, and Washington counties. A narrower band of moderately saline groundwater underlies Austin, Colorado, Trinity, Angelina, San Augustine, and Sabine counties.

The net sand thickness at the southern extent of the 10,000 milligrams per liter contour is less than 50 feet, and the assumed nearly stagnant groundwater flow can be attributed to the low sand content in this portion of the study area. The part of the study area that is classified as very saline is primarily located in Walker, Polk, Tyler, Jasper, and Newton counties.

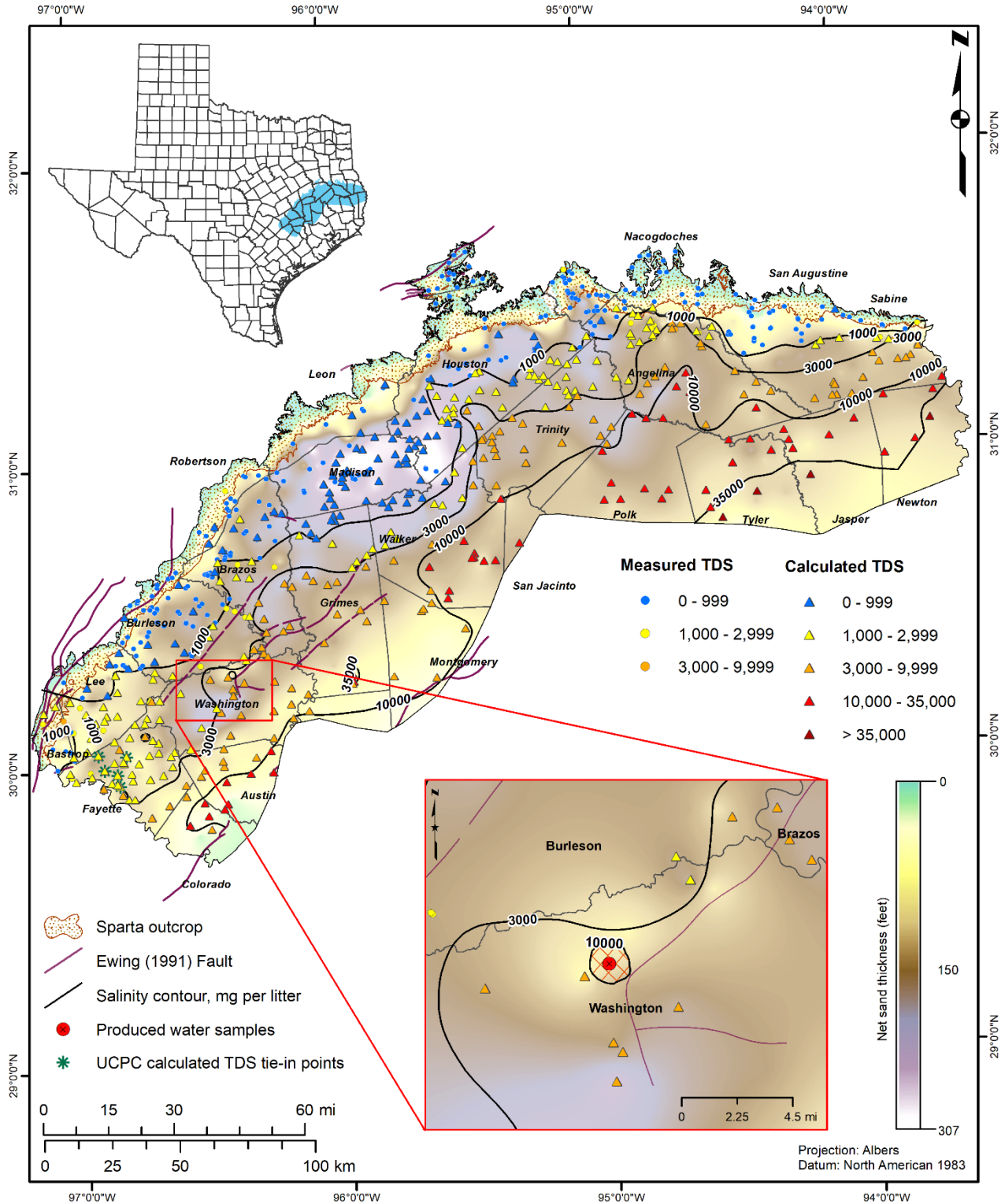


Figure 10.4-1. Measured and calculated water quality results with final total dissolved solids concentration (TDS) contours. The inset map shows the location of calculated and produced water sample data near the Clay Creek salt dome.

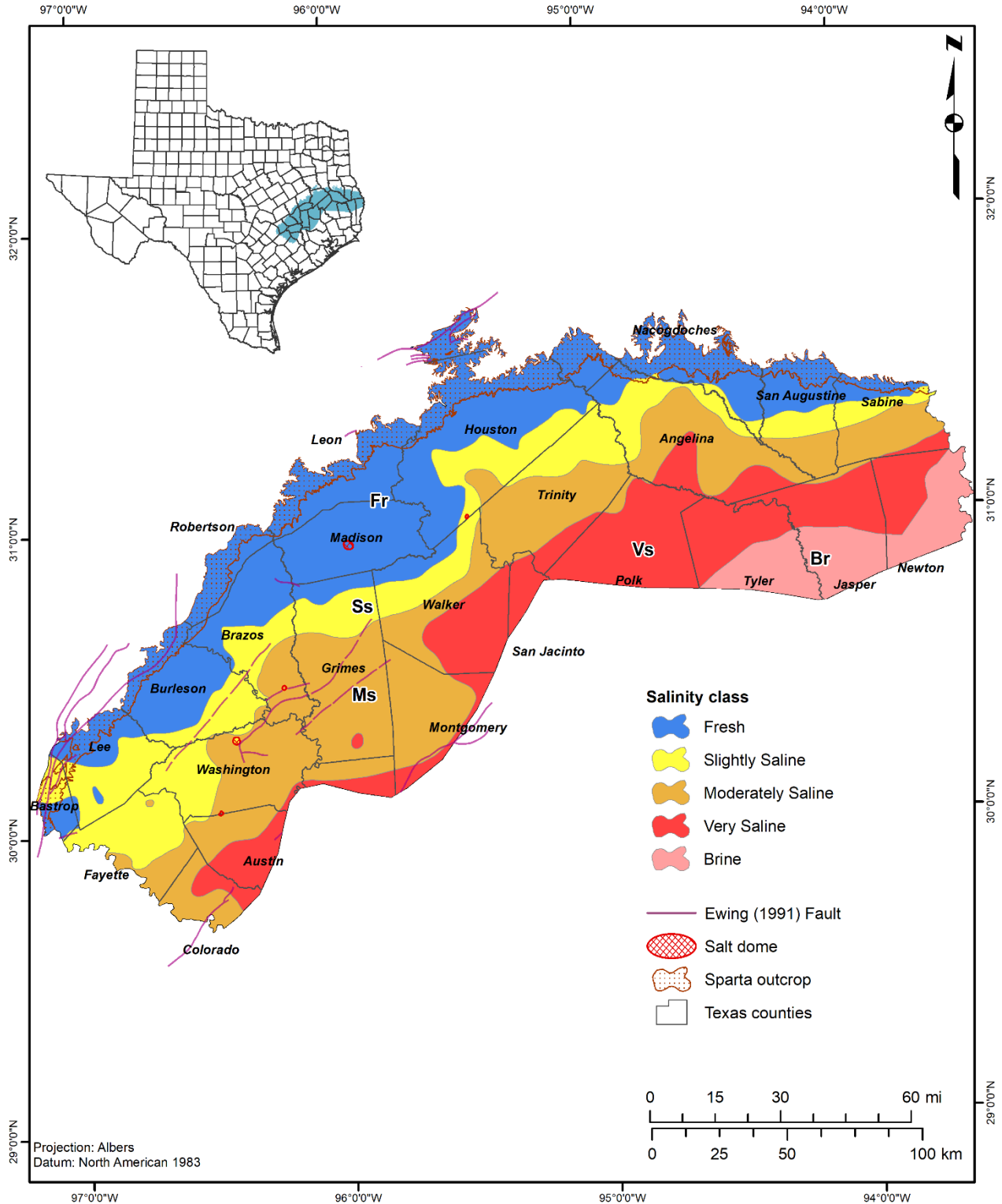


Figure 10.4-2. Salinity zones in the study area.

11 Groundwater volumes

Total aquifer storage volumes were calculated to estimate groundwater volumes in the salinity zones of the East Sparta aquifer. These volumes are for the groundwater salinity classes defined in Section 10.3 (slightly saline, moderately saline, very saline, and brine) that were derived using water quality samples and analysis of geophysical data.

Our primary purpose for calculating these volumes is to provide some form of quantitative volumetric measurement of the brackish groundwater resources in the East Sparta aquifer. These volumes should not be used for formal water planning purposes, nor should they be used in place of site-specific studies when developing a well field.

Figure 11-1 shows a simplified schematic of groundwater conditions in an unconfined aquifer (left) and a confined aquifer (right). Groundwater storage volume in an unconfined aquifer is the volume of storage attributed to drainage ($V_{drained}$) (Equation 11-1a) from declining water level conditions ($V_{drained}$). Groundwater volume calculations in a confined aquifer typically include both 1) the portion of the aquifer storage volume derived from drainage under a declining potentiometric surface condition ($V_{drained}$) and 2) the portion of aquifer storage that is from compressibility of aquifer materials and water ($V_{confined}$) (Equation 11-1b).

We did not calculate the portion of confined storage volume ($V_{confined}$) above the top elevation of the Sparta Formation (above the base of the Cook Mountain confining unit) because we did not have sufficient static water level data in the downdip portion of the aquifer. Also, confined storage ($V_{confined}$) is practically negligible in comparison to the drainable volume ($V_{drained}$). For the Sparta Aquifer, specific yield values for unconfined conditions that were compiled from previous studies range from 0.1 to a maximum of 0.15, and confined storativity ranges from 10^{-5} to 10^{-1} (Kelley and others, 2004).

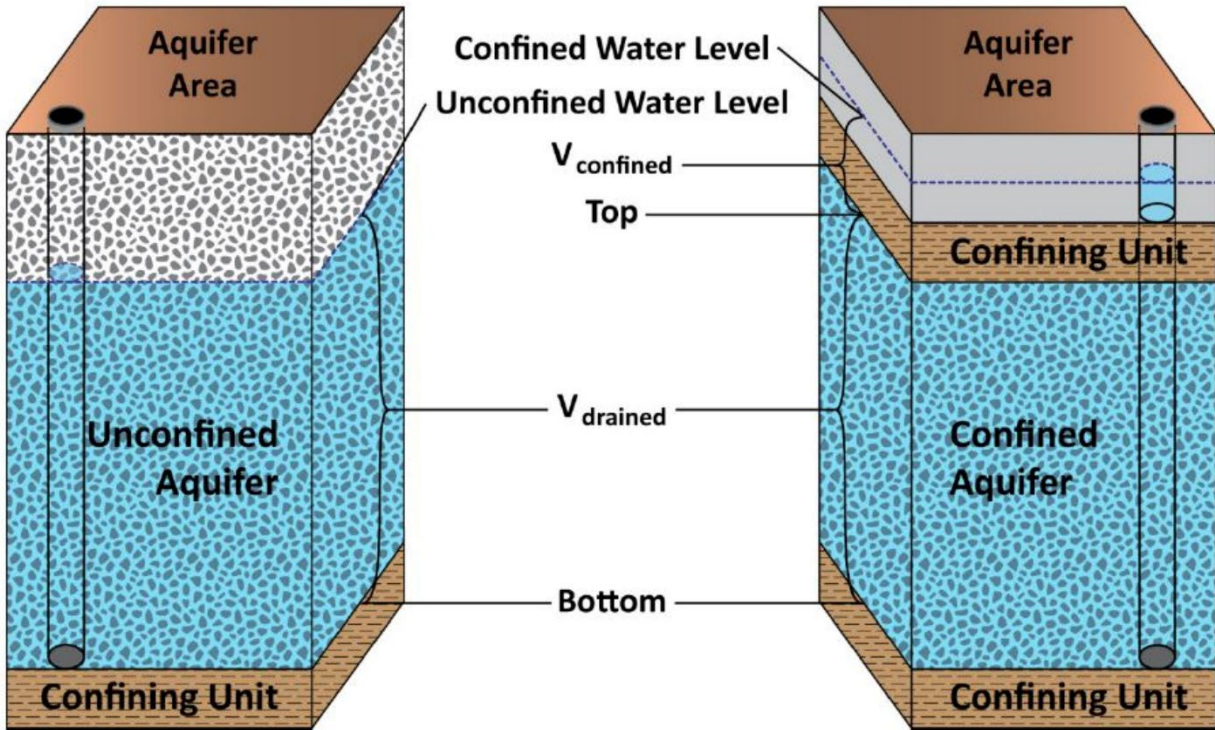


Figure 11-1. Schematic image showing the difference between unconfined and confined aquifer storage (Jigmond and Wade, 2013).

Total aquifer storage volumes for the confined ($V_{drained}$) and unconfined portions of the East Sparta aquifer were estimated using the following equations within each salinity zone:

For unconfined (outcrop):

$$\text{Volume} = V_{drained} = \text{Area} \times (\text{Water level} - \text{Bottom}) \times \text{Percent sand} \times S_y \quad (\text{Equation 11-1a})$$

For confined (subcrop):

$$\text{Volume} = V_{drained} = \text{Area} \times (\text{Top} - \text{Bottom}) \times \text{Net sand thickness} \times S_y \quad (\text{Equation 11-1b})$$

where:

$V_{drained}$ = storage of volume of water draining from the formation (acre-feet)

Area= aquifer area (acres)

Thickness = thickness of aquifer (feet)

Saturated thickness = net thickness of the formation below water level (feet),

Net sand thickness = cumulative portion of aquifer composed of sand(feet)

Percent sand = net sand divided by thickness of the unit multiplied by 100

Water level = groundwater elevation (feet above mean sea level)

Top = elevation of aquifer top (feet above mean sea level)

Bottom = elevation of aquifer bottom (feet above mean sea level)

Sy = specific yield (unitless)

The study area was subdivided into cells, and volumes were calculated for individual cells, which were summed to find the storage volume per salinity zone. Percent sand was calculated for each data location in the study area by dividing the net sand thickness (of a fully penetrating borehole) by the total formation thickness. Net sand was used to characterize saturated sand thickness in the outcrop. Net sand calculations are also discussed in Section 7.5.

11.1 Area

Using ArcGIS 10.7®, we resampled the snapgrid shapefile (the study extent and grid cell template), the Sparta Formation top and bottom rasters, and the net sand thickness raster from 250-foot by 250-foot to 1,500-foot by 1,500-foot cells due to computer processing capabilities. Although bilinear resampling can result in smoothing of the surface, we used this method because it is recommended for continuous data. The area of each 1,500-foot grid cell is then 51.65 acres. This value was manually input using the ArcGIS 10.7® Field Calculator tool.

$$\text{Area per grid cell} = 1,500 \text{ feet} \times 1,500 \text{ feet} \times \frac{1 \text{ acre}}{43,560 \text{ feet}^2} = 51.65 \text{ acres}$$

(Equation 11-2)

11.2 Saturated thickness

Saturated thickness was calculated in one of two ways depending on whether a cell was in the East Sparta aquifer outcrop or subcrop. Cells were assigned either an “O” for outcrop or “S” for subcrop. Where the aquifer is under confined conditions, mostly downdip of the outcrop, it was assumed to be fully saturated with groundwater. Therefore, the net sand value was used for saturated thickness. Where the aquifer is unconfined (in the outcrop) the saturated thickness of each grid cell was based on the static water elevation minus the formation bottom elevation, which was then multiplied by the percent sand to approximate the saturated net sand thickness. Percent sand was calculated by dividing net sand by formation thickness and multiplying by 100. Net sand calculations and raster creation are discussed in section 7.5 of this report.

11.3 Static water level

An interpolated static water level raster was necessary to determine the saturated thickness within the outcrop and downdip to the freshwater line. The TWDB Groundwater Database and Texas Department of Licensing and Regulation databases were imported into MS Access® and the tables were linked to the BRACS Database. Through database queries we utilized the aquifer determination method (described in Section 8) to find wells completed in the Sparta and appended static water level depths into the study static water level table (tblUCPE_SWL_master). To approximate current static water level elevations, we

only included the most recent record for each well with a measurement year greater than or equal to 1999. This process resulted in 72 locations with static water level elevation measurements.

We interpolated a depth to water raster from 1) equidistant points on the base of Sparta Formation contact in the outcrop with an assigned depth of zero feet (sp_ucpe_swl_otc_zero_pt.shp), 2) the depth to water sourced from the TWDB Groundwater Database (sp_ucpe_gwdb_swl_pt.shp), and 3) the depth to water sourced from the State Driller Reports Database (sp_ucpe_tdlr_swl_pt.shp), using the Topo to Raster tool in ArcGIS 10.7®. Depth was interpolated first, then converted to elevation, because the amount of raster correction needed when interpolating elevation was generally greater. We converted the depth raster to elevation using the Raster Calculator tool to add the digital elevation model values to depth. For quality control, wherever our interpolated water level elevations projected above ground surface, we set static water level equal to the digital elevation model. Where static water level elevation projected below the base of the Sparta, static water level was set to the base of Sparta elevation. The resulting raster was then clipped to the outcrop for calculating the volume of water in the unconfined portion of the aquifer.

11.4 Specific Yield

For this study as well as the Upper Coastal Plains Central, the Sparta Aquifer was assigned a specific yield value of 0.1 based on literature review (Young and others, 2018), and (Meyer and others, 2020), and this value was assigned to all cells in the study area.

11.5 Results

The East Sparta aquifer has a total brackish aquifer storage volume of approximately 50 million acre-feet of brackish groundwater with total dissolved solid concentrations between 1,000 and 9,999 milligrams per liter. The total brackish aquifer storage volume is the sum of 22.2 and 27.8 million acre-feet of slightly saline and moderately saline groundwater, respectively (Table 11.5-1). Additionally, we subdivided the volumes for administrative boundaries (Table 11.5-2, Table 11.5-3, and Table 11.5-4).

Brackish groundwater volumes are greatest in Groundwater Management Area 11, with a total of 20.6 million estimated acre-feet from slightly to moderately saline. Bluebonnet Groundwater Conservation District contains the greatest calculated volume of slightly saline to brine groundwater in the Sparta Aquifer. For more information about the calculation of groundwater volume in ArcGIS 10.7®, see Appendix H.

The volumes calculated in this study are estimates to be used to provide insight into the magnitude and distribution of this important resource. We recommend that site-specific studies be conducted to support projects and efforts that will incorporate brackish groundwater resources into water resources planning. It is also important to note that these volume estimates are not the same as the TWDB-calculated total estimated recoverable storage (TERS) volumes, which are confined to the aquifer boundaries used by TWDB groundwater availability models. Furthermore, the area, saturated thickness, and

storage parameters used in the calculations for this study are different from those used in TERS reports, (Wade and others, 2014a, Wade and Shi, 2014b).

The volume calculation method used for this BRACS study is essentially the same as for the total estimated recoverable storage (TERS) volumes. However, the primary variance in the calculations are 1) the $V_{drained}$ calculation incorporates the percent sand value to estimate saturated net sand thickness, 2) the BRACS study has greater data density and stratigraphic control in the downdip portion of the aquifer than what was utilized to calculate the TERS volumes, and 3) the storage volume attributed to specific storage (reduction in pore space and expansion of water) in the confined portion of the aquifer is not included.

Differences in the area used to calculate brackish groundwater volumes arise due to: (1) differences in the areal extent of the GAM models, as brackish groundwater often extends beyond the official TWDB boundaries for major and minor aquifers used to develop TERS, and (2) differences in the grid cell size and orientation of the GAM models used to estimate area.

Differences in the saturated thickness used to calculate brackish groundwater volumes arise due to: (1) differences in aquifer top and bottom elevations and static water levels due to differences in interpretations and data availability during subsurface mapping and (2) whether bulk aquifer thickness (static water level or aquifer top minus aquifer bottom) or net sand, or percent sand, was used to estimate feet of saturated aquifer thickness.

Differences in the storage component used to calculate brackish groundwater volumes include: (1) the value of specific yield (the ratio of drainable water in an aquifer, which is less than porosity), (2) whether volumes calculated from specific yield are further reduced to “recoverable volumes,” and (3) whether confined storage is included, though this is generally a negligible volume.

Additionally, TERS does not take water quality into account and therefore cannot be directly compared to BRACS volumes which are divided by salinity class categories.

Not all brackish groundwater can be produced or economically developed. These volumes do not consider the effects of land surface subsidence, degradation of water quality, or any changes to surface water-groundwater interaction that may result from extracting groundwater from the aquifer. These volumes should not be used for joint groundwater planning or evaluation of achieving adopted desired future conditions in the same way TERS and modeled available groundwater are used according to the joint planning process described in Texas Water Code § 36.108.

Table 11.5-1. Total brackish storage volume in the East Sparta aquifer per salinity class (in millions of acre-feet).

Salinity zone	Slightly saline	Moderately saline	Very saline	Brine	Total volume
Total	22.2	27.8	17.7	4.7	72.5

Table 11.5-2 Total brackish storage volume (in acre-feet) of the East Sparta aquifer in each groundwater management area (GMA) by salinity class.

GMA	Slightly saline	Moderately saline	Very saline	Brine	Total volume
11	8,858,600	11,733,600	2,541,500	0	23,133,700
12	5,780,200	1,852,400	0	0	7,632,600
14	6,307,000	13,183,100	15,036,000	4,742,900	39,269,000
15	1,238,800	1,073,600	145,700	0	2,458,100
Total	22,184,600	27,842,700	17,723,200	4,742,900	72,493,400

Table 11.5-3. Total brackish storage volume (in acre-feet) of the East Sparta aquifer in each regional water planning area (RWPA) by salinity class.

RWPA	Slightly saline	Moderately saline	Very saline	Brine	Total volume
G	8,743,200	9,485,400	94,100	0	18,322,600
H	2,572,000	7,870,200	6,673,600	0	17,115,800
I	8,662,100	9,393,100	10,809,900	4,742,900	33,607,900
K	2,207,400	1,094,100	145,600	0	3,447,100
Total	22,184,600	27,842,700	17,723,200	4,742,900	72,493,400

Table 11.5-4. Total brackish storage volume (in acre-feet) of the East Sparta aquifer in each groundwater conservation district (GCD) per salinity class.

GCD	Slightly saline	Moderately saline	Very saline	Brine	Total volume
Bluebonnet GCD	4,261,300	7,669,300	3,307,400	0	15,238,000
Brazos Valley GCD	1,569,500	1,748,800	0	0	3,318,300
Colorado County GCD	0	396,100	145,600	0	541,700
Fayette County GCD	2,048,600	698,100	0	0	2,746,600
Harris-Galveston Coastal Subsidence District	0	0	15,400	0	15,400
Lone Star GCD	0	1,820,400	341,800	0	2,162,200
Lost Pines GCD	1,788,900	600	0	0	1,789,600
Lower Trinity GCD	0	289,600	5,675,400	0	5,965,000
Mid-East Texas GCD	0	0	0	0	0
Neches & Trinity Valleys GCD	0	0	0	0	0
Pineywoods GCD	2,060,300	3,930,500	1,650,500	0	7,641,300
Post Oak Savannah GCD	1,610,800	79,500	0	0	1,690,300
Southeast Texas GCD	0	151,100	5,614,300	4,742,200	10,507,600
No GCD	8,845,200	11,058,600	972,700	700	20,877,200
Total	22,184,600	27,842,700	17,723,200	4,742,900	72,493,400

12 Desalination

As of 2004, Texas had the third highest number of municipal brackish groundwater desalination plants (20 plants) in the United States, behind Florida (114 plants) and California (33 plants) out of a total of 234 plants in the United States (Mickley, 2018).

According to the latest TWDB Desalination Database (TWDB, 2023d), there were 38 brackish groundwater desalination plants operating in Texas in 2020. Plant production ranged between 0.023 and 27.5 million gallons per day, with a total capacity of 90 million gallons per day (or 100,769 acre-feet per year). In 2018, the total plant capacity in Florida was 279 million gallons per day and in California, brackish groundwater treatment capacity was 124 million gallons per day (Mickley, 2018).

There are no existing desalination plants within the East Sparta aquifer study area. There are no proposed groundwater desalination water management strategies for the East Sparta aquifer study area in the 2022 State Water Plan (TWDB, 2023a).

12.1 Treatment Methods

Most brackish desalination plants in the United States use reverse osmosis, nano filtration, or electro dialysis reversal. There are only two facilities in the United States that use thermal evaporation and distillation following reverse osmosis. All brackish groundwater plants in Texas use reverse osmosis technology, except for one located in Hudspeth County, which uses both reverse osmosis and electro dialysis reversal. Both processes use membranes, which require maintenance and replacement. The primary difference between the processes is that reverse osmosis uses high pressure flow through the membranes, whereas electro dialysis reversal uses low pressure ion exchange membranes (Mickley, 2018).

12.2 Concentrate disposal options

The five conventional disposal options include 1) discharge to surface water, 2) discharge to sewer or wastewater treatment plant, 3) evaporation pond, 4) land application, and 5) injection well. The location of the facility is the primary driver for selecting the best disposal option, because conventional disposal options are site-specific (Mickley, 2018). Facilities with minimal or zero liquid discharge may also include landfill disposal of solids as an option. According to the TWDB Desalination Database (TWDB, 2023d), discharge to surface water is the most common method used in Texas, especially in areas with high salinity surface water features, followed by evaporation ponds, which are practical only for small capacity plants located in an arid climate. Sewer discharge and land application are more widespread than injection wells, primarily due to the high cost associated with the drilling and completion of injection wells (Mickley, 2018).

13 Future improvements

The TWDB collects and disseminates groundwater data and information to help fulfill its mission to lead the state's efforts in ensuring a secure water future for Texas and its citizens. We have continued interest in obtaining additional study area data and information for inclusion into the BRACS Database. Additional data that can be collected include water quality samples, aquifer tests, and geophysical well logs with complete headers. Specific recommendations are:

- Acquire more porosity logs. These are important to provide insight into porosity and interconnected porosity, including neutron porosity logs, density porosity logs, sonic logs, and nuclear magnetic resonance logs. The lack of porosity and density logs is one of the most significant data gaps that exist with old well logs that were used for this study.
- Integrate well log simulation (numerically simulated well logs) to generate a typical full well log suite (like, a well logged with porosity, density, resistivity, gamma ray, sonic, and spontaneous potential) to expand the formation evaluation capabilities.
- Incorporate previously acquired 3D or 2D seismic data. Seismic profiles can be correlated with available well records to determine the geologic structure of the subsurface beyond the single data point in areas where well density is low.
- Conduct a thorough rock property classification analysis for the study area. Obtain and analyze core samples for each identified rock property region to pin down reliable cementation exponent values, as well as accurate porosity and permeability for the hydrogeologic unit of interest.
- Acquire more lab-analyzed water quality samples between 1,000 to 35,000 milligrams per liter total dissolved solids concentration from wells to build a more robust relationship between total dissolved solid and specific conductance. Additionally, obtaining samples that are more spatially representative would be useful, as many of the samples available to us are from wells completed in the outcrop or shallow subsurface portions of the East Sparta aquifer.

14 Conclusions

This study investigated the salinity distribution of groundwater within the East Sparta aquifer. The salinity distribution has been mapped using both measured and calculated total dissolved solids concentrations. East Sparta aquifer groundwater storage volumes were calculated per salinity classification within various administrative boundaries (counties, groundwater conservation districts, groundwater management areas, and regional water planning groups).

The salinity distribution within the study area is primarily influenced by recharge, which in some areas is significantly affected by groundwater discharging as baseflow to a river segment or a large-offset fault (offset greater than 500 feet). Recharge in the study area is also locally influenced by sand distribution that occurred during deposition. Water quality in areas with low net sand thickness tends to deteriorate more rapidly in the downdip direction than it does in areas with greater net sand thickness. Collectively, these factors contribute to locally reduced downdip flow or a “stagnate zone” of higher salinity groundwater relative to adjacent areas.

We calculated a total brackish groundwater storage volume of approximately 50 million acre-feet within the East Sparta aquifer. This is an aggregate volume comprised of approximately 22.2 million acre-feet of slightly saline and 27.8 million acre-feet of moderately saline groundwater and comprises groundwater with total dissolved solids concentrations between 1,000 and 9,999 milligrams per liter.

The estimated volumes of very saline and brine groundwater within the study area are 17.7 and 4.7 million acre-feet, respectively. These volumes are for groundwater with salinities exceeding 10,000 milligrams per liter of total dissolved solids concentration.

The aggregate volume calculations from BRACS studies that have been completed to date (including this study), indicate that a cumulative storage volume of more than 3.8 billion acre-feet of slightly saline and moderately saline groundwater is available in Texas. The BRACS staff recalculates this volume every time a BRACS study is completed. Not all brackish groundwater in storage can be produced or economically developed. However, these estimates and detailed mapping provide users a beneficial tool to evaluate potential sites for brackish groundwater well fields. These volumes do not consider the effects of land subsidence, degradation of water quality, or any changes to surface water-groundwater interaction that may result from extracting groundwater from the aquifer. These volumes should not be used for joint groundwater planning or evaluation of achieving adopted desired future conditions in the same way total estimated recoverable storage (TERS) and modeled available groundwater are used according to the joint planning process described in Texas Water Code § 36.108.

Finally, information contained in this report is not intended to serve as a substitute for site-specific studies that are required to evaluate local aquifer characteristics and groundwater conditions for a desalination plant. Well-field-scale data collection using test and monitor wells is strongly recommended to evaluate the brackish groundwater resource at a particular site. Collection and evaluation of additional well control in a prospective site area is essential in understanding potential target zones for groundwater development.

15 Acknowledgements

We would like to thank John Meyer, retired from the TWDB, for his immense contribution to the development of brackish aquifer studies in Texas in general, and his help in training team members for the start of this project. Much gratitude goes to Mark Robinson for his expertise on the volume calculation process. Thanks to the rest of the BRACS team for their assistance in the completion of this study, in so many ways. Furthermore, to Andrea Croskrey of the Aquifer Storage and Recovery team for her help in trouble-shooting geographic information system applications.

Thanks also to John Dupnik (Deputy Executive Administrator, Office of Water Science and Conservation), Natalie Ballew (Director, Groundwater), and Erika Mancha (Director, Conservation, and Innovative Water Technologies) for their work putting our team together and for much guidance along the way.

We would like to thank Allan Standen, LLC for his team's in-depth work on data gathering for this study. And finally, we would like to acknowledge Andy Donnelly and his extensive bird knowledge, for his suggestions of numerous photogenic bird species that frequent the East Sparta aquifer study area, and for providing the cover photo for this report.

16 References

- Adams, R.L., 2009, Basement tectonics and origin of the Sabine Uplift: Gulf Coast Association of Geological Societies Transactions, v. 59, p. 3–19.
- Alger, R.P., 1966, Interpretation of electric logs in fresh water wells in unconsolidated sediments, *in* Seventh annual logging symposium transactions – Society of Professional Well Log Analysts: Tulsa, Oklahoma, p. 25.
- Archie, G.E., 1942, The electrical resistivity log as an aid in determining some reservoir characteristics: *Petroleum Technology*, v. 5, p. 54–62.
- Asquith, G.B., and Gibson, C.R., 1982, Basic well log analysis for geologists: American Association of Petroleum Geologists, Methods in Exploration Series, 216 p.
- Baker, E.T., 1994, Stratigraphic nomenclature and geologic sections of the Gulf Coastal Plain of Texas: U.S. Geological Survey 94–461, 20 p.
- Burress, G.T., 1951, Spectrochemical correlation of the Clay Creek salt dome formations: Texas Technical College, 84 p.
- Bushaw, D.J., 1968, Environmental synthesis of the East Texas Lower Cretaceous, *in* Gulf Coast Association of Geological Societies Transactions v 18.:
- Christian, B., and Wuerch, D., 2012, Compilation of results of aquifer tests in Texas: Texas Water Development Board 181, 106 p.
- Core Laboratories, 1972, A survey of the subsurface saline water of Texas: Texas Water Development Board 157, 8 volumes, variously paginated p.
- Dillard, J.W., 1963, Availability and quality of groundwater in Smith County, Texas: Texas Board of Water Engineers 6302, 105 p.
- Doveton, J.H., 1999, Basics of oil & gas log analysis: Kansas Geological Survey, 34 p.
- Dutton, S.P., and Loucks, R.G., 2014, Reservoir quality and porosity-permeability trends in onshore Wilcox sandstones, Texas and Louisiana Gulf Coast: Application to deep Wilcox plays, offshore Gulf of Mexico: *GCAGS Journal*, v. 3, p. 33–40.
- Estep, J.D., 1998, Evaluation of ground-water quality using geophysical logs: Texas Natural Resource Conservation Commission, 516 p.
- Estep, J.D., 2010, Determining groundwater quality using geophysical logs: Texas Commission on Environmental Quality, 85 p.

- Ewing, T.E., 1991, Tectonic Map of Texas and accompanying booklet: The University of Texas, Bureau of Economic Geology State Map, 36 p. and 1 plate.
- Galloway, W.E., 2000, Cenozoic depositional history of the Gulf of Mexico basin: American Association of Petroleum Geologists Bulletin, v. 84, p. 1743–1774.
- George, P.G., Mace, R.E., and Petrossian, R., 2011, Aquifers of Texas: Texas Water Development Board Report 380, 172 p.
- Hackley, P.C., 2012, Geologic assessment of undiscovered conventional oil and gas resources - Middle Eocene Claiborne Group: U.S. Geological Survey 2012–1144, 93 p.
- Hem, J.D., 1985, Study and interpretation of the chemical characteristics of natural water: 263 p. and 4 plates: U.S. Geological Survey 2254.
- Hilchie, D.W., 1978, Applied openhole log interpretation for geologist and engineers: Douglas W. Hilchie, Inc., Golden, Co., variously paginated p.
- Hosman, R.L., and Weiss, J.S., 1991, Geohydrologic units of the Mississippi embayment and Texas coastal uplands aquifer systems, south-central United States: Professional Paper 1416B.
- Hutchison, W.R., Davidson, S.C., Brown, B.J., and Mace, R.E., 2009, Aquifers of the Upper Coastal Plains of Texas: Texas Water Development Board 374, 204 p.
- Jackson, M.P.A., and Wilson, B.D. (Eds.), 1982, Fault tectonics of the East Texas basin, *in* The University of Texas at Austin, Bureau of Economic Geology, p. 35.
- Jigmond, M., and Wade, S., 2013, Total estimated recoverable storage for aquifers in Groundwater Management Area 16: Texas Water Development Board 12–025.
- Kelley, V.A., Deeds, N.E., Fryar, D.G., Nicot, J.P., Jones, T.L., Dutton, A.R., Bruehl, G., Unger-Holtz, T., and Machin, J.L., 2004, Groundwater availability models for the Queen City and Sparta Aquifers: INTERA, Inc., University of Texas Bureau of Economic Geology, and R.J. Brandes Company, 867 p.
- Kreitler, C.W., Agagu, O.K., Basciano, J.M., Collins, E.W., Dix, O.R., Dutton, S.P., Fogg, G.E., Giles, A.B., Guevara, E.H., Harris, D.W., Hobday, D.K., McGowen, M.K., Pass, D., and Wood, D.H., 1980, Geology and geohydrology of the East Texas basin, A report of the progress of nuclear waste isolation feasibility studies: The University of Texas at Austin, Bureau of Economic Geology 80–12, 121 p.
- Larkin, T.J., and Bomar, G.W., 1983, Climatic atlas of Texas: Texas Department of Water Resources LP-192, 157 p.

LBG-Guyton & Associates, 2003, Brackish Groundwater Manual for Texas Regional Water Planning Groups: Texas Water Development Board, 199 p.

Meyer, J.E., Croskrey, A.D., Suydam, A.K., and Van Oort, N., 2020, Brackish groundwater in aquifers of the Upper Coastal Plains, Central Texas: Texas Water Development Board 385, 291 p.

Meyer, J.E., Croskrey, A.D., Wise, M.E., and Kalaswad, S., 2014, Brackish groundwater in the Gulf Coast Aquifer, Lower Rio Grande Valley, Texas: Texas Water Development Board 383, 169 p.

Mickley, M., 2018, Updated and extended survey of U.S. municipal desalination plants: Prepared for the U.S. Department of the Interior Bureau of Reclamation Desalination and Water Purification Research and Development Program 155, Treatment of Concentrate, 56 p.

Myers, B.N., 1969, Compilation of results of aquifer tests in Texas: Texas Water Development Board 98, 532 p.

Oliveira, M.F.S., Lima, I., Ferruccio, P.L., Abreu, C.J., Borghi, L., and Lopes, R.T., 2011, Application of nuclear logging to porosity studies in Itaborai Basin, *in* 2011 International Nuclear Atlantic Conference – Belo Horizonte, MG, Brazil.

Parkhurst, D.L., and Appelo, C.A.J., 2013, Description of input and examples for PHREEQC version 3: a computer program for speciation, batch-reaction, one-dimensional transport, and inverse geochemical calculations: Techniques and Methods 6-A43, 519 p.

Payne, J.N., 1968, Hydrologic significance of the lithofacies of the Sparta Sand in Arkansas, Louisiana, Mississippi, and Texas: U.S. Geological Survey 569-A, 22 p.

Payne, J.N., 1970, Geohydrologic significance of lithofacies of the Cockfield Formation of Louisiana and Mississippi and of the Yegua Formation of Texas, Geohydrology of the Claiborne Group: U.S. Geological Survey 569-B, 22 p.

Pearson, K., 2012, Geologic models and evaluation of undiscovered conventional and continuous oil and gas resources - Upper Cretaceous Austin Chalk, U.S. Gulf Coast: U.S. Geological Survey, 33 p.

Pickett, G.R., 1963, Acoustic character logs and their applications in formation evaluation: *Journal of Petroleum Technology*, v. 15, no. 6, p. 659–667.

Ricoy, J.U., 1976, Depositional systems in the Sparta Formation (Eocene) Gulf Coast Basin of Texas: The University of Texas at Austin master's thesis, 110 p.

Ricoy, J.U., and Brown, L.F., Jr., 1977, Depositional systems in the Sparta Formation (Eocene) Gulf Coast basin of Texas: The University of Texas at Austin, Bureau of Economic Geology 77-7, 17 p.

Rittgers, J.B., 2019, Refining Well Log Interpretation Techniques for Determining Brackish Aquifer Water Quality: U.S. Department of the Interior Bureau of Reclamation Research and Development Office Research and Development Office Science and Technology Program ST-2018-7106-01, 191 p.

RRC, 2023d, Railroad Commission of Texas Data Sets for Download, at https://www.rrc.texas.gov/resource-center/research/data-sets-available-for-download/#digital_map.

RRC, 2023e, Railroad commission of Texas Public GIS Viewer, at <https://www.rrc.texas.gov/resource-center/research/gis-viewer/>.

RRC, 2023b, Railroad Commission of Texas Underground Injection Control database.:

RRC, 2023a, Railroad Commission of Texas Wellbore database: Railroad Commission of Texas.

Sandeen, W.M., 1972, Ground-water resources of Washington County, Texas: Texas Water Development Board 162, 111 p.

Schlumberger, 2009, Log interpretation charts, 2009 edition:, 310 p.

Schorr, S., Zivic, M., Hutcison, W.R., Panday, S., and Rumbaugh, J., 2020, Conceptual model report: Groundwater Availability Model for northern portion of the Queen City, Sparta, and Carrizo-Wilcox Aquifers: Montgomery & Associates 1648302063, 240 p.

Seni, S.J., Mullican, W.F.I., and Hamlin, H.S., 1985, Texas salt domes: Natural resources, storage caverns, and extraction technology: The University of Texas at Austin, Bureau of Economic Geology IAC (84-85)-1019, 167 p.

Standen, A.R., Clause, V.A., Hoadley-Leist, A.D., and Peacock, C.W., 2021, Upper Coastal Plains East aquifer data entry for the Brackish Resources Characterization System database: Texas Water Development Board 2000012440, 17 p.

TCEQ, 2023a, Texas Commission on Environmental Quality Source Water Assessment & Protection Viewer version 4.2, at <https://www.arcgis.com/apps/webappviewer/index.html?id=217028ea4a01485f87db4d22aec72755>.

TCEQ, 2023b, Texas Commission on Environmental Quality Water Well Viewer version 5.0, at <https://tceq.maps.arcgis.com/apps/webappviewer/index.html?id=aed10178f0434f2781daff19eb326fe2>.

TDLR, 2023, Texas Department of Licensing and Regulation Submitted Drillers Reports Database, at <https://www.twdb.texas.gov/groundwater/data/drillersdb.asp>.

Torres-Verdin, C., 2017, Integrated geological-petrophysical interpretation of well logs: The University of Texas at Austin, Department of Petroleum and Geosystems Engineering.

TWDB, 2007, The Geologic Atlas of Texas: U.S. Geological Survey, contract geodatabase to the Texas Water Development Board, Version 3.

TWDB, 2023, Brackish Resources Aquifer Characterization System database data dictionary: Texas Water Development Board Open-File 12-02, Sixth Edition, 322 p.

TWDB, 2023a, Texas Water Development Board 2022 State Water Plan, Interactive, at <https://2022.texasstatewaterplan.org/statewide>.

TWDB, 2023b, Texas Water Development Board Brackish Resources Aquifer Characterization System (BRACS), at <http://www.twdb.texas.gov/groundwater/bracs/index.asp>.

TWDB, 2023c, Texas Water Development Board Brackish Resources Aquifer Characterization System (BRACS) Database, at <https://www.twdb.texas.gov/groundwater/bracs/database.asp>.

TWDB, 2023d, Texas Water Development Board Desalination Plant Database, at <http://www.twdb.texas.gov/innovativewater/desal/maps.asp>.

TWDB, 2023e, Texas Water Development Board Groundwater Database, at <https://www.twdb.texas.gov/groundwater/data/gwdbbrpt.asp>.

TWDB, 2023f, Texas Water Development Board Texas Water Service Boundary Viewer, at <https://www3.twdb.texas.gov/apps/WaterServiceBoundaries>.

TWDB, 2023g, Texas Water Development Board Water Data Interactive Groundwater Data Viewer, at <https://www3.twdb.texas.gov/apps/WaterDataInteractive/GroundWaterDataViewer>.

USGS, 2023a, U.S. Geological Survey GeoLog Locator, at <https://webapps.usgs.gov/GeoLogLocator/#!/search>.

USGS, 2023b, U.S. Geological Survey National Produced Waters Geochemical Database v2.3, at <https://data.usgs.gov/datacatalog/data/USGS:59d25d63e4b05fe04cc235f9>.

Wade, S., Ph.D., and Shi, J., Ph.D., 2014b, Total estimated recoverable storage for aquifers in groundwater management area 12: Texas Water Development Board 13-035 version 2, 43 p.

Wade, S., Ph.D., Shi, J., Ph.D., and Selter-Weatherford, C., 2014a, Total estimated recoverable storage for aquifers in groundwater management area 11: Texas Water Development Board 13-034, 30 p.

William F. Guyton & Associates, 1970, Ground-water conditions in Angelina and Nacogdoches Counties, Texas: Texas Water Development Board 110, 167 p.

William F. Guyton & Associates, 1972, Ground-water conditions in Anderson, Cherokee, Freestone and Henderson Counties, Texas: Texas Water Development Board 150, 193 p.

Williams, J.H., Lane, J.W., Jr., Singha, K., and Haeni, F.P., 2002, Application of advanced geophysical logging methods in the characterization of a fractured-sedimentary bedrock aquifer, Ventura County, California: United States Geological Survey Water Resources Investigations Report 00-4083, 28 p.

Winslow, A.G., and Kister, L.R., 1956, Saline-water resources of Texas: U.S. Geological Survey Water Supply Paper 1365, 105 p.

Woodruff, C.M., Jr., and McBride, M.W., 1979, Regional assessment of geothermal potential and the Balcones and Luling-Mexia-Talco fault zones, Central Texas: The University of Texas at Austin, Bureau of Economic Geology U.S. Department of Energy, Geothermal Energy ET-78-S-05-5864, 247 p.

Yin, H., and Groshong, R.H., Jr., 2006, Balancing and restoration of piercement structures: geologic insights from 3D kinematic models: *Journal of Structural Geology*, v. 28, p. 99-114.

Young, S., Jigmond, M., Jones, T., Ewing, T.E., Panday, S., Harden, R.W., and Lupton, D., 2018, Groundwater availability model for the central portion of the Sparta, Queen City, and Carrizo-Wilcox aquifers: INTERA, Inc., Frontera, and RW Harden and Associates, 944 p.

Young, S., Jigmond, M., Jones, T., Lupton, D., Ewing, T.E., and Harden, R.W., 2017, Draft report: Conceptualization, investigation, and sensitivity analysis regarding the effects of faults on groundwater flow in the Carrizo-Wilcox aquifer in Central Texas: INTERA, Inc., Frontera, and RW Harden and Associates, 170 p.

17 Appendices

Appendix A. Public water supplies	A-1
Appendix B. BRACS Database	B-1
Appendix C. Geophysical logging tools	C-1
Appendix D. Comparison of stratigraphic interpretations	D-1
Appendix E. Geographic information System datasets	E-1
Appendix F. Porosity calculations	F-1
Appendix G. Modeled water quality data (PhreeqC)	G-1
Appendix H. Calculation of groundwater volumes	H-1

Appendix A. Public water supplies

This appendix provides maps of public water supply systems for the East Sparta aquifer study area. This appendix is referenced from section 4.1 of the report. The maps are tiled into three separate sections for the east, central and west portions of the study area (Figure A-1 through A-3, respectively). The source for the public water supply polygon data is the TWDB Water Service Boundary Viewer (TWDB, 2023f).

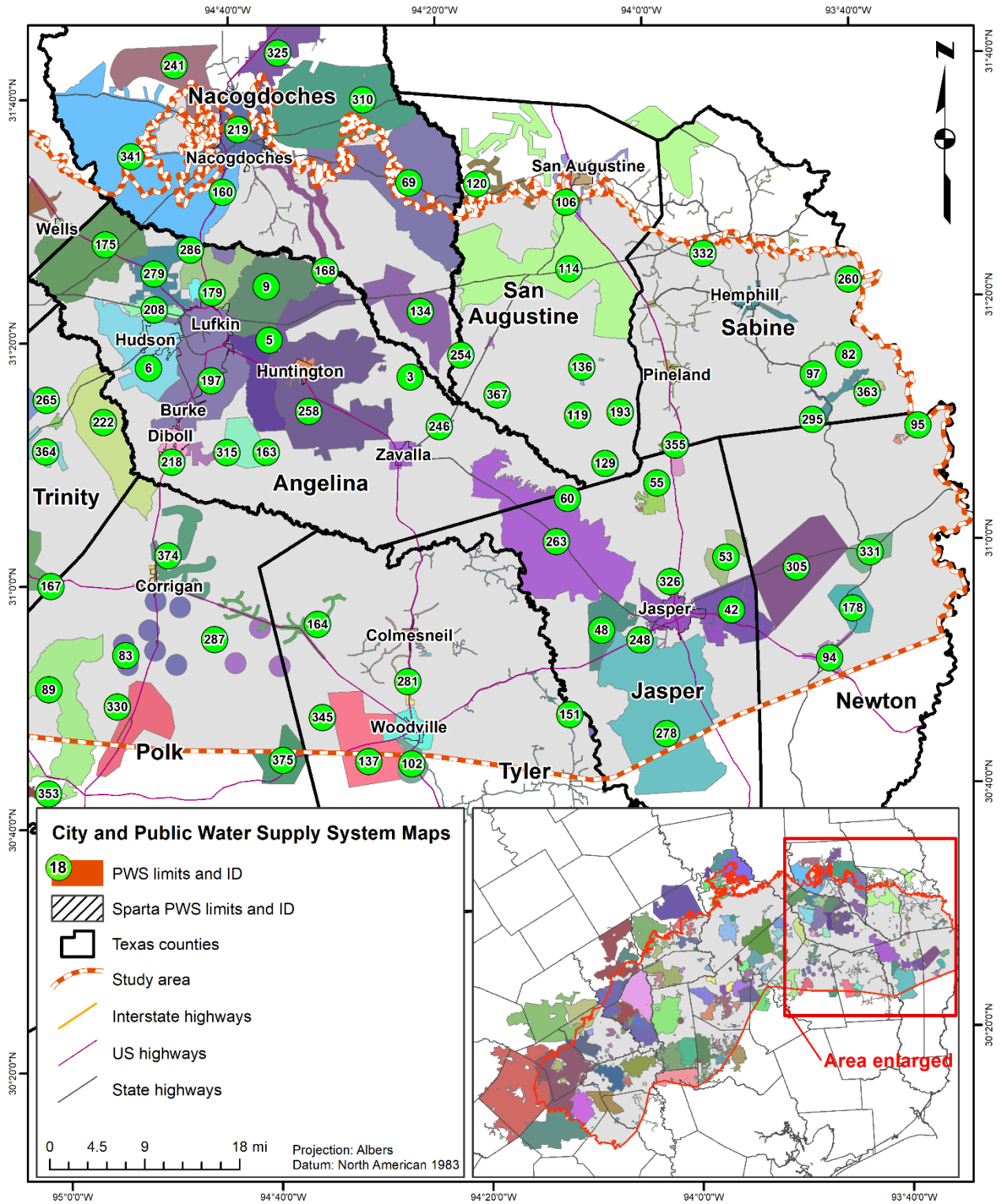


Figure A-1. City and public water supply limits in the eastern part of the study area.

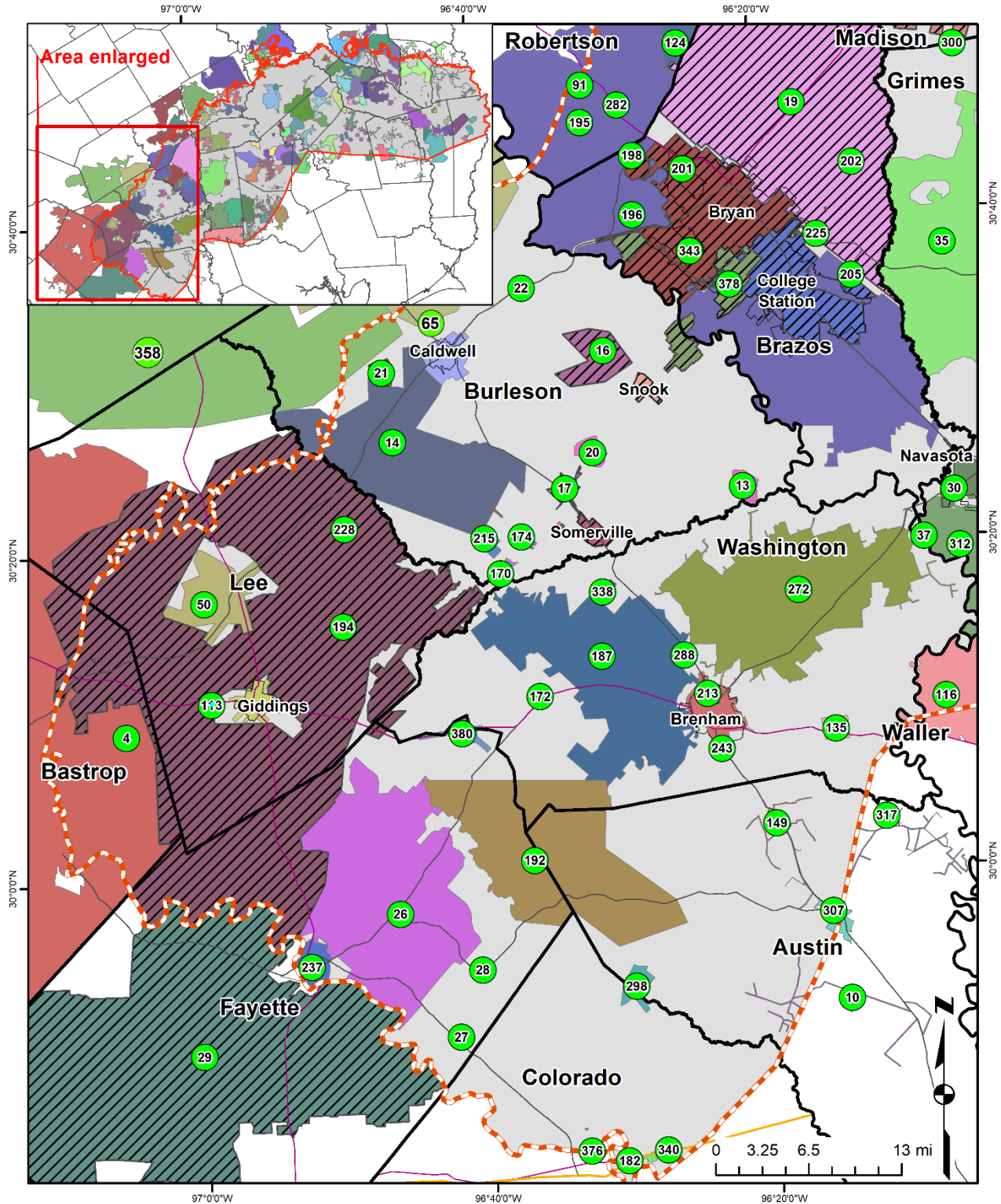


Figure A-3. City and public water supply limits in the western part of the study area.

Table A-1. Cross-reference table between map identification number (green circles) and the public water supply in Figures A-1 through A-3.

Map ID	PWS ID	PWS name	Map ID	PWS ID	PWS name
1	0030002	City of Huntington	35	0030036	Wickson Creek SUD Grimes
2	0030003	Walnut Ridge Estates Water Sys	36	0030037	Poe Bracewell Water Sys
3	0030004	Walnut Bend Water Sys	37	0030038	G & W WSC Field Store
4	0030005	Aqua WSC	38	0030039	Dobbin Plantersville WSC 2
5	0030006	Angelina WSC	39	0030040	Consolidated WSC Rural Sys
6	0030007	Hudson WSC	40	0030041	West Magnolia Forest
7	0030008	Pleasure Point	41	0030042	Anderson Water Sys
8	0030009	Rayburn Water	42	0030043	Holly Huff WSC
9	0030010	M & M WSC	43	0030044	City of Grapeland
10	0030011	Austin County WSC 4	44	0030045	Ratcliff WSC
11	0030012	City of Zavalla	45	0030046	City of Lovelady
12	0030013	City of Snook	46	0030047	City of Browndell
13	0030014	Clay WSC	47	0030048	TDCJ Eastham Unit
14	0030015	Deanville WSC	48	0030049	Rural WSC
15	0030016	Clara Hills Water Sys	49	0030050	Montgomery County MUD 9
16	0030017	Tunis WSC	50	0030051	Lincoln WSC
17	0030018	Lyons WSC	51	0030052	Consolidated WSC Central Sys
18	0030019	Yegua Water Sys	52	0030053	Rayburn Country MUD
19	0030020	Wickson Creek SUD	53	0030054	Harrisburg WSC
20	0030021	Centerline WSC	54	0030055	Lakewood On Lake Conroe
21	0030022	Cade Lakes WSC	55	0030056	Mulberry WS Brookeland FWSD
22	0030023	Cooks Point WSC	56	0030057	City of Magnolia
23	0030024	Forest WSC	57	0030058	Ranch Crest Subd
24	0030025	Barten WSC	58	0030059	City of Normangee
25	0030026	Shiro Water Sys	59	0030060	Hunters Retreat
26	0030027	Fayette WSC East	60	0030061	Westwood WSC
27	0030028	Ellinger Sewer and WSC	61	0030062	Hulon Lakes Subd
28	0030029	City of Fayetteville	62	0030063	Hidden Forest Estates
29	0030030	Fayette WSC West	63	0030064	Caney Creek Utility
30	0030031	City of Navasota	64	0030065	Del Lago Estates WSC
31	0030032	Highway 90 Estates	65	0030066	Milano WSC
32	0030033	Richards Water Sys	66	0030067	Crystal Springs Water Co Chasewood
33	0030034	B & J Water Co	67	0030068	Diamond Head WSC
34	0030035	Roans Prairie	68	0030069	Cimarron Country

Table A-1 (continued). Cross-reference table between map identification number (green circles) and the public water supply in Figures A-1 through A-3.

Map ID	PWS ID	PWS name	Map ID	PWS ID	PWS name
69	0030070	Melrose WSC	103	0030104	Timberlane Water Sys
70	0030071	Lake Livingston Kickapoo Estates	104	0030105	Lakeside WS3
71	0030072	Emerald Lakes Subd	105	0030106	Lake South WSC
72	0030073	Lake Conroe Forest Subd	106	0030107	San Augustine Rural WSC
73	0030074	Lake Windcrest Water Sys	107	0030108	Clear Creek Forest Section 12
74	0030075	Caddo Village	108	0030109	Montgomery County MUD 8
75	0030076	Vista Verde Water Sys	109	0030110	Lake Conroe West
76	0030077	Old Mill Lake	110	0030111	Harborside
77	0030078	Toledo Village WSC	111	0030112	City of Trinity
78	0030079	White Oak Ranch Section One	112	0030113	Walker County SUD F
79	0030080	City of Corrigan	113	0030114	Westwood Villa Apartments
80	0030081	Dogwood Hills	114	0030115	New WSC
81	0030082	City of Willis	115	0030116	Lake Louise Subd
82	0030083	Timberlane Estates Property Owners Association	116	0030117	G & W WSC
83	0030084	Moscow WSC 1	117	0030118	Walston Springs WSC
84	0030085	City of Madisonville	118	0030119	Lake Livingston Sandy Ridge Water
85	0030086	Rolling Forest Subd	119	0030120	El Pinon Estates Water Sys
86	0030087	Saddle & Surrey Acres WSC	120	0030121	Denning WSC
87	0030088	Arrowhead Lake & Frontier Lake	121	0030122	Lake Livingston Sportsmans Retreat
88	0030089	Forest Hills Water Supply	122	0030123	Emerald Woods
89	0030090	Tempe WSC 1	123	0030124	San Jo Utilities
90	0030091	Tanglewood Forest Subd	124	0030125	Wickson SUD Wheelock
91	0030092	Post Oak	125	0030126	Dobbin Plantersville WSC 1
92	0030093	Walker County SUD A	126	0030127	Dodge Oakhurst WSC 2
93	0030094	Far Hills Utility District	127	0030128	Yesterdays Crossing
94	0030095	City of Newton	128	0030129	City of Wells
95	0030096	Tall Timbers WSC	129	0030130	Powell Point Water Sys
96	0030097	Conroe Resort	130	0030131	Yaupon Cove
97	0030098	Shawnee Shores	131	0030132	Montgomery County UD 4
98	0030099	Glen Oaks Water Sys	132	0030133	Walker County SUD D
99	0030100	City of Giddings	133	0030134	Lake Lorraine WS
100	0030101	Branch Wood WSC	134	0030135	Etoile WSC
101	0030102	Montgomery County MUD 126	135	0030136	Chappell Hill WSC
102	0030103	Seneca WSC	136	0030137	Anthony Harbor Subd

Table A-1 (continued). Cross-reference table between map identification number (green circles) and the public water supply in Figures A-1 through A-3.

Map ID	PWS ID	PWS name	Map ID	PWS ID	PWS name
137	0030138	Cypress Creek WSC	171	0030172	Walker County SUD B Crabbs Prairie
138	0030139	Holiday Villages of Livingston	172	0030173	City of Burton
139	0030140	City of Panorama Village	173	0030174	Shorewood Forest Water Sys
140	0030141	Lakeside WS 1	174	0030175	Lakeview N Marshall Oaks Sommerville
141	0030142	Lakeside WS 5	175	0030176	Pollok-Redtown WSC
142	0030143	Harbor Point	176	0030177	Montgomery County MUD 42
143	0030144	Indigo Ranch	177	0030178	Lakeside Estates Subd
144	0030145	Lakewood Water Sys	178	0030179	East Newton WSC
145	0030146	Deep River Plantation	179	0030180	Redland WSC
146	0030147	Indigo Lakes Water Sys	180	0030181	Gulf Coast Trades Center
147	0030148	Whispering Woods	181	0030182	Lakeside WS 4
148	0030149	Lake Conroe Hills MUD	182	0030183	Columbus Oaks Apartments
149	0030150	Austin County WSC 1	183	0030184	Barlow Lake Estates
150	0030151	High Meadows Ranch WS	184	0030185	Angelina County FWSD 1
151	0030152	Town Bluff Water Sys	185	0030186	Bell Water
152	0030153	Forest Woods Subd	186	0030187	Glendale WSC
153	0030154	Hickory Hollow Water Sys	187	0030188	Central Washington County WSC
154	0030155	Doucette Water Sys	188	0030189	Montgomery County UD 3
155	0030156	Burleson County MUD 1	189	0030190	Apache Hills
156	0030157	Green Rich Shores and Sterling Island	190	0030191	Holiday Oaks Subd
157	0030158	Westwood Shores MUD	191	0030192	City of New Waverly
158	0030159	Mostyn Manor	192	0030193	West End WSC
159	0030160	Walker County SUD C	193	0030194	Parkway Water Sys
160	0030161	Nacogdoches County MUD 1	194	0030195	Lee County WSC
161	0030162	City of Elkhart	195	0030196	Wellborn SUD
162	0030163	Lake Livingston Heights WSC	196	0030197	Smetana Forest
163	0030164	Beulah WSC	197	0030198	City of Lufkin
164	0030165	Chester WSC	198	0030199	Lakewood Estates
165	0030166	Anderson County Cedar Creek WSC	199	0030200	Watson Lakes WSC
166	0030167	City of San Augustine	200	0030201	Lakes of Magnolia
167	0030168	Woodlake Jossierand WSC	201	0030202	City of Bryan
168	0030169	Woden WSC	202	0030203	Al Leonard Ranch
169	0030170	Mill Creek Estates	203	0030204	Somerville Place
170	0030171	Birch Creek Recreation WSC	204	0030205	Point Blank & Stephens Creek WSC

Table A-1 (continued). Cross-reference table between map identification number (green circles) and the public water supply in Figures A-1 through A-3.

Map ID	PWS ID	PWS name	Map ID	PWS ID	PWS name
205	0030206	City of College Station	239	0030240	Keenan WSC
206	0030207	Port Adventure	240	0030241	River Oaks Sunshine Acres
207	0030208	Concord-Robbins WSC	241	0030242	Lilly Grove SUD
208	0030209	Woodlawn WSC	242	0030243	Rolling Hills Colony Water Sys
209	0030210	Raylake WSC	243	0030244	Brenham State Supported Living Cent
210	0030211	Oakwood Water Sys	244	0030245	Montgomery County UD 2
211	0030212	High Prairie WS Corporation	245	0030246	Alleyton Water Sys
212	0030213	Riley Road Estates WS	246	0030247	Tx Airstream Harbor Water
213	0030214	City of Brenham	247	0030248	Woodland Lakes Estates WSC
214	0030215	Shannon Place Water Sys	248	0030249	Holmwood Angelina & Neches River Authority
215	0030216	Little Oak Forest Subd	249	0030250	Lakeview Pointe Apartments
216	0030217	City of Broaddus	250	0030251	Leggett WSC
217	0030218	Benchley Oaks Subd	251	0030252	Rogers Road Water Sys
218	0030219	City of Diboll	252	0030253	Magnolia Reserve Water Plant
219	0030220	City of Nacogdoches	253	0030254	Apple Springs WSC
220	0030221	Big Oaks Ranchette Subd	254	0030255	Sutton Hills Estates
221	0030222	Robertson County WSC	255	0030256	Bentwood Bend Water Sys
222	0030223	Nigton Wakefield WSC	256	0030257	City of Pineland
223	0030224	Southeast WSC Sys 4	257	0030258	Loch Ness Cove Subd Water Sys
224	0030225	City of Colmesneil	258	0030259	Four Way SUD
225	0030226	Glen Oaks MHP	259	0030260	Bridgepoint Subd
226	0030227	City of Conroe	260	0030261	El Camino Bay Water Sys
227	0030228	City of Woodville	261	0030262	Cape Malibu WSC
228	0030229	Lee County FWSD 1	262	0030263	Montgomery County FWSD 6
229	0030230	Trinity Rural WSC 3	263	0030264	Upper Jasper County Water Authority 1
230	0030231	Crown Ranch Subd	264	0030265	Pennington WSC
231	0030232	Southeast WSC Sys 3	265	0030266	Nogalus Centralia WSC
232	0030233	Clover Creek MUD	266	0030267	Woodhaven Estates
233	0030234	Enchanted Cove Water Sys	267	0030268	Flamingo Lakes Lot Owners Association Inc
234	0030235	Pinehurst Decker Prairie WSC	268	0030269	Texas Grand Ranch
235	0030236	Mount Pleasant Village Water Sys	269	0030270	Gun & Rod Estates
236	0030237	Conroe Bay Water Sewer Supply	270	0030271	Twin Creek WSC
237	0030238	City of La Grange	271	0030272	Grand Harbor Water Sys
238	0030239	Waterwood MUD 1	272	0030273	Northeast Washington County

Table A-1 (continued). Cross-reference table between map identification number (green circles) and the public water supply in Figures A-1 through A-3.

Map ID	PWS ID	PWS name	Map ID	PWS ID	PWS name
273	0030274	Southeast WSC Sys 2	307	0030308	City of Bellville
274	0030275	Bee Creek Estates	308	0030309	Canyon Park WSC
275	0030276	Onalaska WSC	309	0030310	Grand Oaks MUD
276	0030277	Shadow Bay Subd	310	0030311	Swift WSC
277	0030278	Riverside SUD	311	0030312	Wildwood Shores
278	0030279	Upper Jasper County Water Authority 2	312	0030313	TDCJ W Pack Unit
279	0030280	Lufkin State Supported Living Cent	313	0030314	Walnut Cove WSC
280	0030281	Blaketree MUD 1	314	0030315	Havenshire Water Sys
281	0030282	Windmill Mobile Home Estates	315	0030316	Prairie Grove WSC
282	0030283	Oak Forest Lakeway Manor	316	0030317	Shady Brook Acres
283	0030284	Carousel MHP	317	0030318	Austin County WSC 2
284	0030285	Montgomery Trace Water Sys	319	0030320	Lake Conroe Terrace Water Sys
285	0030286	Corinthian Point MUD 2	320	0030321	Hazy Hollow East Estates
286	0030287	Central WC&ID of Angelina County	321	0030322	Deer Run and White Rock City Marina
287	0030288	Moscow WSC 2	322	0030323	Paradise Cove Water Sys
288	0030289	Oak Hill FWSD 1	323	0030324	Beau View Utilities
289	0030290	City of Leona	324	0030325	Phelps SUD
290	0030291	Lake Bonanza WSC	325	0030326	Appleby WSC
291	0030292	Stanley Lake MUD	326	0030327	City of Jasper
292	0030293	Point Aquarius MUD	327	0030328	New Danville Community
293	0030294	Slocum WSC	328	0030329	Mink Branch Valley
294	0030295	Clear Water Cove Incorporated	329	0030330	Fountain Lake Owners WSC
295	0030296	South Sabine WSC	330	0030331	Texas Water Supply
296	0030297	Shady Oaks Estates	331	0030332	Burkeville WSC
297	0030298	Falls of Wildwood	332	0030333	G M WSC
298	0030299	New Ulm WSC	333	0030334	Trinity Rural WSC 2
299	0030300	Southeast WSC Sys 1	334	0030335	Shady Oaks MHP
300	0030301	North Zulch MUD	335	0030336	City of Huntsville
301	0030302	City of Groveton	336	0030337	City of Midway
302	0030303	City of Kennard	337	0030338	City of Crockett
303	0030304	Stillwater Estates	338	0030339	Lake Forest Water Sys
304	0030305	City of Caldwell	339	0030340	Flo Community WSC
305	0030306	Jamestown WSC	340	0030341	Happy Oaks
306	0030307	City of Montgomery	341	0030342	D & M WSC

Table A-1 (continued). Cross-reference table between map identification number (green circles) and the public water supply in Figures A-1 through A-3.

PWS ID	PWS name	Map ID	PWS ID	PWS name
0030343	Pine Lake Subd North WSC	365	0030366	Trinity Rural WSC 1
0030344	Ramblewood MHP	366	0030367	Spring Preserve Water Sys
0030345	City of Somerville	367	0030368	La Playa Subd Water Sys
0030346	White Tail Ridge Lakes Estates	368	0030369	G & W WSC Woodland Lakes Water Sys
0030347	Pine Vista Mobile Home Village	369	0030370	Lake Forest Falls Subd
0030348	Montgomery County MUD 18	370	0030371	TDCJ Ferguson Unit
0030349	Starlite MHP	371	0030372	Grassy Creek MHP
0030350	Whispering Pines Lake Water	372	0030373	Lake Conroe Village
0030351	Lazy River MHP	373	0030374	Lake Livingston Oakridge North
0030352	Tyler County SUD	374	0030375	Damascus Stryker WSC
0030353	TDCJ Luther Units	375	0030376	Woods Creek WSC
0030354	Lake Livingston Pineshadows East	376	0030377	Cardon Loop
0030355	Bft Family Trailer Park	377	0030378	Wood Acres MHP
0030356	Brookeland FWSD	378	0030379	Texas A&M University Main Campus
0030357	Westmont Mobile Home Community	379	0030380	Leaning Oak MHP
0030358	Hilltop Lakes WSC	380	0030381	City of Carmine
0030359	Southwest Milam WSC	381	0030382	The Oaks
0030360	Thousand Oaks	382	0030383	Lake Livingston WS& Sewer Ser
0030361	Emerald Estates	383	0030384	Sunrise Ranch
0030362	Kickapoo Preserve Subd	384	0030385	Lakeside WS 2
0030363	North Lake Estates	385	0030386	Oak Hollow Subd
0030364	Beechwood WSC	386	0030387	Meazell MHP
0030365	Centerville WSC			

FWSD = Fresh water supply district
MHP = Mobile home park
MUD = Municipal utility district
Subd = Subdivision
SUD = Special utility district
Sys = System
TDCJ = The Texas department of Criminal Justice
UD = Utility district
WSC = Water supply corporation
WS = Water supply

Appendix B. BRACS Database

This appendix contains a brief overview of the BRACS Database. Descriptions of selected tables housed in the BRACS Database are included for general reference. For additional info, please refer to the latest edition of the BRACS Database Data Dictionary (TWDB, 2023) which is available for download from the BRACS Database webpage.

Figure B-1 shows the BRACS Database table relationships. Each rectangle represents a unique category of information in a primary table linked to the other tables based on key fields represented by colored lines. The well location table, in the upper left, is the primary table where the well record identification number, Well_ID, is assigned.

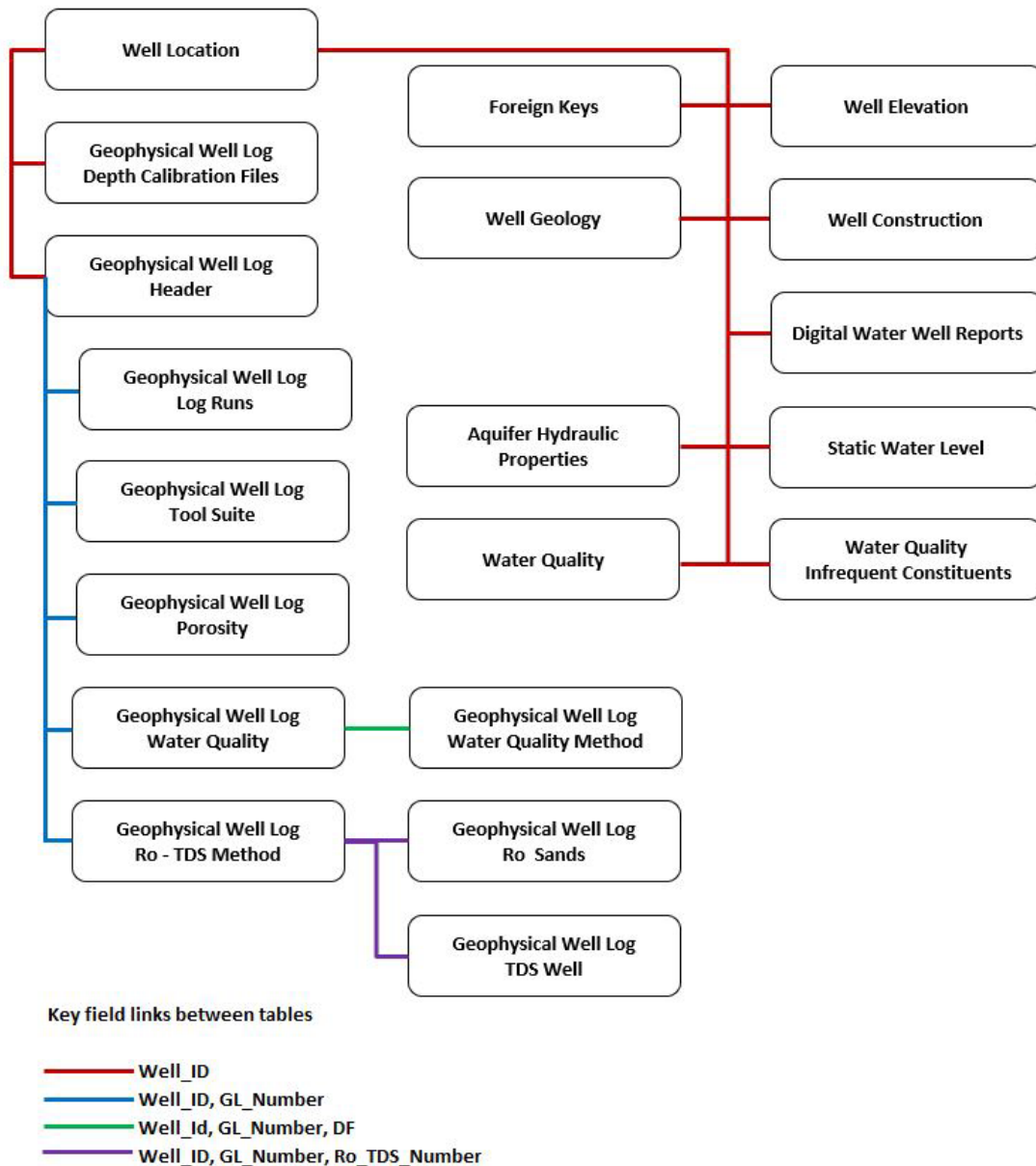


Figure B-1. BRACS Database table relationships.

Well location: tblWell_Location

The well location table contains one record per well. When a new well record is appended into the BRACS Database, the record is first added to this table, which assigns its unique identification number using an autonumber data type in the field [WELL_ID]. The table contains attributes about the well, such as owner, location, source of well information, and well depth information.

Elevation: tblBracs_Elevation

The elevation information resides in a separate table to handle the zero-to-many relationship between a well record and site elevation. The elevation values may differ depending on the elevation model used. The two primary sources of elevation information used are digital elevation models, one with a 30-meter grid cell and the other with a 10-meter grid cell. The table contains attributes about the well elevation such as method, elevation datum, agency, and date collected.

Foreign keys: tblBracs_ForeignKey

The foreign key table contains the identification (ID) names or numbers assigned to a well. This information resides in a separate table to handle the zero-to-many relationship between a well record and assigned IDs. This table is used to 1) record all the different names and numbers of the well and 2) link the BRACS well records with equivalent well records in supporting databases or written reports, such as the TWDB Groundwater Database (TWDB, 2023e), the Railroad Commission of Texas Oil and Gas Well Database (RRC, 2023a), or the Texas Department of Licensing and Regulation Submitted Driller's Report Database (TDLR, 2023).

Well geology: tblWell_Geology

The well geology table contains records of 1) well site lithology, 2) simplified lithologic descriptions, 3) stratigraphic picks, 4) faults, 5) salinity zones, and 6) hydrogeologic units. The information resides in a separate table to handle the zero-to-many relationship between a well record and well site geology.

Aquifer hydraulic properties: tblBracs_AquiferTestInformation

The aquifer test table contains records of hydraulic properties such as well yield, specific capacity, and transmissivity. The information resides in a separate table to handle the zero-to-many relationship between a well record and aquifer test results. Sources of information include, but are not limited to: 1) TWDB aquifer test spreadsheet, 2) TWDB Groundwater Database (TWDB, 2023e) remarks table, compilations of aquifer test data from 3) (Myers, 1969) and 4) (Christian and Wuerch, 2012), 5) Texas Department of Licensing and Regulation Submitted Driller's Report Database (TDLR, 2023), 6) scanned State of Texas Water Well Reports (TCEQ, 2023c), 7) TWDB published reports, 8) U.S. Geological Survey published reports, 9) Bureau of Economic Geology published reports, and 10) miscellaneous published and unpublished reports.

Geophysical well log, header: tblGeophysicalLog_Header

This table contains geophysical well log attributes, file names and types, and digital file locations for each log in the TWDB BRACS collection. The information resides in a separate

table to handle the zero-to-many relationship between a well record and a geophysical well log. The top page of a geophysical well log is commonly called the header and contains the operator name, well lease and number, location, dates, depths, logging parameters, and other attributes essential in understanding the conditions under which the logging was performed.

Geophysical well log, log runs: tblGeophysicalLog_Header_LogRuns

This table contains geophysical well log attributes from each log run for each geophysical well log used for log analysis. An oil or gas well may be drilled and logged in different depth stages. Attributes (for example top and bottom depth of the log run, temperature of bottom hole, drilling mud resistivity) will be different and must be recorded in a separate table to handle the one-to-many relationship between a geophysical well log and each log run.

Well construction: tblBracs_Casing

The well construction table contains the diameter, top and bottom depths, and construction interval (casing, well screen, open hole) (Table 15-1). The design of the table is exactly like the table in the original TWDB Groundwater Database (Rein and Hopkins, 2008) except the state well number field is replaced with the BRACS [Well_ID] field. The information resides in a separate table to handle the zero-to-many relationship between a well record and the well construction.

Digital water well reports: tblBracsWaterWellReports

This table contains file names and types, file locations, and hyperlinks for each digital well report in the BRACS Database collection. The majority of reports are for water wells. However, any non-geophysical well log report for oil and gas wells (such as a scout ticket) is contained in this table and filing system. The information resides in a separate table to handle the zero-to-many relationship between a well record and the digital well report.

Water quality: tblBracsWaterQuality

The water quality table contains records of water chemistry data organized with one record per well per date sampled with constituents in separate fields. The design of the table is almost exactly like the table in the original TWDB Groundwater Database (Rein and Hopkins, 2008). The information resides in a separate table to handle the zero-to-many relationship between a well record and water quality sample.

Porosity: tblGeophysicalLog_Porosity

The geophysical log porosity table holds records of geophysical well log types and the calculated porosity for specific geologic intervals. There may be multiple inputs for one well ID given number of logs or formations with calculated porosity.

Static water level: tblBRACS_SWL

Static water level information is contained in this table which is designed similarly to its equivalent in the original Groundwater Database. Information includes dates, water levels, and source of measurement.

Appendix C. Geophysical logging tools

Geophysical logging enables geoscientists to characterize downhole physical properties to gain understanding of geologic materials, groundwater and/or other fluids, and the mechanical integrity of boreholes. Geophysical logging tools measure rock and fluid properties using geophysical well logging tools. These tools are typically dropped to the lowest depth of the hole to be logged and are lifted at a constant rate until the logging tool passes the desired section of the hole. Interpretations of geophysical well logs are conducted using the combination of several geophysical well logging techniques. Common geophysical logs used in this study include:

Spontaneous-potential (SP) logs – results from naturally occurring electrical currents flowing between borehole mud and formation. SP curve deflection occurs opposite permeable bed (Schlumberger, 2009), and depending on the salinity of the mud filtrate vs salinity of the formation water, deflection of SP curve appears as negative or positive. Spontaneous-potential logs can be used in the determination of lithology and water quality.

Resistivity logs – record the electrical resistivity (fluid conductivity) of fluid in the borehole as measured by variably-spaced potential electrodes on the logging probe (logs measure the geological formation at shallow, medium, and deep depths) (Rittgers, 2019). Log response shows separation between deep resistivity and shallow resistivity curves opposite permeable formation due to the borehole mud invasion of the formation (Schlumberger, 2009). This causes a different resistivity to occur close to the borehole wall compared to deeper in the formation. Formation resistivity logs can be useful in indicating permeable zones, comparing different lithologies and fluid resistivity which reflect difference in dissolved solids concentration of water.

Gamma Ray logs – record the amount of natural gamma radiation emitted by the rocks surrounding the borehole. The most significant naturally occurring sources of gamma radiation are potassium-40 and daughter products of the uranium- and thorium-decay series (Williams and others, 2002). Clay- and shale-bearing rocks commonly emit relatively high gamma radiation because they include weathering products of potassium feldspar and mica and tend to concentrate uranium and thorium by ion absorption and exchange. The gamma log is often used to define lithology and correlate geologic units between boreholes.

Caliper logs – provide a continuous record of average borehole diameter. Used to identify fractures, water-bearing openings, and changes in lithology. Changes in borehole diameter are related to drilling and construction procedures, caving in of rocks, and the presence of fractures (Williams and others, 2002).

Acoustic logs – provide record of formation's interval transit time and are commonly referred to as sonic logs (Schlumberger, 2022). Acoustic logs have become a widely used porosity tool in formation evaluation (Pickett, 1963).

Nuclear logs (neutron and density logs) – provide a record of formation porosity variations, bulk density, types of pore fluids, and rock characteristics by measuring the intensity of scattered radiation induced by radioactive sources (Oliveira and others, 2011).

Appendix D. Comparison of stratigraphic interpretations

A comparison of picks between this study, Ricoy (1976) and applicable groundwater availability models (GAMs) for the Sparta, Queen City and, Carrizo-Wilcox aquifers (Kelley and others, 2004; Young and others, 2018; and Schorr and others, 2020) was completed to verify congruence with previously published studies. A summary of the results is included in Tables D-1 and D-2, and Figure D-1.

Overall, this study picked shorter intervals, excluding the more subtle fining-upwards sequences occurring near the top and the coarsening-upwards sequences occurring near the base of the Sparta Formation. Ricoy (1976) picked the longest intervals overall and included most of these sequences. Intervals for the GAMs are a hybrid between these interpretations.

It should be noted that picks from the U. S. Geological Survey's Regional Aquifer System Analysis (RASA) of the Texas Gulf Coast (Hosman and Weiss, 1991) that have been carried over from the legacy GAMs were excluded from the comparison for the purposes of this study. The tops from that study differed significantly in some locations. The difference ranges between 227 and 772 feet.

The RASA study was based upon best available science at the time it was completed. However, the definition of best available science evolves over time and the confidence level of the data from this study is variable. In some locations within the East Sparta aquifer study area, these data vary significantly when compared to data from more recent investigations.

Table D-1. Comparison of Sparta Formation picks that are congruent.

County	Well_ID	Q-number	Study ^a	Top Sparta (depth in feet)	Base Sparta (depth in feet)	Sparta thickness (feet)
Tyler	6361	Q-141	BRACS	4776	5031	255
			Ricoy	4690	5275	585
			SPQC04	4580	5135	555
Angelina	20891	Q-57	BRACS	184	490	306
			Ricoy	180	515	335
			SPQC04		510	
			nQCSCW	230		
Houston	37382	Q-144	BRACS	345	572	227
			Ricoy	340	680	340
			SPQC04	345	695	350
San Jacinto	22637	Q-6	BRACS	3897	4152	255
			Ricoy	3790	4300	510
			SPQC04	3780	4230	450
			nQCSCW	same as SPQC04		
Madison	9689	Q-9	BRACS	595	889	294
			Ricoy	600	950	350
			SPQC04	550	935	385
			nQCSCW	same as SPQC04		
Grimes	67789	Q-37	BRACS	3993	4205	212
			Ricoy	3910	4420	510
			SPQC04	3830	4360	530
			nQCSCW	same as SPQC04		
Brazos	38516	Q-27	BRACS	509	753	244
			Ricoy	415	785	370
			SPQC04	415	770	355
			nQCSCW	same as SPQC04		
Washington	87616	Q-24	BRACS	2739	2992	253
			Ricoy	2720	3170	450
Fayette	9699	Q-28	BRACS	2798	2988	190
			Ricoy	2710	3040	330
			SPQC04	2620	3003	383

^a BRACS is the current study, SPQC04 is Kelley and others (2004), nQCSCW is Schorr and others (2020), and Ricoy is Ricoy (1976).

Well ID 20891 – Angelina Co.

Well ID 22637 – San Jacinto Co.

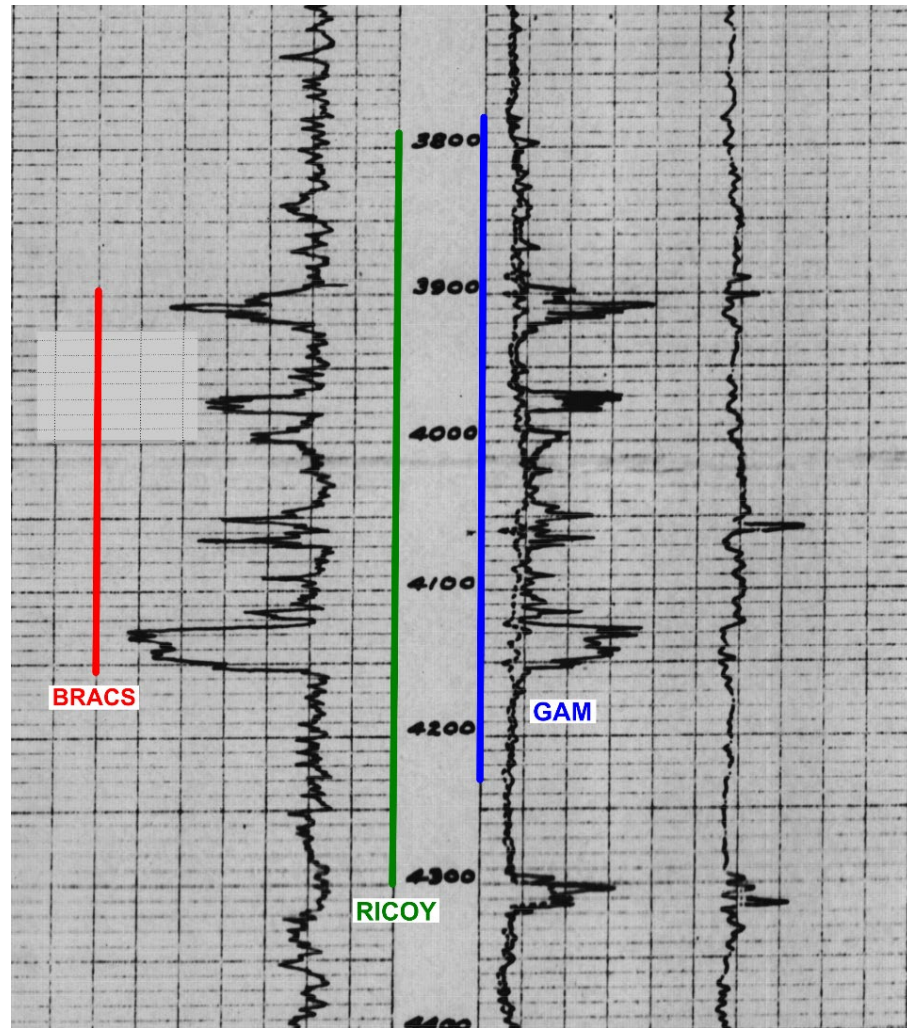
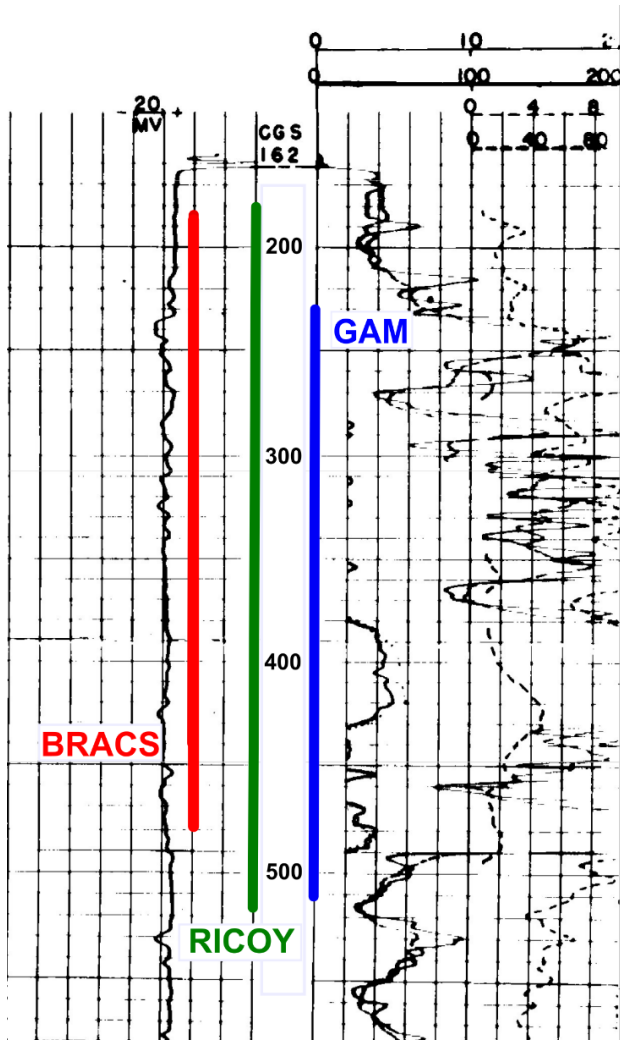


Figure D-1. Comparison of Sparta Formation picks between this study, Ricoy (1976), Kelley and others (2004), and Schorr and others (2020).

Table D-2. Comparison of Sparta Formation picks that are incongruous.

County	Well ID	Q-number	Study ^a	Top Sparta (depth in feet)	Base Sparta (depth in feet)	Sparta thickness (feet)	Difference (feet)
Waller	4631	Q-134	BRACS	5,811	5,994	183	610
			Ricoy	5,720	6,220	500	
			nQCSCW	5,201			
Montgomery	6338	Q-100	BRACS	5,156	5,379		772
			nQCSCW	4,384			
			Ricoy	n/a			
Polk	26142	Q-187	Ricoy	2,770	3,170	400	419
			nQCSCW	2,351			
			BRACS	2,816	3,090	274	
Angelina	6250	Q-59	BRACS	940	1,161	221	440
			Ricoy	950	1,365	415	
			nQCSCW	500			
Newton	66660	Q-225	BRACS	4,175	4,442	267	399
			Ricoy 1	3,990	4,560	570	
			nQCSCW	3,776			
Sabine	6345	Q-41	BRACS	560	789	229	227
			Ricoy	560	900	340	
			cQCSCW	333			

^a BRACS is the current study, nQCSCW is Schorr and others (2020), cQCSCW is Young and others (2018), and Ricoy is Ricoy (1976).

Appendix E. Geographic information system datasets

Many GIS datasets were created for this study and each of the GIS files prepared for this BRACS study is available for download from the Texas Water Development Board website. GIS techniques used to build the files are noted in the GIS file metadata. For further info on GIS raster interpolation methodology, see Meyer and others 2020. ArcGIS® and the Spatial Analyst® extension software by Environmental Systems Research Institute, Inc. (ESRI) were used to create the GIS files.

We have developed a file naming scheme for all GIS files created for this study. The full list of study-specific codes is presented in Table E-1.

Table E-1. GIS filename codes applied to the Sparta East aquifer study.

Code	Code type	Code description
UCPE	BRACS study	Upper Coastal Plains - East Texas (project acronym)
BRACS	General	Brackish Resources Aquifer Characterization System
GCD	General	Groundwater Conservation District
GMA	General	Groundwater Management Area
GWDB	General	Groundwater Database
PWS	General	Public Water System
Desal	General	Desalination Plant
RWPA	General	Regional Water Planning Area
czwx	Stratigraphic	Carrizo-Wilcox
qc	Stratigraphic	Queen City Formation
sp	Stratigraphic	Sparta Formation
yj	Stratigraphic	Jackson Group-Yegua Formation
ns	Value	Net sand in cumulative feet
tk	Value	Isochrone thickness in feet
te	Value	Top elevation in feet relative to mean sea level
be	Value	Bottom elevation in feet relative to mean sea level
td	Value	Top depth in feet below ground surface
bd	Value	Bottom depth in feet below ground surface
tds	Value	Total dissolved solids in milligrams per liter
swl	Value	Static water level
swle	Value	Static water level elevation, in feet relative to mean sea level
guide	Value	Guide point value
dem	Value	Digital Elevation Model, ground surface elevation in feet relative to mean sea level
i	Raster data value	Integer
nd	Raster data value	Null data values are set
snap	Snap raster	Snap raster file used to snap all project cells
250K	Data type	Shapefile was digitized from a 1:250,000 original
AD	Data type	Aquifer determination
AT	Data type	Aquifer test

Table E-1 (continued). GIS filename codes applied to the UCPE Sparta East aquifer study.

Code	Code type	Code description
calc	Data type	Calculated
con	Data type	Contour
depo	Data type	Depositional
ext	Data type	Extent
ft	Data type	Feet
meas	Data type	Measured
otc	Data type	Outcrop
pg	Data type	Polygon
pl	Data type	Polyline
pt	Data type	Point
sbc	Data type	Subcrop
sys	Data type	System

Study GIS files organized by folder structure

All surface files (for example elevation, depth, net sand) are in the Tag Image File Format (.tif) with Albers projection and the North American Datum 1983 as the horizontal datum. All raster files are snapped (coincident cell boundaries) to the study snap grid raster with a cell size of 250 by 250 feet.

Polygon, polyline and point files are in the ArcGIS® shapefile (.shp) format with Groundwater Availability Model projection and the North American Datum 1983 as the horizontal datum. Various tables are provided in dBASE table file format (.dbf), which represents dBase database file.

The codes from Table E-1 are used consistently in all digital files in the project. Each code is separated from the next code with an underscore character.

Table E-2. GIS files for regional geology in the East Sparta Aquifer study area. Folder structure: BRACS_UCPE_GIS_data\sp_ucpe_StudyArea.

File type	Point file name	Polyline file name	Polygon file name	Raster
Cross section	sp_ucpe_cross_section_pt.shp sp_ucpe_estimated_cross_section_pt.shp	sp_ucpe_cross_section_pl.shp sp_ucpe_estimated_cross_section_pl.shp		
Type logs	sp_ucpe_type_log_pt.shp			
Project snap grid				ucpe_snap.tif
Project elevation				dem_i_ucpe.tif sp_ucpe_otc_dem.tif
Study area		sp_ucpe_study_area_pl.shp	sp_ucpe_study_area_pg.shp ucpe_study_area_pg.shp tx_usgs_coastal_uplands.shp	sp_ucpe_ext_nd.tif sp_ucpe_otc_nd.tif
Texas counties			sp_ucpe_tx_counties.shp ucpe_tx_counties.shp tx_counties.shp tx_outline.shp	
Texas cities and urban areas			sp_ucpe_City_TxDOT_2015.shp tx_urban_areas.shp	
PWS			sp_ucpe_pws_service_areas.shp	
PWS with Sp wells			sp_pws_service_areas.shp	
Well control	sp_ucpe_well_control_pt.shp			
GWDB well control	sp_ucpe_gwdb_well_control_pt.shp			
Porosity logs	sp_ucpe_porosity_logs.shp			
Aquifer test	sp_ucpe_AT_pt.shp			

Table E-2 (continued). GIS files for regional geology in the East Sparta Aquifer study area. Folder structure: BRACS_UCPE_GIS_data\sp_ucpe_StudyArea.

File type	Point file name	Polyline file name	Polygon file name	Raster
GMA			GMA.shp	
RWPA			RWPA.shp	
GCD			sp_ucpe_GCD.shp	
U.S. highways		sp_ucpe_US_highways_tsms.shp		
Interstate highways		sp_ucpe_interstate_highways_tsms.shp		
State highways		sp_ucpe_state_highways_tsms.shp		
Major Texas rivers		major_tx_rivers.shp sp_ucpe_tx_rivers.shp		
Figure feathering			sp_ucpe_boundary_feathered_mask.pg ucpe_boundary_feathered_mask.pg	

Table E-3. GIS files for regional geology in the East Sparta Aquifer study area. Folder structure: BRACS_UCPE_GIS_data\ucpe_Stratigraphy.

File type	Point file name	Polyline file name	Raster
Top elevation	spte_ucpe_pt.shp spte_ucpe_guide_pt.shp sp_ucpe_LA.pt	spte_ucpe_con_1000ft_pl.shp spte_ucpe_con_guide_pl.shp	spte_ucpe.tif
Bottom elevation	spbe_ucpe_pt.shp spbe_ucpe_guide_pt.shp	spbe_ucpe_con_1000ft_pl.shp	spbe_ucpe.tif
Top depth		sptd_ucpe_con_1000ft_pl	sptd_ucpe.tif
Bottom depth		spbd_ucpe_con_1000ft_pl	spbd_ucpe.tif
Thickness	sp_ucpe_tk_guide_pt.shp	sptk_ucpe_con_50ft_pl.shp	sptk_ucpe.tif
Outcrop control	spbe_ucpe_otc_ext_dem_pt.shp		

Table E-4. GIS files for regional geology in the East Sparta Aquifer study area. Folder structure: BRACS_UCPE_GIS_data\sp_ucpe_Lithology.

File type	Point file name	Polyline file name	Raster
Net sand	spns_ucpe_pt.shp spns_ucpe_guide_pt.shp	spns_ucpe_con_40ft_pl.shp	spns_ucpe.tif
Outcrop control	sp_ucpe_otc_zero_pt.shp		

Table E-5. GIS files for regional geology in the East Sparta Aquifer study area. Folder structure: BRACS_UCPE_GIS_data\sp_ucpe_SalinityClass.

File type	Point file name	Polyline file name	Polygon file name
Salinity class		sp_ucpe_salinity_class_pl.shp	sp_ucpe_salinity_class_pg.shp
Measured water quality	sp_ucpe_TDS_meas_pt.shp		
Calculated water quality	sp_ucpe_TDS_calc_pt.shp sp_ucpe_TDS_calc_tie_in_pt.shp		
Produced water samples	sp_ucpe_produced_water_samples.shp		

Table E-6. GIS files for regional geology in the East Sparta Aquifer study area. Folder structure: BRACS_UCPE_GIS_data\sp_ucpe_Geology.

File type	Point file name	Polyline file name	Polygon file name
Outcrop			sp_ucpe_otc_pg.shp
Subcrop			sp_ucpe_otc_sbc_pg.shp
Depositional settings		sp_ucpe_depo_sys_axis_pl.shp sp_ucpe_depo_sys_boundary_pl.shp	
Mapped geological features			sp_ucpe_salt_domes_modified.shp
Mapped faults		sp_ucpe_normal_fault_downthroun_Ewing.shp sp_ucpe_normal_fault_Ewing.shp sp_ucpe_Fault250_GAT.shp ucpe_normal_fault_downthrown_Ewing.shp ucpe_normal_fault_Ewing.shp	
Mapped structure		ucpe_embayment_axes.shp ucpe_arch_axes.shp	ucpe_sabine_uplift.shp
Surface geology			sp_ucpe_rock_unit_pl_250K_GAT.shp

Table E-7. GIS files for regional geology in the East Sparta Aquifer study area. Folder structure: BRACS_UCPE_GIS_data\sp_ucpe_Volumes.

File type	Point file name	Polygon	Raster
Static water level	sp_ucpe_gwdb_swl_pt.shp sp_ucpe_tdlr_swl_pt.shp		sp_ucpe_swl_otc.tif
Static water level outcrop control	sp_ucpe_swl_otc_zero_pt.shp		
Volume grid	sp_ucpe_master_grid_pt.shp sp_ucpe_master_grid_manual_pt.shp	sp_ucpe_master_grid_pg.shp	
Volumes by county	sp_ucpe_volumes_by_county.dbf		
Volumes by GCD	sp_ucpe_volumes_by_GCD.dbf		
Volumes by GMA	sp_ucpe_volumes_by_GMA.dbf		
Volumes by RWPA	sp_ucpe_volumes_by_RWPA.dbf		
Volumes by salinity class	sp_ucpe_volumes_by_salinity_class.dbf		

Appendix F. Porosity calculations

We read five apparent density porosity measurements directly from the density geophysical well log.

We calculated eight neutron-density porosity measurements in the Sparta Formation using a concentration of shale correction. The following calculations used equations in (Torres-Verdin, 2017):

Read the apparent neutron and density in porosity units directly from the geophysical well log.

Calculate the shale index using gamma ray values from the sand being evaluated and a “pure” sand and “pure” shale in the same geological formation with the equation:

$$I_{sh} = \frac{\gamma_{formation} - \gamma_{sand}}{\gamma_{shale} - \gamma_{sand}}$$

where:

I_{sh} = shale index

$\gamma_{formation}$ = formation sand gamma ray value in API units

γ_{sand} = “pure” sand unit gamma ray value in API units

γ_{shale} = “pure” shale unit gamma ray value in API units

Calculate the concentration of shale using the Larionov I method used for Tertiary clastics with the equation:

$$C_{sh} = 0.083 \cdot (2^{3.7 \cdot I_{sh}} - 1)$$

where:

C_{sh} = concentration of shale

I_{sh} = shale index

Calculate corrected apparent neutron and density porosity values with the concentration of shale with the equations:

$$\text{cor } \phi_D = \frac{(\phi_D - C_{sh}) \cdot \phi_{D sh}}{1 - C_{sh}}$$

$$\text{cor } \phi_N = \frac{(\phi_N - C_{sh}) \cdot \phi_{N sh}}{1 - C_{sh}}$$

where:

$\text{cor } \phi_D$ = corrected apparent density porosity

$\text{cor } \phi_N$ = corrected apparent neutron porosity

- ϕ_D = apparent density porosity, read from geophysical well log
- ϕ_N = apparent neutron porosity, read from geophysical well log
- $\phi_{D\ sh}$ = apparent density porosity of a “pure” shale unit, read from geophysical well log
- $\phi_{N\ sh}$ = apparent neutron porosity of a “pure” shale unit, read from geophysical well log
- C_{sh} = concentration of shale

Calculate corrected neutron-density estimated total porosity using corrected apparent density and neutron porosity with the equation:

$$\text{cor } \phi_{N-D} = \sqrt{\frac{\text{cor } \phi_N^2 + \text{cor } \phi_D^2}{2}}$$

where:

- $\text{cor } \phi_{N-D}$ = corrected neutron-density porosity
- $\text{cor } \phi_D$ = corrected apparent density porosity
- $\text{cor } \phi_N$ = corrected apparent neutron porosity

We calculated 19 neutron-density porosity measurements in the formations of interest without using a concentration of shale correction. The following calculations used the equation in (Torres-Verdin, 2017)

Read the apparent neutron and density in porosity units directly from the geophysical well log.

Calculate neutron-density estimated total porosity using the apparent neutron and density porosity with the equation:

$$\phi_{N-D} = \sqrt{\frac{\phi_N^2 + \phi_D^2}{2}}$$

where:

- ϕ_{N-D} = neutron-density porosity
- ϕ_D = apparent density porosity
- ϕ_N = apparent neutron porosity

We calculated one porosity estimate using the density tool in units of grams per cubic centimeter and the (Asquith and Gibson, 1982) equation:

Read the apparent density in units of grams per cubic centimeter directly from the geophysical well log.

A density total porosity was calculated using the apparent density with the equation:

$$\phi_D = \frac{\rho_m - \rho_{fm}}{\rho_m - \rho_{fl}}$$

where: ϕ_D = density porosity

ρ_m = density of the matrix, sandstone (2.65 grams per cubic centimeter)

ρ_{fl} = density of the borehole fluid is fresh mud (1 gram per cubic centimeter)

ρ_{fm} = density of the formation, read from the geophysical well log (grams per cubic centimeter)

We calculated 17 porosity estimates using the sonic (acoustic) tool interval transit time in units of microseconds per foot and the (Asquith and Gibson, 1982) equation:

Read the sonic interval transit time in units of microseconds per foot directly from the geophysical well log.

A sonic total porosity was calculated using the sonic interval transit time with the equation:

$$\phi_s = \frac{1}{C} \cdot \frac{\Delta_{Tfm} - \Delta_{Tm}}{\Delta_{Tfl} - \Delta_{Tm}}$$

where:

ϕ_s = sonic porosity

Δ_{Tfm} = time of formation is read from the geophysical well log (microseconds per foot)

Δ_{Tm} = time of matrix in sandstone (55.5 microseconds per foot)

Δ_{Tfl} = time of borehole fluid in fresh mud (189 microseconds per foot)

C = compaction factor = $\frac{\Delta_{Tsh} \cdot Cn}{100}$

where: Δ_{Tsh} = time of adjacent shale unit in microseconds per foot

Cn = constant which is normally 1 (Hilchie, 1978)

Appendix G. Modeled water quality data (Phreeqc)

Sample	Silica (mg/L)	Calcium (mg/L)	Magnesium (mg/L)	Sodium (mg/L)	Potassium (mg/L)	Strontium (mg/L)	Carbonate (mg/L)	Bicarbonate (mg/L)	Sulfate (mg/L)	Chloride (mg/L)	Fluoride (mg/L)	Nitrate (mg/L)	pH (su)	TDS (mg/L)	Alkalinity (mg/L)	SC (estimated)
1	14	392	135	899	-	-	-	369	-	1,153	0.5	1.0		4,087	251	5,936
2	-	15	9	2,512	-	-	-	796	27	3,443	-	-	7.7	6,802	-	11,331
3	13	287	60	1,463	-	-	-	584	621	1,786	1.1	2.0	6.5	4,817	351	7,494
4	13	114	85	1,889	-	-	-	358	589	2,256	1.3	3.0	6.7	5,308	662	8,993
5	11	21	16	2,198	-	-	-	-	621	2,984	2.0	3.0	7.6	6,877	874	10,734
6	12	28	19	2,452	-	-	-	979	594	3,351	1.9	2.8	7.6	7,440	837	11,750
7	12	35	22	2,706	-	-	-	937	567	3,710	1.8	2.5	7.6	7,993	800	12,749
8	12	42	25	2,960	-	-	-	895	540	4,058	1.7	2.3	7.6	8,536	763	13,720
9	11	49	28	3,214	-	-	-	853	513	4,258	1.6	2.0	7.7	8,930	726	14,438
10	10	56	31	3,468	-	-	-	811	384	4,712	1.5	1.8	7.7	9,475	689	15,506
11	13	63	34	3,722	-	-	-	769	459	4,909	1.4	1.5	7.7	9,972	652	16,294
12	14	70	37	3,976	-	-	-	727	432	5,250	1.3	1.3	7.8	10,509	615	17,240
13	14	77	40	4,230	-	-	-	685	405	5,591	1.2	1.0	7.8	11,044	578	18,186
14	14	84	43	4,484	-	-	-	643	378	5,932	1.1	0.8	7.8	11,580	541	19,129
15	15	91	46	4,738	-	-	-	601	351	6,273	1.0	0.5	7.9	12,117	504	20,068
16	15	98	49	4,992	-	-	-	559	324	6,614	0.9	0.3	7.9	12,652	467	20,999
17	16	105	52	5,246	-	-	-	517	297	7,012	0.8	-	7.9	13,246	430	22,025
18	16	112	55	5,500	-	-	-	475	270	7,296	0.7	(0.3)	7.9	13,724	393	22,859
19	17	112	61	7,800	-	-	-	432	284	9,897	1.0	0.5	7.7	18,605	335	30,481
20	17	110	51	9,763	-	-	-	410	263	-	1.0	-	7.6	20,762	301	33,636
21	-	175	62	8,722	-	-	-	952	22	-	-	-	7.0	23,302	-	37,316
22	-	175	62	8,722	-	-	-	952	22	-	-	-	7.0	23,303	-	37,349
23	18	104	54	-	-	-	-	405	410	-	1.0	-	7.5	23,641	297	37,952
24	-	67	53	8,888	-	-	-	-	14	-	-	-	7.4	24,657	-	35,669
25	18	100	52	-	-	-	-	398	574	-	1.0	-	7.4	26,839	284	42,463
26	-	199	98	-	-	-	-	-	21	-	-	-	7.7	28,850	-	44,921
27	18	95	53	-	-	-	-	356	658	-	1.0	-	7.3	30,100	261	47,204
28	19	87	51	-	-	-	-	312	789	-	1.0	-	7.2	34,990	251	54,150

Appendix H. Calculation of groundwater volumes

A master grid polygon file was created using the Fishnet tool in ArcGIS® to compile various data based on complex geometric shapes and administrative boundaries into smaller three-dimensional cubes for the groundwater volume calculations. Grid cells were assigned to administrative boundaries into the master polygon and, ultimately, point shapefile containing the centroid of grid cells (UCPE_master_grid_sp_pt.shp).

As discussed in section 11, the grid cell sizes were increased to 1,500 feet to optimize calculation tools using the program. Using the latest shapefiles for polygons of each administrative boundary, administrative titles were assigned. Administrative boundaries we included are County names, Groundwater Conservation Districts (GCDs), Groundwater Management Area numbers (GMAs), and Regional Water Planning Areas (RWPAs).

To assign administrative boundary properties, cells were selected by attribute where the centroids were located within a specific boundary. We then used the Field Calculator tool to attribute the name of the feature. For example, grid cells were selected by location with their centroid within Sabine County, then, using the Field Calculator, we assigned the name “Sabine” under the field “COUNTYNAME” to only those selected cells.

For further information on the methodology used for calculations in ArcGIS, please see the BRACS study titled, Brackish Groundwater in Aquifers of the Upper Coastal Plains, Central Texas (Meyer and others, 2020). For quick reference, volume calculations involved the following equations:

Groundwater volume per grid cell = cell area * saturated thickness * specific yield

Once calculated per grid cell, we summed grid cell volumes per salinity class to calculate total volumes.

*Area*_{of study} = number of cells * cell length * cell width * conversion factor from feet to acres

$$157,642 * 1500 * 1500 * \frac{1 \text{ acre}}{13,560 \text{ feet}^2} = 8,142,666 \text{ acres}$$

Saturated thickness (STK) represents the portion of the formation that could hold and produce water. Two different calculations were used based on whether in the outcrop or subcrop.

Outcrop:

$$\text{STK}_{\text{outcrop}} = (\text{static water level elevation} - \text{bottom elevation}) * \text{percent sand}$$

$$\text{percent sand} = (\text{formation net sand} / \text{formation thickness}) * 100$$

Subcrop:

$$\text{STK}_{\text{subcrop}} = \text{formation net sand}$$

Specific Yield = value derived from (Young and others, 2018). Specific yield for this study was 0.1.

Percent sand data clean-up

Percent sand is an important aspect for calculating the saturated thickness for each cell within the outcrop portion of the studies master grid shapefile. Given the dendritic nature of the many drainage pathways within the East Sparta outcrop, the variability of the data control, and the inherent limitations of the Topo to Raster predictive interpolation tool, about 4,000 cells indicated a Sparta net sand thickness greater than formation thickness, which would have resulted in erroneous value with percent sand greater than one hundred. Therefore, we decided to manually input the percent sand for 4,219 cells, 1,302 of which were located within the subcrop and had no effect on the saturated thickness calculations. The remaining cells account for 1.8 percent of the 157,642 total study area cells used for volume calculations.

Those cells that were manually evaluated, based on the following criteria, were also flagged in a separate field named "SPPS_m" for manual input (SPPS_m = 1). We selected those cells with Sparta percent sand greater than 100 located in the outcrop (SPOTC = 0), and changed those to 100, to assume outcrop cells have 100 percent sand (Figure 17H-1). This accounted for eleven percent of the manually input cells, or 0.3 percent of the total study area.

The following did not affect volume calculations but was still performed to eliminate incorrect null or negative values based on best professional judgement. Within a few areas immediately downdip from the outcrop, clusters of cells erroneously showed net sand greater than thickness. This appears to be a result of having sparse net sand or thickness control data in the surrounding areas. However, most of the calculated net sand values within these clusters showed about 80 percent net sand. Therefore, a value of 80 was manually input for percent sand for ten percent of these cell clusters. Next, we selected cells with Sparta percent sand erroneously greater than 100 percent within the subcrop (SPOTC = S). These cells were in obvious drainage pathways eroded through the outcrop (net sand = 0). Therefore, seven percent of the manually evaluated cells were edited to show percent sand equal to zero.

The remaining cells either contained zero feet thickness or zero feet net sand, and when calculating percent sand, they yielded erroneous null values. Therefore, we manually input zero for percent sand for these cells and denoted then with the number two for manual input (SPPS_m =2).

For further detail on ArcGIS® volumetrics methodology, see Meyer and others (2020).

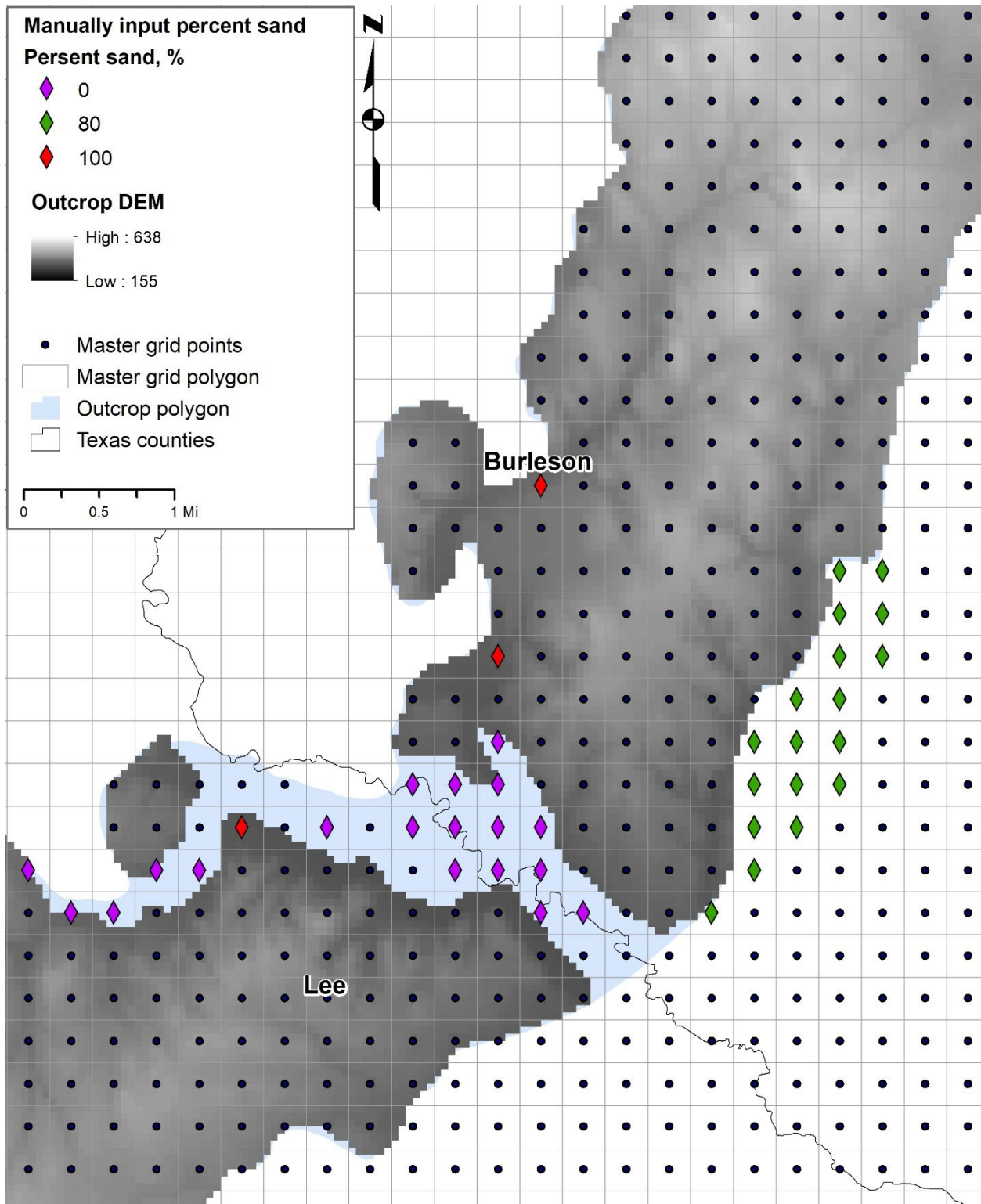


Figure H-1. Example of percent sand manual input.